The Role of F-box Only Protein 2 (Fbxo2) in Amyloid Precursor Protein Processing and Synaptic Dynamics

by

Graham Michael Atkin

A dissertation submitted in partial fulfillment
of the requirements for the degree of
Doctor of Philosophy
(Neuroscience)
in the University of Michigan
2014

Doctoral Committee
- Professor Henry Paulson, Chair
- Professor Eva Feldman
- Professor Kojo Elenitoba-Johnson
- Associate Professor Michael Sutton
- Assistant Professor Vikram Shakkottai

Acknowledgements: I wish to thank Geoff Murphy, Shannon Moore, Jack Hunt, Eiko Minakawa, Nate Tipper, William Tennant, Chris Valdez, and Asim Beg for their assistance with the design and execution of these research projects. This work was funded by NIH grant RO1 AG034228, pilot research funds from the Michigan Alzheimer's Disease Center, NIA grant T32-AG000114, and the University of Michigan Protein Folding Diseases Initiative.

TABLE OF CONTENTS

LIST OF FIGURES

ABSTRACT
Proper protein quality control is essential for neuronal health and function, and there is substantial evidence for the dysregulation of proteostasis in a wide range of neuropathological conditions including the most common neurodegenerative diseases. Diminished function of the Ubiquitin Proteasome System, the major cellular pathway for the clearance of toxic or unwanted proteins, likely contributes to disease pathogenesis through numerous - and as yet, incompletely understood - mechanisms. Here, I review recent studies exploring the role of the Ubiquitin Proteasome System in the most common neurodegenerative diseases. I then describe in-depth two research projects directed at further investigating one agent of the Ubiquitin Proteasome System whose expression is reduced in Alzheimer's disease, the F-box Only Protein 2 (Fbxo2). Using cell-based models and an *Fbxo2* knockout mouse, I present evidence for a role for Fbxo2 in the turnover and processing of the Amyloid Precursor Protein, believed to be the major causative protein in Alzheimer's disease. I then show that the loss of Fbxo2 results in greater expression and surface localization of NMDA receptor subunits, and enhances the formation of axo-dendritic shaft synapses. Taken together, these studies support a central role for the Ubiquitin Proteasome System, and in particular Fbxo2, in the turnover and handling of key proteins in the pathogenesis of Alzheimer's disease and the regulation of synaptic connections.

Chapter One: Ubiquitin Pathways in Neurodegenerative Disease

ABSTRACT

Control of proper protein synthesis, function, and turnover is essential for the health of all cells. In neurons these demands take on the additional importance of supporting and regulating the highly dynamic connections between neurons that are necessary for cognitive function, learning, and memory. To meet the demands of regulating multiple unique synaptic protein environments within a single neuron, while maintaining cell health, requires the highly regulated processes of ubiquitination and degradation of ubiquitinated proteins through the proteasome. In this review, we examine the effects of dysregulated ubiquitination and protein clearance on the handling of disease-associated proteins and neuronal health in the most common neurodegenerative diseases.

INTRODUCTION

The unique demands placed on neurons by their exquisitely complicated and dynamic architecture have been appreciated by investigators for over a hundred years (1-3). Recent studies place the number of neurons in the human brain at approximately 85 billion (4). With each neuron making upwards of 10 thousand synaptic connections, the estimated total number of synapses reaches toward 8.5 hundred trillion (8.5×10^{14}). Astonishingly, plasticity can occur selectively at

particular subsets of synapses within a neuron, even down to the level of a single specified synapse (5). Failure to maintain these synaptic connections and their proper plasticity are hallmarks of a host of neurodegenerative diseases, and loss of synaptic connections correlates with diminished cognitive function even before neurons degenerate (6,7). With 2,788 unique proteins already identified as integral to the composition of each synapse (8), the management of unique protein environments requires sufficiently complex and modifiable systems of protein quality control. The Ubiquitin Proteasome System (UPS), a set of interacting enzymes and associated proteins, is able to address these diverse proteostatic needs through the orchestrated activity of over 500 components working in versatile combinations to regulate protein-protein interactions and eliminate unwanted proteins. As newly synthesized proteins form new structures and connections, the UPS works to insure that old proteins are degraded to make way and that the proper complement of building materials is available. To achieve these functions, components of the UPS are recruited to dendritic spines in response to synaptic activity (9,10). Evidence continues to mount for the necessity of UPS involvement in the dynamic remodeling of synaptic structures following synaptic activity (11-17). This contribution to synaptic plasticity requires that the UPS function properly. For example, pharmacologic inhibition of the UPS reveals leads to a robust reduction in activity-dependent synaptic plasticity (12) and a dose-dependent loss of synaptic connections (18). Robust loss of synaptic connections is evident in all of the major neurodegenerative disorders. Precisely how these synapses are lost remains unclear, but given its role in the

degradation of synaptic scaffolding proteins and cytoskeletal elements, ubiquitination is almost certainly involved.

As important as the contribution of the UPS to maintaining the plasticity of synapses are its diverse roles in ensuring general cell health, including the elimination of misfolded or damaged proteins, mediation of receptor signaling pathways, response to DNA damage and oxidative stress, progression of the cell cycle, among other roles (19,20). UPS function is essential to cell health and survival in all cell types. Improper clearance of proteins is a causative or contributing factor in many neurodegenerative diseases, which are often characterized by the accumulation of aggregated proteins (21,22). Whether aggregation itself is the cause of toxicity or merely represents a strategy by which neurons sequester toxic proteins remains contested (23), but the failure of quality control pathways to eliminate these unwanted proteins is evident. UPS dysfunction has been reported in the most common neurodegenerative diseases, including Alzheimer's Disease (AD), Parkinson's Disease (PD), Amyotrophic Lateral Sclerosis (ALS), and Huntington's Disease (HD), as well as less common disorders and various animal models of protein aggregation (24-28). How the UPS becomes impaired in disease states is not always clear, as too little is known about how disease-related proteins are handled under normal conditions. Research into these areas has begun to reveal just how intricate and extensive the UPS is, and hopefully will uncover potential therapeutic interventions.

UBIQUITINATION AND THE UBIQUITIN PROTEASOME SYSTEM

Ubiquitin is a 76 amino acid (~8 kDa) protein expressed in all eukaryotic cells. It is highly conserved throughout evolution; the amino acid sequence of human ubiquitin is identical to that of Aplysia (29) and nearly identical to that of yeast (30). Through the coordinated activity of multiple enzymes, ubiquitin is covalently added to substrate proteins through the formation of an iso-peptide bond between the C-terminal diglycine motif of ubiquitin and lysine residues on the target (Figure 1) (31). This cascade begins with the ATP-dependent attachment of ubiquitin's C-terminal glycine through a thio-ester bond to an active-site cysteine on an Ubiquitin Activating Enzyme (E1). This ubiquitin is then transferred to a Ubiquitin Conjugating Enzyme (E2) through a thio-ester bond. From there, the E2 enzyme will cooperate with a Ubiquitin Ligase (E3) to transfer the ubiquitin molecule to the target lysine on a substrate protein. This last step occurs differently depending on the type of E3 involved, but it is at this step that substrate specificity is believed to occur, with E3 ligases selecting substrates for ubiquitination. However, this view has recently come under some scrutiny, as evidence emerges for a role for E2s in the process of substrate selection (32).

E3s are typically grouped into three classes, with each defined by the specific protein domains it possesses. These domain-based classes include: 1) Really Interesting New Gene (RING) finger-containing E3s, 2) Homologous to E6-AP (HECT) domain-containing E3s, and 3) E3s composed of multiple subunits. RING finger-containing E3s bring the E2 and the substrate protein into

sufficiently close proximity for the transfer of the ubiquitin to its target lysine (33). HECT-domain containing proteins possess an active-site cysteine to which the ubiquitin is first transferred from the E2 before being passed to the substrate protein (34). In contrast to these single-unit E3 ligases, multi-subunit ligases are composed of multiple adaptor proteins, cofactors, and scaffolding proteins that confer substrate specificity and facilitate ubiquitination (35). The Skp1/Cul1/F-box (SCF) protein complex and the Anaphase-promoting Complex (APC) are among the best studied of these multi-subunit E3s. SCF complexes can include various combinations of scaffolding proteins called cullins, F-box proteins, and substrate adaptors (36). APC is less variable, containing Apc2, Apc11, and either Cdh1 or Cdc20 for substrate recognition (37). Further contributing to the complexity of these multi-subunit E3 ligases is the developmental and spatial restriction of their expression within cells (38). There are estimated to be at least 500 different E3 ligases, with more continuing to be discovered (39). Each E3 can recognize multiple substrates; Fbxw1/β-TRCP1, for example, has upwards of 40 documented substrates itself (40).

This highly regulated process adds ubiquitin to target lysines on the substrate, but it can also add other ubiquitin molecules onto lysines of a ubiquitin already conjugated to a substrate. By this process, ubiquitin chains of varying length and composition can be formed. The elongation of ubiquitin chains can occur at any of ubiquitin's own seven lysines, resulting in the formation of different linkage types (41). Although all possible linkage types are present in cells, their precise

functions remain only partially understood (42). Chains formed through the addition of ubiquitin exclusively at lysine 48 (K48) have been recognized to signal protein degradation (43), whereas K63-linked ubiquitin chains seem to subserve diverse functions beyond protein degradation (44). For example, K63-linked chains regulate NF-κB signaling not by promoting protein degradation but by influencing ubiquitin-dependent protein-protein interactions (45). Elsewhere, however, they been implicated in promoting the lysosomal degradation of the low density lipoprotein receptor (LDLR) (46) and the epidermal growth factor receptor (EGFR) (47). Both K48- and K63-linked chains have been observed to modify kinase activity in response to cellular stress, as have K11-linked chains (48,49). K11-linked chains are critical for cell-cycle regulation and cell division (50). Other linkages, including atypical, mixed-type linkages are less well studied, but have been implicated in similar processes within the cell (51,52).

The functions thus far attributed to specific chain linkages represent only a fraction of the diverse roles ubiquitin is known to play in cellular processes (51), many of which do not depend on proteasome function (53). Ubiquitination regulates DNA repair (54), protein localization and endocytosis (55-57), and protein-protein interactions (58,59). Free, unanchored chains of ubiquitin molecules are also present in cells and can regulate numerous functions including kinase activation (60). The UPS has been also been implicated in the turnover of mRNA, although whether this regulation is direct or indirect remains unclear (61). Intriguingly, E3 ligases can themselves be targeted for

ubiquitination, offering an additional level of control for this important pathway (62,63). The ubiquitination of E3 ligases can result either in their degradation or in the modification of their activity (64).

Once a substrate is tagged for elimination through the addition of a ubiquitin chain, it must be targeted to the cell's degradation machinery by chaperone proteins which recognize and bind to poly-ubiquitin chains. One such chaperone is Valosin-containing protein (VCP), which has been shown to physically interact with and shuttle poly-ubiquitinated substrates to the proteasome to facilitate their degradation (Figure 2) (65). The proteasome contains a catalytic protein complex referred to as the 20S core (66), which is capped at each end by a regulatory protein complex (19S) (67,68). It is responsible for breaking down substrate proteins into small peptides (69,70).

The ubiquitination of substrate proteins is a reversible process. The removal of ubiquitin is carried out by De-ubiquitinating Enzymes (DUBs). DUBs play two important roles, allowing for the editing of existing chains (71) and the removal of ubiquitin chains altogether from a substrate. As the presence of ubiquitin chains prevents substrates from entering the proteasome due to spatial restrictions, DUBs play an essential role in determining the rate of protein clearance in cells (31,72), and certain DUBs including USP14 are known to associate directly with the19S regulatory complex of the proteasome (73).

Numerous studies report proteasome dysfunction and the accumulation of ubiquitinated proteins in disease states. But it is important to consider that proteasomal degradation is only one of several potential outcomes of ubiquitination. Indeed, there are numerous examples of dysregulated protein handling due to failures in ubiquitination that do not necessarily implicate the proteasome. Whether the effects of proteasomal failure reach upstream to impact the activity and efficacy of E1s, E2s, or E3s is not clear. Given that K48-linked chains are among the most common found in cells (74), it is conceivable that impaired proteolysis could deplete cellular pools of free ubiquitin and thereby induce further dysfunction. Accordingly, an imbalance in ubiquitination/ deubiquitination activities may result in improper chain formation, preventing the proteasome from recognizing and handling targeted substrates. To examine these two separate yet related phenomena, it will be helpful to distinguish whether dysfunction occurs in UPS per se or, more broadly in the Ubiquitin Signaling System (USS) which includes the labeling of proteins with ubiquitin for any number of intended outcomes beyond degradation. While impaired clearance characterizes UPS failure, it remains to be seen whether and how the other, non-proteasomal components of the USS contribute to disease processes. One example of this distinction is evident in the ubiquitin-mediated fate of Caspase proteins.

Though the precise methods by which neurons degenerate in disease remain unclear, substantial evidence supports a role for proteases of the Caspase family.

For example, activated caspases are elevated in Alzheimer's Disease (AD) patient tissue (75). Upon activation, caspases can either activate other proteases (initiator caspases) or damage essential components of the cell and promote apoptosis (effector caspases). Sublethal amounts of caspase activation have been linked to synaptic dysfunction in an animal model of AD (76). Caspase-mediated effects can be inhibited both by the inactivation of caspase enzyme activity and by their targeted degradation through the proteasome. The X-linked Inhibitor of Apoptosis Protein (XIAP) and its family member cIAP1 are RING-type E3 ligases that directly bind to and target caspases for degradation; XIAP is also able to inhibit the proteolytic activity of caspases (77,78). The regulation of caspases by XIAP is limited, however, in oxidative stress conditions. Both acute and chronic inflammation, which are often associated with disease, elevate the levels of nitric oxide in neurons. This elevation can lead to the aberrant addition of nitric oxide to proteins (nitrosylation). Dysregulated nitrosylation of proteins is evident in several neurodegenerative diseases, including AD (79). The addition of nitric oxide (nitrosylation) to the active cysteine of XIAP's RING domain inactivates its E3 ligase activity. Nitrosylated XIAP is unable to ubiquitinate caspases and thus unable to inhibit apoptosis (80). The relative amount of nitrosylated XIAP is increased in AD patient tissue, suggesting a role in the accelerated apoptosis observed in disease (80). Here, then, is one example in which the state of the proteasome in disease is secondary to the decreased ability of E3 ligases to target caspases for degradation. Therefore, it is essential to consider how disease-related proteins are modified by agents of

the USS while also examining whether affected neurons can execute the intended consequences of that modification.

To further illustrate the complexity of ubiquitin-mediated pathway involvement, we review key findings about the handling of disease-related proteins by the USS and UPS in several of the most common neurodegenerative diseases.

ALZHEIMER'S DISEASE

AD is the most common form of dementia and the most common neurodegenerative disorder. Its symptoms include a progressive decline in memory and other cognitive functions. Histologically, AD involves extensive neurodegeneration and loss of synaptic connections, resulting in progressive atrophy of the temporal, frontal and parietal lobes of the cerebral cortex. It is characterized by the hallmark deposition of intracellular, filamentous aggregates mainly consisting of hyper-phosphorylated Tau (neurofibrillary tangles) and extracellular plaques rich in Amyloid-Beta (amyloid plaques) (81-83). Ubiquitinated forms of Tau and Amyloid-Beta, as well as other ubiquitinated proteins, are major components of these aggregates (84). Amyloid-Beta, produced by the cleavage of the Amyloid Precursor Protein (APP), is thought to have numerous deleterious effects on neuronal health and connectivity (85). Mutations in the genes encoding APP or the Presenilin protease enzymes that cleave APP to generate Amyloid-Beta cause early-onset AD, and support the notion that Amyloid-Beta metabolism is a central component of AD pathogenesis

(86). The generation of hyper-phosphorylated Tau is less clearly understood. It has been suggested that Amyloid-Beta is able to stimulate the kinase GSK3-B, resulting in the aberrant phosphorylation of Tau (87). The mechanisms governing the synthesis, processing, and degradation of these proteins remain incompletely understood. Inhibition of the proteasome causes an increase in Amyloid-Beta (88), and numerous studies have begun to describe an extensive role for both ubiquitination and the proteasome in the production and handling of APP, Amyloid-Beta, and Tau (Figure 3).

APP is produced in the endoplasmic reticulum (ER). HRD1, an E3 ligase associated with the clearance of newly synthesized proteins through ER-associated degradation (ERAD), has been shown to interact with APP. Decreasing HRD1 expression evokes ER stress and apoptosis, accompanied by the accumulation of APP and Amyloid Beta. The disease relevance of the HRD1/ APP relationship is supported by the reduced levels of HRD1 in AD brain tissue (89). Similarly, the levels of Fbxo2, a brain-enriched E3 ligase substrate adaptor protein also implicated in ERAD, have been reported to be decreased in AD patient tissues (90). Fbxo2 was also found to facilitate the degradation of APP, and a knockout mouse model for Fbxo2 revealed elevated levels of APP and Amyloid Beta in a brain region-specific manner (91). In the following chapter, I will describe the identification of APP as a substrate for Fbxo2, and the changes to APP levels and processing that follow the loss of Fbxo2.

In the Golgi apparatus, APP is ubiquitinated by unknown E3 ligases stimulated by ubiquilin-1, a protein with chaperone-like properties. This ubiquitination is K63-linked and does not cause the degradation of APP. Instead, it causes the retention of APP in the early secretory pathway, impairing its maturation and delaying its subsequent processing by secretases into Amyloid Beta (92). The process by which this ubiquitination of APP is normally removed to allow processing remains unclear. Ubiquilin-1 levels are significantly decreased in AD patient brain tissues, further suggesting a role in AD pathogenesis (92). Single-nucleotide polymorphisms (SNPs) in the UBQLN1 gene have recently been linked to late-onset AD (93).

After being produced and trafficked to the surface, APP is internalized via endocytosis into the trans-Golgi network and sequentially cleaved to produce Amyloid-Beta (85). The C-terminus of HSP70 Interacting Protein (CHIP) is an E3 ligase associated with polyglutamine neurodegenerative disorders (94,95), Williams 2009). In AD models, CHIP has been shown to interact with Amyloid-Beta in the Golgi, in a manner that increases upon inhibition of the proteasome. Over-expression of CHIP results in a decrease in Amyloid-Beta levels and may stabilize levels of APP (88).

Beyond targeting APP or Amyloid-Beta directly, the USS affects numerous other components of the Amyloid pathway, including the secretase enzymes responsible for the production of Amyloid Beta. FBXW7 (SEL-10) facilitates the

ubiquitination of the gamma-secretase component Presenilin 1 (PS1), although this ubiquitination unexpectedly increases Amyloid Beta production through mechanisms that remain unclear (96). Fbxo2, described above, has also been implicated in the turnover of the Beta-secretase protein BACE1 (90).

The effects of Amyloid-Beta on neurons is also influenced by the complex actions of the USS. For example, the intracellular response to Amyloid-Beta is thought to be mediated through numerous proteins including GSK3B, a kinase that is reportedly increased in AD and has Tau as one of its substrates. GSK3B has been investigated as a possible link between the two characteristic protein pathologies of AD (87). The kinase activity of GSK3B is enhanced by forming a complex with the tumor suppressor protein p53. Under normal conditions, this interaction is limited by the degradation of p53 by the E3 ligase Mouse double minute 2 homolog (MDM2). Under conditions of cellular stress, however, MDM2 levels are decreased, leading to the increased association of GSK3B and p53. This enhancement is thought to contribute to the hyperphosphorylation of Tau seen in AD (97). The observed decrease in MDM2 under conditions of stress actually stems from its own governance by the UPS. Under normal conditions, MDM2 is modified by the small, ubiquitin-like modifier protein SUMO. Sumoylation of MDM2 prevents its auto-ubiquitination. Under conditions of cellular stress, sumoylation of MDM2 is diminished, causing it to become auto-ubiquitinated which then triggers its own degradation by the proteasome (63). The level of GSK3B in neurons is also mediated by yet another E3-ligase, Nedd8

ultimate buster 1 (NUB1). NUB1 directly binds to GSK3B and promotes its degradation by the proteasome, while also inhibiting the interaction between GSK3B and Tau. NUB1 activity thereby diminishes the levels of hyper-phosphorylated Tau and Tau aggregates (98).

NUB1 was originally identified for its role in regulating Nedd8 (99,100). Nedd8 is a small signaling protein similar to ubiquitin both in structure (approximately 60% identity and 80% homology to human ubiquitin) and in function (99,101). The conjugation of Nedd 8, “neddylation,” to cullin proteins promotes the ubiquitination activity of SCF complexes (102). Nedd8 also modifies other proteins, including transmembrane proteins such as APP, and may influence their degradation (103). Dysregulated clearance of Neddylated proteins in disease states is evinced by the accumulation of Nedd8 in ubiquitin-positive tau filamentous inclusions in some cases of AD and in Lewy bodies in Parkinson’s Disease (104).

CHIP, described above for its role in the turnover of Amyloid-Beta, has also been shown to play a role in regulating phosphorylated Tau. Through its interaction with two heat-shock induced proteins, Hsp70 and Hsp90, CHIP is able to ubiquitinate phosphorylated Tau. Under normal conditions, this ubiquitination leads to an accumulation of ubiquitinated tau, which then becomes aggregated into high molecular-weight, detergent-insoluble aggregates. CHIP immunoreactivity decorates neurofibrillary tangles (NFTs) in several tauopathies,

including AD (105). However, over-expression of Hsp70 shifts the handling of ubiquitinated Tau toward a pathway of clearance through the UPS, rather than aggregation, and reduces Tau levels in vitro (105). Intriguingly, in vitro the ubiquitination of Tau also is carried out in an E3-ligase independent manner by the E2 Ube2w (32). Ube2w, whose levels are increased under cellular stress, also ubiquitinates CHIP and regulates its activity (64). Additionally, a role for CHIP in the ubiquitin-mediated turnover of caspases has been described. Mice which are homozygous null for Chip show increased levels of cleaved and uncleaved caspase-3 (106).

Although not considered causative themselves, additional proteins have been shown to exacerbate disease pathogenesis, and are similarly subject to regulation by ubiquitination. NMDA receptors are ionotropic glutamate receptors whose regulated conductance of calcium into postsynaptic sites has been linked to learning and memory. Aberrant activation and signaling of these receptors has been implicated in numerous disease processes, including AD (107). It has been suggested that the Amyloid-Beta-induced loss of synapses requires the activation of extra-synaptic NMDA receptors containing the GluN2B subunit (108,109), underscoring the importance of regulating NMDA receptor levels and localization in AD pathology. GluN2B is ubiquitinated in response to synaptic activity by the E3 ligase Mind Bomb-2 (110). Fbxo2, described above for its regulation of APP, also regulates the levels and localization of NMDA receptors in vitro and in vivo by facilitating the activity-dependent ubiquitination and elimination of NMDA

receptor subunits GluN1 and GluN2A (111). In the third chapter of this thesis, I will further examine the effects of Fbxo2 on synaptic content, localization, and transmission using an *Fbxo2* knockout mouse model.

The downstream effects of NMDA receptor activation are extensive. In one example, following NMDA receptor activation, the cyclin-dependent kinase 5 (Cdk5) phosphorylates Cdh1, a key regulator of the E3 ligase complex APC; in doing so, the turnover of its cyclin B1 by APC is inhibited, promoting neurotoxicity following NMDA receptor activation (112).

PARKINSON'S DISEASE

Parkinson's Disease (PD) is the second most common neurodegenerative disease and the most common neurodegenerative movement disorder. It is characterized by progressive abnormalities in gait and posture, as well as difficulty initiating and completing voluntary and involuntary movements. Histopathologically, PD involves the loss of dopaminergic neurons of the substantia nigra and locus ceruleus accompanied by astrocytosis and increased numbers of microglia. Throughout the brainstem of PD patients, proteinaceous intracellular aggregates called Lewy bodies can be found, comprised primarily of alpha-synuclein. With slightly altered appearance, these synuclein-containing aggregates can be seen in other brain regions, and the question of their contribution to disease pathogenesis remains an area of intense study (113). Although the majority of PD cases are of sporadic origin, the small fraction of

inherited cases has provided valuable insight into the role of the USS and UPS in PD pathology (Figure 4).

Mutations in alpha-synuclein have been described in cases of familial PD (114,115), and the proteasome is at least partially responsible for the turnover of this protein (116). Proteasome dysfunction is reported in the substantia nigra in PD, and proteasomal inhibition itself can cause the formation of protein inclusions and eventual degeneration of neurons in the substantia nigra in rats, although with some inconsistency (117-119). The expression of mutant alpha-synuclein induces the formation of filaments which interact directly with the 20S core of the proteasome and decrease its proteolytic activity (120). This deficit in proteasome function is ameliorated by the concomitant expression of the E3 ligase Parkin (121).

Of patients with inherited PD, nearly 40 percent of those with an early onset of symptoms have mutations in the gene encoding Parkin (122). First described in Japan, multiple mutations in Parkin have now been described in one or both alleles (123). While mutations in alpha-synuclein cause autosomal dominant PD, mutations in Parkin cause autosomal recessive PD. These mutations result in the loss of Parkin function, one aspect of which is to regulate the ubiquitination of alpha-synuclein. Because the accumulation of ubiquitinated alpha-synuclein is evident in both familial and sporadic PD, Parkin dysfunction may also play a role in idiopathic PD and the formation of Lewy bodies (124,125). Consistent with this

view, targeted expression of mutant Parkin in disease-related brain regions of animal models yields similar pathologies to those observed in PD (126).

Parkin is also involved in the intricate regulation of pro-survival signaling through the Akt pathway by Epidermal Growth Factor (EGF) (127). EGF-Akt signaling occurs through Epidermal Growth Factor Receptors (EGFR) which are decreased in disease-related brain regions of patients with PD (128). Accordingly, increased activation of EGFR in an animal model of PD prevents the loss of dopaminergic neurons (128). EGF signaling is regulated by ubiquitin in several ways. Ligand binding of the epidermal growth factor receptor (EGFR) stimulates Akt signaling, but triggers the endocytosis and degradation of EGFR, ostensibly as a means for limiting the extent of EGF signaling. This process is mediated by the activity-dependent ubiquitination of EGFR by an unknown E3 ligase, which makes it eligible for recognition by the ubiquitin-interacting motif (UIM) of the EGFR Protein tyrosine kinase Substrate #15, Eps15. Interaction with Eps15 is necessary for the internalization of EGFR, as Eps15 links ubiquitinated EGFRs to the machinery which traffics them to the proteasome for degradation (129). Parkin, which contains an amino-terminal ubiquitin-like (UBL) domain, blocks the Eps15-EGFR interaction by binding to the UIM of Eps15 through this UBL domain, and then facilitating the ubiquitination of Eps15. In this manner, EGFR internalization is prevented, and EGF signaling and activation of pro-survival pathways are enhanced. But interaction between Eps-15 and Parkin suggests yet a further level of ubiquitin-dependent regulation. Eps-15 promotes

its own ubiquitination by stimulating Parkin's E3 ligase activity upon interaction. This ubiquitination, which is believed to be K63-linked, prevents the interaction of ubiquitinated Eps15 with other ubiquitinated proteins such as EGFR and Parkin itself. Notably, Parkin deficiency causes a reduction in EGF signaling (127). Here, again, dysfunctional ubiquitin signaling, independent of proteasomal cleavage, is able to regulate the health of neurons in a disease context.

Parkin has been shown to function as part of a macromolecular E3 ligase complex which includes the pten-induced kinase (PINK1) and the peptidase Dj-1 (62). Mutations in both PINK1 and Dj-1 contribute to hereditary PD (130,131). Together, these proteins facilitate the degradation of Parkin substrates. Synphillin-1, which interacts with alpha-synuclein and is also present in Lewy bodies, is one such substrate, as is Parkin itself (62). Additionally, the interaction between PINK1 and Parkin facilitates the degradation and turnover of mitochondria (132,133). In order to do so, Parkin targets proteins in the outer mitochondrial membrane for degradation, inlcuding Tom20 (134). These findings suggest that Parkin dysfunction may contribute to global cellular health problems, even beyond the accumulation of alpha-synuclein and synphillin-1.

Rare mutations associated with familial, early-onset PD are also found in the de-ubiquitinating enzyme UCH-L1 (135). These mutations reduce the DUB activity of UCHL1. UCH-L1's role is significant for the health and function of neurons through its regulation of substrates involved in governing mRNA transcription,

protein translation, synaptic plasticity, and pro-survival signaling. These processes are potently influenced by the activity of a serine/threonine protein kinase originally identified for its susceptibility to inhibition by Rapamycin, the Mammalian Target of Rapamycin, mTOR (136-139). Intriguingly, mTOR function requires both the correct ubiquitination of interacting proteins and proteasome activity (139,140). mTOR asserts its effects through the formation of large protein complexes. mTOR can function in combination with Raptor (mTOR Complex 1 or mTORC1) or Rictor (mTORC2). mTOR1 regulates transcription and is important for local protein synthesis, a necessary component of several types of synaptic plasticity. mTORC2, on the other hand, influences Akt signaling, cytoskeletal dynamics, and actin polymerization (141). The balance between mTORC1 and mTORC2 formation depends on the interaction of Raptor with a multi-subunit E3 ligase composed of DNA Damage-Binding Protein (DDB1), Cullin 4A (CUL4), and the RING-type E3 ligase RING box 1 (RBX1) (139). Although the exact mechanism is still unclear, the DDB1-CUL4 complex appears to ubiquitinate Raptor in a manner that facilitates its incorporation into the mTORC1 complex including DDB1, CUL4, Raptor, and mTOR (139). UCHL1 deubiquitinates Raptor, thereby destabilizing mTORC1 complex formation and shifting the balance toward mTORC2-dependent signaling (142). This shift may have a significant impact on the ability of neurons to modify their synaptic content to promote learning and memory, and may also represent a neuroprotective response mechanism.

The loss of UCHL1's DUB activity result in an accumulation of alpha-synuclein at presynaptic terminals rather than increased clearance (143). Surprisingly, UCH-L1 had been proposed to act as an E3 ligase when it self-dimerizes; this new activity is independent of the state of UCHL1's DUB activity (144). Acting as an E3 ligase, UCHL1 causes the K63-linked ubiquitination of alpha-synuclein, which, in turn, worsens PD pathology (144). Accordingly, a mutant form of UCH-L1 with decreased E3 ligase activity upon dimerization, but normal DUB activity, decreases PD pathogenesis (144). The intended role of UCHL1's ubiquitination of alpha-synuclein remains unclear.

There have been several ubiquitin-linked proteins whose involvement in neurotoxicity overlaps between AD and PD. Of those described above, CHIP, MDM2, and HRD1 support the importance of the UPS in pathological mechanisms in multiple disease states. CHIP also interacts with Parkin and stimulates its ligase activity (145). Down-regulation of MDM2 is toxic to dopaminergic neurons even without a toxic insult (146). And HRD1 levels are increased in dopaminergic neurons under conditions of neurotoxicity, suggesting a role in the response to cellular stress (147).

AMYOTROPHIC LATERAL SCLEROSIS

Amyotrophic Lateral Sclerosis (ALS) is the most common fatal neurodegenerative disease affecting motor neurons. The loss of motor neurons in the brain and spinal cord of ALS patients typically results in progressive

paralysis and death within a few years of onset. Non-motor pathologies, particularly cognitive deficits, can also accompany motor deficits. Histopathologically, ubiquitin-rich cytoplasmic inclusions appear in the remaining motor neurons of ALS patients, accompanied by marked gliosis. Ubiquitin-positive inclusions can also be observed in cortical brain regions, consistent with the observed cognitive decline in many ALS patients (148,149). Sporadic ALS (SALS) represents greater than 90 percent of all ALS cases, with familial ALS (FALS) accounting for the remaining <10 percent. The etiology of ALS remains unclear, and what is known to date has been determined largely through the study of genes originally identified as mutated in FALS. Importantly, the disease genes that cause FALS are also found mutated in some SALS cases, and the histopathologies of familial and sporadic cases are essentially indistinguishable (150), suggesting that studies of FALS will offer useful insight into all forms of ALS. Among the disease genes associated with FALS, mutations in the gene encoding Superoxide Dismutase 1 (SOD1) were described first (151), and mutations in the Transactivation Response DNA-binding protein 43 (TDP-43) are probably the most common (152). These two proteins accumulate in ubiquitin-positive inclusions in disease-related neuronal populations, and the mechanisms of their turnover and clearance provide insight into the importance of the UPS in ALS (Figure 5).

SOD1 plays an important role in the elimination of free superoxide radicals. Its expression is regulated by several agents of the UPS. The canonical HECT-type

E3 ligase E6-AP directly binds to and ubiquitinates SOD1 (153). Levels of E6-AP are decreased prior to the onset of neurodegeneration in a mouse model of ALS expressing mutant SOD1, and over-expression of E6-AP reduces the aggregation of mutant SOD1 in vitro (153). NEDL1, a homologue of E6-AP, is reported to selectively bind to mutant SOD1 but not wild-type SOD1, facilitating its ubiquitination and clearance (154). NEDL1 is thought to function in concert with the endoplasmic reticulum translocon-associated protein TRAP-δ, suggesting a role for NEDL1in the ERAD of mutant SOD1 (155). The interaction between NEDL1 and mutant SOD1 increases with disease severity, and NEDL1 immunoreactivity is observed in SOD1-positive inclusions in human spinal cord tissue from FALS patients (154). Also reportedly present in SOD1-positive inclusions is the RING-finger type E3 ligase Dorfin, which shares NEDL1's selectivity in ubiquitinating mutant, but not wild-type, SOD1 (156). Over-Expression of Dorfin in a mouse model of FALS reduces expression and aggregation of SOD1 while also diminishing motor neuron degeneration (157).

TDP-43, the major component of most aggregates in ALS cases, is normally a predominantly nuclear protein. It has two RNA binding domains and has been implicated in RNA splicing and trafficking (158,159). Ubiquitinated TDP-43 is a major component of cytoplasmic inclusions in ALS (160). Mutations associated with ALS result in the redistribution of TDP-43 from the nucleus to the cytoplasm (161), although the precise mechanisms by which TDP-43 contributes to ALS pathogenesis remain the subject of intensive study (162). TDP-43 expression

inhibits proteasome function and increases levels of Parkin mRNA and protein (163) by binding to Parkin mRNA (164). Parkin, in turn, is able to mediate both K48 and K63-linked ubiquitination of TDP-43, though this modification does not cause a reduction in the levels of TDP-43 (163). TDP-43 is unlike other substrates of Parkin-dependent K63-linked ubiquitination, which are targeted for degradation through the autophagic pathway (165). The interaction between TDP-43 and Parkin requires the histone deacetylase protein HDAC6 and promotes the translocation of TDP-43 from the nucleus to the cytoplasm (163).

HUNTINGTON'S DISEASE

Huntington's disease (HD) is the most common of the polyglutamine (polyQ) disorders. While polyglutamine repeats are common motifs facilitating protein-protein interactions, expansion of these repeats is associated with at least nine different neurodegenerative disorders (166,167). The threshold length at which this expansion begins to elicit adverse effects varies among these diseases, determined in part by the specific protein context neighboring the repeat in the expanded protein (168). Expansion of the CAG repeat in exon 1 of the gene coding for the Huntingtin protein increases the length of the polyglutamine domain (169,170). The repeat length threshold for disease in HD is 38 or more repeats (171), with longer repeats causing earlier onset and more severe disease. Symptoms of HD include progressive cognitive impairment, mood disorder and other psychiatric symptoms, and highly disordered movement and motor control including abnormal movements such as chorea. These

progressive symptoms lead to mortality within 20 years of onset (172). Histopathologically, HD is characterized by the degeneration of striatal and cortical neurons and the presence of intraneuronal, intranuclear aggregates and dystrophic neurites. Both of these latter features are marked by the presence of ubiquitinated Huntingtin. These aggregates can be found in cortical and striatal neurons, with some variance in cortical localization related to the age of onset (173).

The normal function of Huntingtin remains unknown. Structural analyses and numerous other studies have led scientists to propose several functions including intracellular protein trafficking, modulation of gene transcription, and regulation of scaffolding proteins and NMDA receptors at the synapse (174,175). NMDA receptors are improperly localized to extra-synaptic sites in HD, and their signaling at those sites contributes to the onset of symptoms in HD animal models (176,177). This mislocalization decreases synaptic NMDA receptor activation, which has been shown to promote Huntingtin aggregation and neuronal survival (178). Whether HD arises exclusively from a toxic gain of function for mutant Huntingtin or from an additional partial loss of normal Huntingtin function remains unclear. In either case, ubiquitin plays a significant role in the handling of normal and mutant Huntingtin protein (Figure 6).

The presence of ubiquitinated Huntingtin suggests a failure of the UPS. Huntingtin is ubiquitinated (179), but it has been proposed that the proteasome

may be unable to process expanded polyglutamine stretches, resulting instead in the accumulation of peptide fragments containing polylgutamine (180). The fate of these peptide fragments is unclear, but they may remain associated with the proteasome and inhibit its function (181,182). Intriguingly, components of the UPS, including proteasomes, have been identified within Huntingtin aggregates (183). This may represent deleterious proteasomal sequestration in aggregates, even though aggregation of mutant Huntingtin may itself be neuroprotective (178,181). The idea that Huntingtin-induced pathology includes a deficiency in UPS-mediated clearance is supported by the beneficial effects observed following efforts to increase proteasomal activity in models of HD (184). The upregulation of UPS agents through the action of histone deacetylase inhibitors may also improve the aggregation phenotype of HD model mice (185).

The precise mechanisms by which Huntingtin is ubiquitinated are not well understood. It is unclear whether, like TDP-43, ubiquitination of Huntingtin includes both K48 and K63 linkages. Most studies investigating this question have used models over-expressing a fragment of Huntingtin with a polyQ expansion. While such over-expression models induce aggregation and toxicity, their physiological relevance to the human disease state remains an area of some debate. That said, in these model systems several components of the UPS contribute to the clearance of mutant Huntingtin. HRD1, described above for its role in several diseases, is implicated in the clearance of mutant Huntingtin. The activity of HRD1 increases with Huntingtin polyQ expansion length, suggesting

that HRD1 regulation may not typically handle normal, unexpanded Huntingtin (186). The Tumor Necrosis Receptor Associated Factor 6 (TRAF6) is an E3-ligase which binds to both unexpanded and mutant Huntingtin and facilitates non-canonical ubiquitination through K6, K27, and K29-linked chains (187). The physiological role of this modification is unclear, but it promotes the aggregation of mutant Huntingtin without changing the localization of the wild-type protein. Additionally, NUB1, described above for its role in AD, works in conjunction with Cullin 3 to facilitate the ubiquitination and clearance of mutant Huntingtin (188).

Sumoylation also can regulate HD pathogenesis. Rhes, a striatal protein which acts as a SUMO E3 ligase, binds to mutant Huntingtin selectively and facilitates its sumoylation (189). The sumoylation of mutant Huntingtin promotes disaggregation; however, disaggregated, sumoylated, mutant Huntingtin inhibits transcription, increases cytotoxicity through Caspase-3, and may impair the induction of autophagy (190-192).

Huntingtin is also reported to interact with the E2 enzyme hE2-25k (Ube2K) (179). The presence of Ube2k immunoreactivity in HD patient brains has been observed, and the Huntingtin-Ube2k interaction promotes aggregation and cytotoxicity in a manner that requires E2 catalytic function (193). Ube2k has been shown to interact with numerous RING-finger E3 ligases (194). It is possible that Ube25k cleaves the polyubiquitin chains attached to Huntingtin to an extent that degradation is no longer signaled.

CONCLUSIONS: TOO BIG NOT TO FAIL

Befitting its extensive contributions to a wide range of cellular processes, the systems of protein ubiquitination and ubiquitin-dependent clearance are implicated at many levels of the most common neurodegenerative disorders. Is this implied involvement in disease incidental, or does dysregulated ubiquitination and clearance represent an inevitable and common pathway for the worsening of all neurodegenerative diseases? Because alterations in ubiquitin-dependent gene transcription, translation, control of protein quality and maturation, trafficking, mitochondrial turnover, and the handling of protein-protein interactions are found in combination in neurodegenerative disease, it seems likely that dysregulated ubiquitination will not remain limited to a single ubiquitin-dependent process in a given disease. Instead, the UPS and USS will be widely involved. To what degree this involvement might begin the pathogenic cascade is currently unclear. But based on the studies reviewed here, it seems more likely that through a complex web of dysfunction in the UPS and USS, involvement of these systems causes the pathogenicity of aberrant proteins to diversify and flourish, affecting additional systems and promoting the loss of synapses and cell death.

The UPS is not alone in its handling of unwanted or toxic proteins. The autophagic system is the other major pathway by which protein clearance is achieved. Autophagy especially regulates the turnover of organelles and aggregated protein species, and accordingly its role in neurodegenerative

disease has been extensively pursued. Upon failure of the proteasome, autophagic mechanisms can be induced as a compensatory response to UPS inhibition in numerous neurodegenerative diseases (195-197). Further activation of autophagic mechanisms through pharmacologic or genetic manipulation has proven useful as a therapeutic intervention in model systems (198). It seems evident, however, from the continued accumulation of ubiquitin-positive proteins in neurodegeneration, that autophagic induction is not sufficient to overcome this failure. Moreover, it is unclear what effect sustained, heightened autophagy might have on already weakened neurons.

The overlapping involvement of certain E3 ligases like HRD1, NUB1, and CHIP not only speaks to their significance as key regulators of proteostasis but also nominates them as important targets for research. While knocking out CHIP has been shown to exacerbate polyglutamine pathology (95), CHIP over-expression can reduce proteotoxicity and the effects of cellular stress in numerous models ((94,199,200). But CHIP induction without concurrent upregulation of Hsp70 might worsen tau pathology, suggesting that combinatorial approaches to therapy will be required.

In considering the specific goals and appropriate timing for interventions intended to prevent or delay disease onset, it is important to acknowledge that the loss of synapses precedes neurodegeneration and is thought to underlie many of the earliest cognitive impairments in numerous diseases. As such, it may represent

a key step in the disease cascade and a critically important target for therapies. Alternatively, synaptic connections may simply be too costly for unhealthy neurons to properly maintain, and the loss of synaptic connections is, in effect, a response intended to limit inappropriate and potentially dangerous synaptic signaling in disease states. In the latter case, this dauer-like state is ultimately ineffective in staving off neurodegeneration, but may slow the process. With respect to human disease, perhaps restoring synapses could improve quality of life - regardless of whether such a change ultimately lengthens or shortens the life-span of affected neurons. For this reason, elucidation of the processes by which ubiquitin governs synapse formation, maintenance, and removal under normal conditions may prove invaluable.

FIGURE LEGENDS

Figure 1. The Process of Ubiquitin Conjugation

1. Ubiquitin (U) is bound via a thioester bond to the active-site cysteine of an E1 Ubiquitin-Activating enzyme, through a process requiring ATP. 2. The ubiquitin molecule is then passed to an E2 Ubiquitin-Conjugating Enzyme through trans (thio)esterification. 3. An E3 ubiquitin ligase brings the E2 into sufficiently close proximity and correct alignment with a substrate protein to facilitate the transfer of ubiquitin to a target residue. In the case of HECT-type E3s, the ubiquitin is first transferred to an active site cysteine on the E3 before being conjugated to the substrate. E3s can also exist as multi-subunit complexes including scaffolding and adaptor proteins that confer substrate specificity to the process of

ubiquitin transfer. 4. Additional ubiquitin molecules can be added onto the first to create polyubiquitin chains on substrate proteins.

Figure 2. The Ubiquitin Proteasome System

The 26S proteasome is composed of a cylindrical, proteolytic 20S core which is capped at both ends by a 19S regulatory cap. Polyubiquitinated substrate proteins, typically bearing K48-linked chains, are targeted to the proteasome by trafficking proteins. The proteasome digests these substrates into smaller peptides and free ubiquitin molecules, which then can be used to modify further substrates.

Figure 3. Regulation of Protein Trafficking, Receptor Signaling, and Protein Clearance by Ubiquitination

Improper processing of APP and Tau contribute to the pathology of AD. Excessive or improperly folded APP is cleared from the ER by HDR1 and Fbxo2 through the addition of K-48 linked chains. Ubiquitin-mediated processes are indicated by dashed lines. Maturation of APP is arrested in the early secretory pathway by non-degradative, K-63 linked ubiquitination that is stimulated by Ubiquilin 1. Surface APP is endocytosed to the late Golgi, where it is cleaved by secretases including BACE-1 and PS-1, whose levels are regulated by the E3 ligases Fbxo2 and FBXW-7, respectively. The cleavage of APP results in the production of Amyloid-Beta, which can be targeted for degradation by CHIP. Uncleared Amyloid-Beta is exocytosed to the extracellular space, where it

aggregates to form plaques. Amyloid-Beta can influence NMDA receptor signaling. NMDA receptor activation stimulates the kinase Cdk5, which results in the downstream inhibition of the E3 ligase APC and blocks the degradation of cyclin B1. NMDA receptor signaling also increases the activation of GSK3B, which phosphorylates Tau. GSK3B is targeted for degradation by NUB1, which also blocks the interaction between GSK3B and Tau. GSK3B activity is increased by complexing with p53, whose levels are regulated by the E3 ligase MDM2. Under conditions of cellular stress, MDM2 auto-ubiquitinates and targets itself for degradation. The E3 ligase CHIP targets Tau, but can have divergent effects on its handling. When working in combination with Hsp70, CHIP targets Tau for degradation. However, when Hsp90 is involved, CHIP facilitates an alternative ubiquitination of unknown linkage type, resulting in the accumulation of phosphorylated tau. Through an unknown mechanism, this accumulated Tau then forms insoluble protein aggregates.

Figure 4. Ubiquitination in Pro-survival Pathways, Mitochondria Stability, and Protein Clearance in Parkinson's Disease

Dysregulation of Parkin and UCHL1, both of which are associated with PD, has widespread effects on neuronal health. The Epidermal Growth Factor (EGF) binds to EGFR and initiates pro-survival signaling through the Akt and mTOR pathways. Ligand-binding to EGFR stimulates its ubiquitination, which allows for its UIM-dependent recognition by Eps15. Eps15 internalizes EGFR, allowing it to be trafficked to the proteasome for degradation. The EGFR-Eps15 interaction is

blocked by the interaction of the UBL of the E3 ligase Parkin with the UIM of Eps15; this interaction increases Parkin's ligase activity, causing Eps15 to become ubiquitinated and dissociated from its UIM-dependent interactors. Downstream of EGFR signaling, mTOR's participation in the protein complex mTORC1 requires the ubiquitination of Raptor by DDB1 and Cul4. This ubiquitination is undone by the de-ubiquitinating enzyme UCHL1. Parkin also plays a role in the degradation of mitochondrial outer membrane proteins including Tom20, and through its involvement with PINK1 and Dj-1, facilitates the degradation of Synphilin-1 and itself. Synphilin interacts with alpha-synuclein, which can be degraded by Parkin in association with CHIP. Dimerized UCHL1 may also modify alpha-synuclein, though the result is non-degradative, K-63 linked ubiquitination which promotes its accumulation. Accumulated alpha-synuclein binds to the 20S core of the proteasome and inhibits proteasome function.

Figure 5. A Role for Ubiquitination in the Pathogenesis of Amyotrophic Lateral Sclerosis

Impaired turnover of SOD1 and TPD-43 are implicated in the etiology of ALS. Mutated or excess SOD1 in the ER is targeted for degradation by the E3 ligase NEDL1 via the translocon protein TRAP. SOD1 in the cytosol is targeted by the canonical HECT-type E3 ligase, E6-AP, and the RING-type E3 Dorfin. TDP-43 can be ubiquitinated by Parkin in association with HDAC6. This modification can include both K48 and K63-linked chains and does not lead to the degradation of

TDP-43, instead increasing the proportion of TDP-43 in the cytosol. In the nucleus, TDP-43 regulates the transcription of genes including Parkin. In the cytosol, accumulated TDP-43 can inhibit the proteasome and form protein aggregates.

Figure 6. Ubiquitin-mediated Handling of the Pathologic Huntingtin Protein in Huntington's Disease

The Huntingtin protein is improperly cleared from neurons in HD. Mutant Huntingtin can be targeted for degradation in the ER by HRD1, and in the cytosol by NUB1. However, this ubiquitination can be edited by UCHL1, inhibiting the degradation of Huntingtin and promoting its aggregation in the cytosol. Traf6 facilitates the non-canonical ubiquitination of Huntingtin through the formation of K6, K27, and K29-linked polyubiquitin chains, and these modifications selectively promote the aggregation of mutant Huntingtin. Aggregates of mutant Huntingtin include components of the UPS including proteasomes. Rhes promotes the sumoylation of Huntingtin, which promotes its disaggregation but then causes mutant Huntingtin to interfere with other cellular processes including gene transcription in the nucleus.

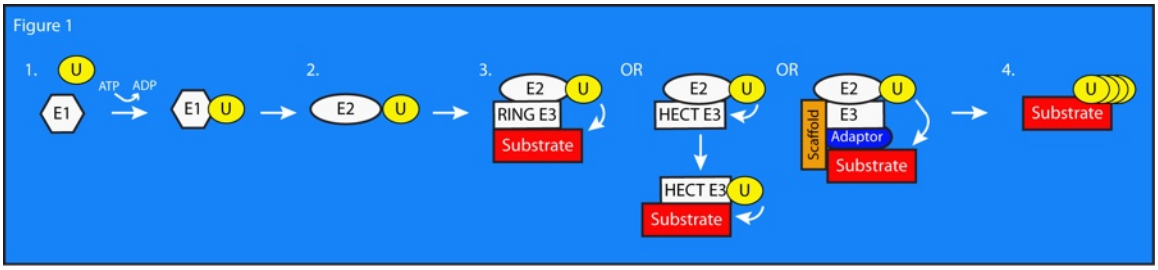

Figure 1. The Process of Ubiquitin Conjugation

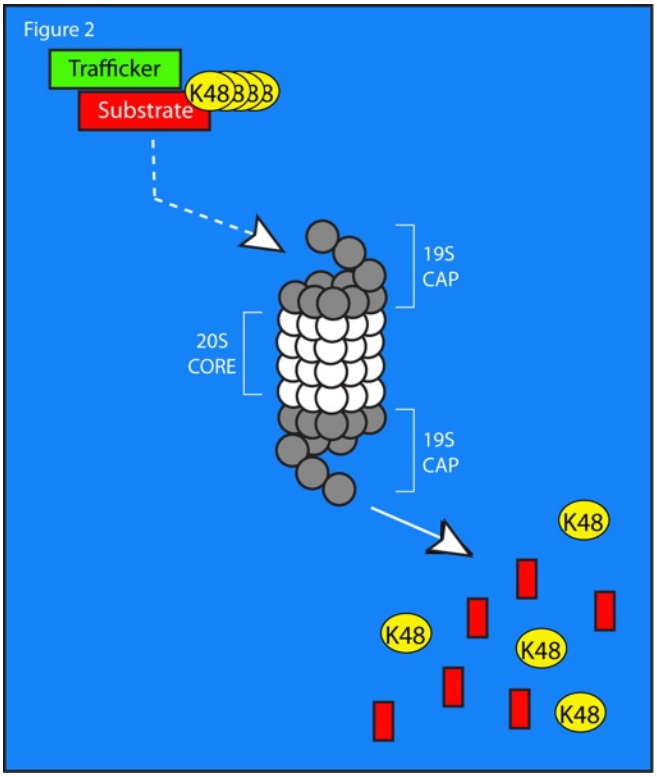

Figure 2. The Ubiquitin Proteasome System

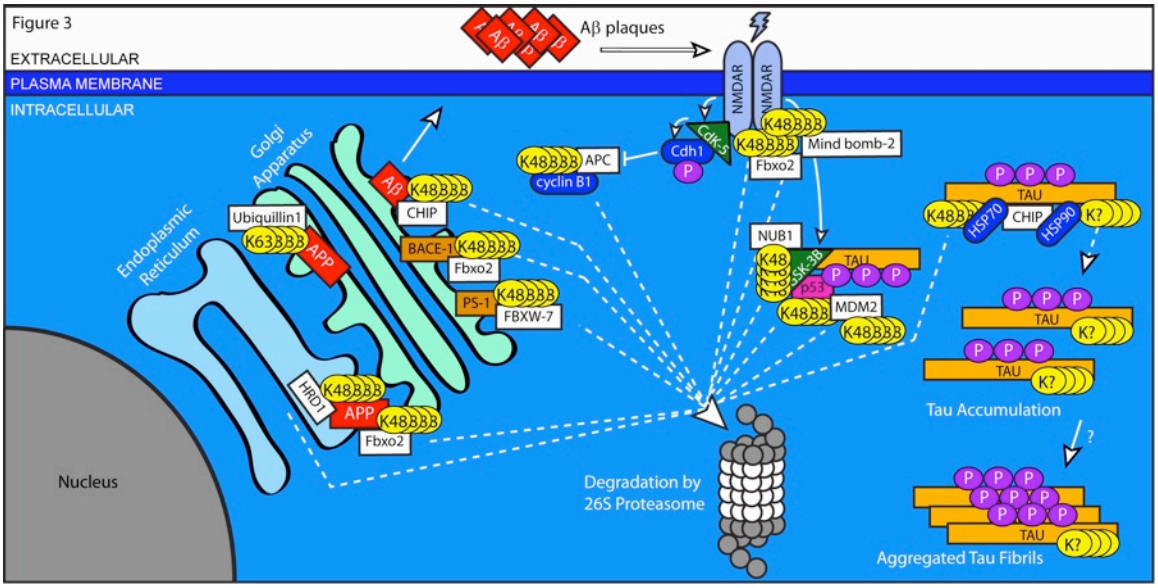

Figure 3. Regulation of Protein Trafficking, Receptor Signaling, and Protein Clearance by Ubiquitination

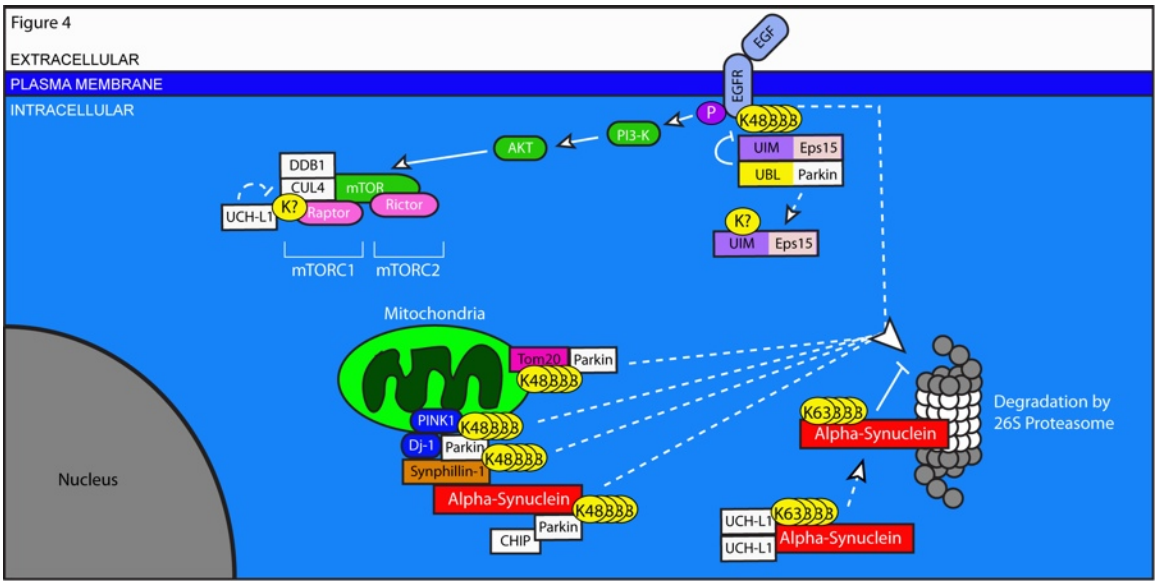

Figure 4. Ubiquitination in Pro-survival Pathways, Mitochondria Stability, and Protein Clearance in Parkinson's Disease

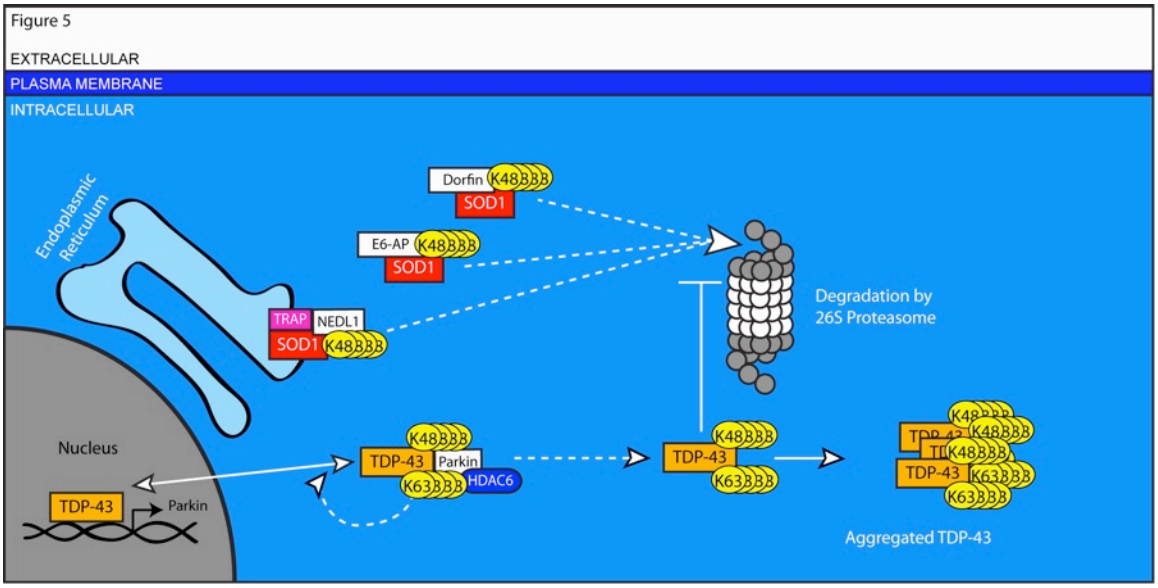

Figure 5. A Role for Ubiquitination in the Pathogenesis of Amyotrophic Lateral Sclerosis

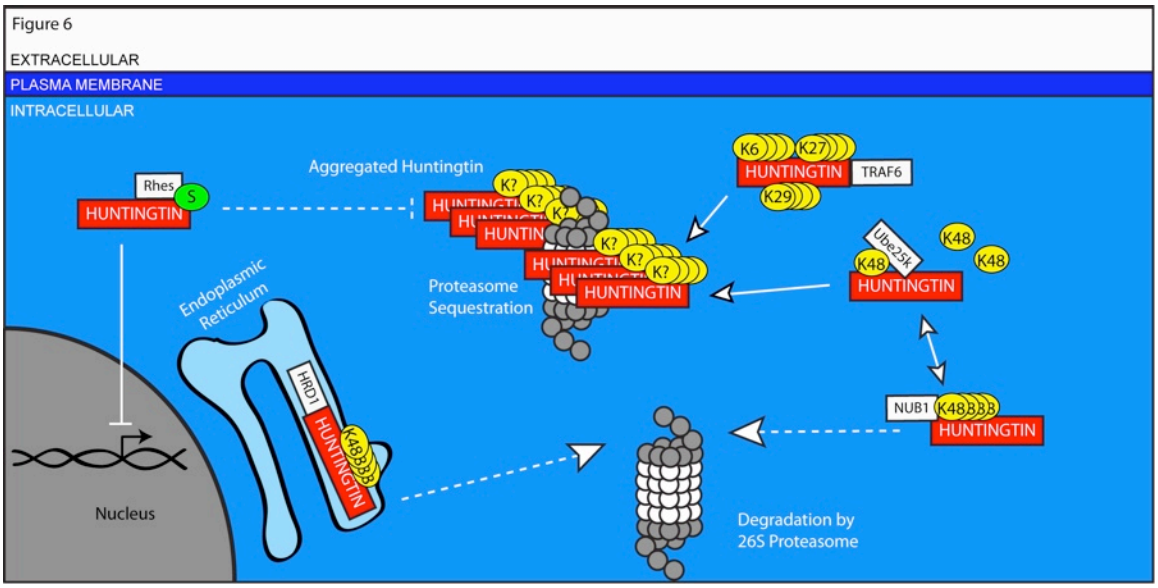

Figure 6. Ubiquitin-mediated Handling of the Pathologic Huntingtin Protein in Huntington's Disease

Bibliography

1. Golgi, C. (1886) *Sulla fina anatomia degli organi centrali del sistema nervoso*, U. Hoepli, Milane,
2. Ramon y Cajal, S. (1909) *Histologie du systeme nerveux de l'homme & des vertebres*, A. Maloine, Paris
3. Herculano-Houzel, S. (2011) Scaling of brain metabolism with a fixed energy budget per neuron: implications for neuronal activity, plasticity and evolution. *PLoS One* **6**, e17514
4. Azevedo, F. A., Carvalho, L. R., Grinberg, L. T., Farfel, J. M., Ferretti, R. E., Leite, R. E., Jacob Filho, W., Lent, R., and Herculano-Houzel, S. (2009) Equal numbers of neuronal and nonneuronal cells make the human brain an isometrically scaled-up primate brain. *J Comp Neurol* **513**, 532-541
5. Lee, M. C., Yasuda, R., and Ehlers, M. D. (2010) Metaplasticity at single glutamatergic synapses. *Neuron* **66**, 859-870
6. Masliah, E., Hansen, L., Albright, T., Mallory, M., and Terry, R. D. (1991) Immunoelectron microscopic study of synaptic pathology in Alzheimer's disease. *Acta Neuropathol* **81**, 428-433
7. Masliah, E., Terry, R. D., Alford, M., DeTeresa, R., and Hansen, L. A. (1991) Cortical and subcortical patterns of synaptophysinlike immunoreactivity in Alzheimer's disease. *Am J Pathol* **138**, 235-246
8. Pielot, R., Smalla, K. H., Muller, A., Landgraf, P., Lehmann, A. C., Eisenschmidt, E., Haus, U. U., Weismantel, R., Gundelfinger, E. D., and Dieterich, D. C. (2012) SynProt: A Database for Proteins of Detergent-Resistant Synaptic Protein Preparations. *Front Synaptic Neurosci* **4**, 1
9. Bingol, B., and Schuman, E. M. (2006) Activity-dependent dynamics and sequestration of proteasomes in dendritic spines. *Nature* **441**, 1144-1148
10. Bingol, B., Wang, C. F., Arnott, D., Cheng, D., Peng, J., and Sheng, M. (2010) Autophosphorylated CaMKIIalpha acts as a scaffold to recruit proteasomes to dendritic spines. *Cell* **140**, 567-578
11. Hegde, A. N., Inokuchi, K., Pei, W., Casadio, A., Ghirardi, M., Chain, D. G., Martin, K. C., Kandel, E. R., and Schwartz, J. H. (1997) Ubiquitin C-terminal hydrolase is an immediate-early gene essential for long-term facilitation in Aplysia. *Cell* **89**, 115-126
12. Ehlers, M. D. (2003) Activity level controls postsynaptic composition and signaling via the ubiquitin-proteasome system. *Nat Neurosci* **6**, 231-242
13. Pak, D. T., and Sheng, M. (2003) Targeted protein degradation and synapse remodeling by an inducible protein kinase. *Science* **302**, 1368-1373
14. Patrick, G. N., Bingol, B., Weld, H. A., and Schuman, E. M. (2003) Ubiquitin-mediated proteasome activity is required for agonist-induced endocytosis of GluRs. *Curr Biol* **13**, 2073-2081
15. Bingol, B., and Schuman, E. M. (2004) A proteasome-sensitive connection between PSD-95 and GluR1 endocytosis. *Neuropharmacology* **47**, 755-763

16. Fu, A. K., Hung, K. W., Fu, W. Y., Shen, C., Chen, Y., Xia, J., Lai, K. O., and Ip, N. Y. (2011) APC(Cdh1) mediates EphA4-dependent downregulation of AMPA receptors in homeostatic plasticity. *Nat Neurosci* **14**, 181-189
17. Hung, A. Y., Sung, C. C., Brito, I. L., and Sheng, M. (2010) Degradation of postsynaptic scaffold GKAP and regulation of dendritic spine morphology by the TRIM3 ubiquitin ligase in rat hippocampal neurons. *PLoS One* **5**, e9842
18. Bajic, N., Jenner, P., Ballard, C. G., and Francis, P. T. (2012) Proteasome inhibition leads to early loss of synaptic proteins in neuronal culture. *J Neural Transm* **119**, 1467-1476
19. Bernassola, F., Ciechanover, A., and Melino, G. (2010) The ubiquitin proteasome system and its involvement in cell death pathways. *Cell Death Differ* **17**, 1-3
20. Shang, F., and Taylor, A. (2011) Ubiquitin-proteasome pathway and cellular responses to oxidative stress. *Free Radic Biol Med* **51**, 5-16
21. Alves-Rodrigues, A., Gregori, L., and Figueiredo-Pereira, M. E. (1998) Ubiquitin, cellular inclusions and their role in neurodegeneration. *Trends Neurosci* **21**, 516-520
22. Huang, Q., and Figueiredo-Pereira, M. E. (2010) Ubiquitin/proteasome pathway impairment in neurodegeneration: therapeutic implications. *Apoptosis* **15**, 1292-1311
23. Ross, C. A., and Poirier, M. A. (2005) Opinion: What is the role of protein aggregation in neurodegeneration? *Nat Rev Mol Cell Biol* **6**, 891-898
24. Keller, J. N., Hanni, K. B., and Markesbery, W. R. (2000) Impaired proteasome function in Alzheimer's disease. *J Neurochem* **75**, 436-439
25. Lonskaya, I., Desforges, N. M., Hebron, M. L., and Moussa, C. E. (2013) Ubiquitination Increases Parkin Activity to Promote Autophagic alpha-Synuclein Clearance. *PLoS One* **8**, e83914
26. McNaught, K. S., Belizaire, R., Isacson, O., Jenner, P., and Olanow, C. W. (2003) Altered proteasomal function in sporadic Parkinson's disease. *Exp Neurol* **179**, 38-46
27. Seo, H., Sonntag, K. C., and Isacson, O. (2004) Generalized brain and skin proteasome inhibition in Huntington's disease. *Ann Neurol* **56**, 319-328
28. Bence, N. F., Sampat, R. M., and Kopito, R. R. (2001) Impairment of the ubiquitin-proteasome system by protein aggregation. *Science* **292**, 1552-1555
29. Hegde, A. N., Broome, B. M., Qiang, M., and Schwartz, J. H. (2000) Structure and expression of the Aplysia polyubiquitin gene. *Brain Res Mol Brain Res* **76**, 424-428
30. Finley, D., and Chau, V. (1991) Ubiquitination. *Annu Rev Cell Biol* **7**, 25-69
31. Hershko, A., and Ciechanover, A. (1998) The ubiquitin system. *Annu Rev Biochem* **67**, 425-479
32. Scaglione, K. M., Basrur, V., Ashraf, N. S., Konen, J. R., Elenitoba-Johnson, K. S., Todi, S. V., and Paulson, H. L. (2013) The ubiquitin-

conjugating enzyme (E2) Ube2w ubiquitinates the N terminus of substrates. *J Biol Chem* **288**, 18784-18788
33. Lorick, K. L., Jensen, J. P., Fang, S., Ong, A. M., Hatakeyama, S., and Weissman, A. M. (1999) RING fingers mediate ubiquitin-conjugating enzyme (E2)-dependent ubiquitination. *Proc Natl Acad Sci U S A* **96**, 11364-11369
34. Huibregtse, J. M., Scheffner, M., Beaudenon, S., and Howley, P. M. (1995) A family of proteins structurally and functionally related to the E6-AP ubiquitin-protein ligase. *Proc Natl Acad Sci U S A* **92**, 2563-2567
35. Cardozo, T., and Pagano, M. (2004) The SCF ubiquitin ligase: insights into a molecular machine. *Nat Rev Mol Cell Biol* **5**, 739-751
36. Hao, B., Zheng, N., Schulman, B. A., Wu, G., Miller, J. J., Pagano, M., and Pavletich, N. P. (2005) Structural basis of the Cks1-dependent recognition of p27(Kip1) by the SCF(Skp2) ubiquitin ligase. *Mol Cell* **20**, 9-19
37. Biggs, J. R., Peterson, L. F., Zhang, Y., Kraft, A. S., and Zhang, D. E. (2006) AML1/RUNX1 phosphorylation by cyclin-dependent kinases regulates the degradation of AML1/RUNX1 by the anaphase-promoting complex. *Mol Cell Biol* **26**, 7420-7429
38. Pines, J. (2006) Mitosis: a matter of getting rid of the right protein at the right time. *Trends Cell Biol* **16**, 55-63
39. Ardley, H. C., and Robinson, P. A. (2005) E3 ubiquitin ligases. *Essays Biochem* **41**, 15-30
40. Skaar, J. R., Pagan, J. K., and Pagano, M. (2009) SnapShot: F box proteins I. *Cell* **137**, 1160-1160 e1161
41. Peng, J., Schwartz, D., Elias, J. E., Thoreen, C. C., Cheng, D., Marsischky, G., Roelofs, J., Finley, D., and Gygi, S. P. (2003) A proteomics approach to understanding protein ubiquitination. *Nat Biotechnol* **21**, 921-926
42. Xu, P., Duong, D. M., Seyfried, N. T., Cheng, D., Xie, Y., Robert, J., Rush, J., Hochstrasser, M., Finley, D., and Peng, J. (2009) Quantitative proteomics reveals the function of unconventional ubiquitin chains in proteasomal degradation. *Cell* **137**, 133-145
43. Glickman, M. H., and Ciechanover, A. (2002) The ubiquitin-proteasome proteolytic pathway: destruction for the sake of construction. *Physiol Rev* **82**, 373-428
44. Jacobson, A. D., Zhang, N. Y., Xu, P., Han, K. J., Noone, S., Peng, J., and Liu, C. W. (2009) The lysine 48 and lysine 63 ubiquitin conjugates are processed differently by the 26 s proteasome. *J Biol Chem* **284**, 35485-35494
45. Hadian, K., Griesbach, R. A., Dornauer, S., Wanger, T. M., Nagel, D., Metlitzky, M., Beisker, W., Schmidt-Supprian, M., and Krappmann, D. (2011) NF-kappaB essential modulator (NEMO) interaction with linear and lys-63 ubiquitin chains contributes to NF-kappaB activation. *J Biol Chem* **286**, 26107-26117

46. Zhang, L., Xu, M., Scotti, E., Chen, Z. J., and Tontonoz, P. (2013) Both K63 and K48 ubiquitin linkages signal lysosomal degradation of the LDL receptor. *J Lipid Res* **54**, 1410-1420
47. Huang, F., Zeng, X., Kim, W., Balasubramani, M., Fortian, A., Gygi, S. P., Yates, N. A., and Sorkin, A. (2013) Lysine 63-linked polyubiquitination is required for EGF receptor degradation. *Proc Natl Acad Sci U S A* **110**, 15722-15727
48. Bertrand, M. J., Lippens, S., Staes, A., Gilbert, B., Roelandt, R., De Medts, J., Gevaert, K., Declercq, W., and Vandenabeele, P. (2011) cIAP1/2 are direct E3 ligases conjugating diverse types of ubiquitin chains to receptor interacting proteins kinases 1 to 4 (RIP1-4). *PLoS One* **6**, e22356
49. Ben-Neriah, Y. (2002) Regulatory functions of ubiquitination in the immune system. *Nat Immunol* **3**, 20-26
50. Matsumoto, M. L., Wickliffe, K. E., Dong, K. C., Yu, C., Bosanac, I., Bustos, D., Phu, L., Kirkpatrick, D. S., Hymowitz, S. G., Rape, M., Kelley, R. F., and Dixit, V. M. (2010) K11-linked polyubiquitination in cell cycle control revealed by a K11 linkage-specific antibody. *Mol Cell* **39**, 477-484
51. Husnjak, K., and Dikic, I. (2012) Ubiquitin-binding proteins: decoders of ubiquitin-mediated cellular functions. *Annu Rev Biochem* **81**, 291-322
52. Ikeda, F., and Dikic, I. (2008) Atypical ubiquitin chains: new molecular signals. 'Protein Modifications: Beyond the Usual Suspects' review series. *EMBO Rep* **9**, 536-542
53. Mukhopadhyay, D., and Riezman, H. (2007) Proteasome-independent functions of ubiquitin in endocytosis and signaling. *Science* **315**, 201-205
54. Jackson, S. P., and Durocher, D. (2013) Regulation of DNA damage responses by ubiquitin and SUMO. *Mol Cell* **49**, 795-807
55. Hicke, L., and Dunn, R. (2003) Regulation of membrane protein transport by ubiquitin and ubiquitin-binding proteins. *Annu Rev Cell Dev Biol* **19**, 141-172
56. Schnell, J. D., and Hicke, L. (2003) Non-traditional functions of ubiquitin and ubiquitin-binding proteins. *J Biol Chem* **278**, 35857-35860
57. Haglund, K., Di Fiore, P. P., and Dikic, I. (2003) Distinct monoubiquitin signals in receptor endocytosis. *Trends Biochem Sci* **28**, 598-603
58. Hoege, C., Pfander, B., Moldovan, G. L., Pyrowolakis, G., and Jentsch, S. (2002) RAD6-dependent DNA repair is linked to modification of PCNA by ubiquitin and SUMO. *Nature* **419**, 135-141
59. Moldovan, G. L., Pfander, B., and Jentsch, S. (2007) PCNA, the maestro of the replication fork. *Cell* **129**, 665-679
60. Xia, Z. P., Sun, L., Chen, X., Pineda, G., Jiang, X., Adhikari, A., Zeng, W., and Chen, Z. J. (2009) Direct activation of protein kinases by unanchored polyubiquitin chains. *Nature* **461**, 114-119
61. Cano, F., Miranda-Saavedra, D., and Lehner, P. J. (2010) RNA-binding E3 ubiquitin ligases: novel players in nucleic acid regulation. *Biochem Soc Trans* **38**, 1621-1626
62. Xiong, H., Wang, D., Chen, L., Choo, Y. S., Ma, H., Tang, C., Xia, K., Jiang, W., Ronai, Z., Zhuang, X., and Zhang, Z. (2009) Parkin, PINK1, and

DJ-1 form a ubiquitin E3 ligase complex promoting unfolded protein degradation. *J Clin Invest* **119**, 650-660
63. Buschmann, T., Fuchs, S. Y., Lee, C. G., Pan, Z. Q., and Ronai, Z. (2000) SUMO-1 modification of Mdm2 prevents its self-ubiquitination and increases Mdm2 ability to ubiquitinate p53. *Cell* **101**, 753-762
64. Scaglione, K. M., Zavodszky, E., Todi, S. V., Patury, S., Xu, P., Rodriguez-Lebron, E., Fischer, S., Konen, J., Djarmati, A., Peng, J., Gestwicki, J. E., and Paulson, H. L. (2011) Ube2w and ataxin-3 coordinately regulate the ubiquitin ligase CHIP. *Mol Cell* **43**, 599-612
65. Dai, R. M., and Li, C. C. (2001) Valosin-containing protein is a multi-ubiquitin chain-targeting factor required in ubiquitin-proteasome degradation. *Nat Cell Biol* **3**, 740-744
66. Lowe, J., Stock, D., Jap, B., Zwickl, P., Baumeister, W., and Huber, R. (1995) Crystal structure of the 20S proteasome from the archaeon T. acidophilum at 3.4 A resolution. *Science* **268**, 533-539
67. Finley, D. (2009) Recognition and processing of ubiquitin-protein conjugates by the proteasome. *Annu Rev Biochem* **78**, 477-513
68. Zhang, F., Hu, M., Tian, G., Zhang, P., Finley, D., Jeffrey, P. D., and Shi, Y. (2009) Structural insights into the regulatory particle of the proteasome from Methanocaldococcus jannaschii. *Mol Cell* **34**, 473-484
69. Hough, R., Pratt, G., and Rechsteiner, M. (1987) Purification of two high molecular weight proteases from rabbit reticulocyte lysate. *J Biol Chem* **262**, 8303-8313
70. Hadari, T., Warms, J. V., Rose, I. A., and Hershko, A. (1992) A ubiquitin C-terminal isopeptidase that acts on polyubiquitin chains. Role in protein degradation. *J Biol Chem* **267**, 719-727
71. Wilkinson, K. D. (1997) Regulation of ubiquitin-dependent processes by deubiquitinating enzymes. *FASEB J* **11**, 1245-1256
72. Wilkinson, K. D. (2009) DUBs at a glance. *J Cell Sci* **122**, 2325-2329
73. Borodovsky, A., Kessler, B. M., Casagrande, R., Overkleeft, H. S., Wilkinson, K. D., and Ploegh, H. L. (2001) A novel active site-directed probe specific for deubiquitylating enzymes reveals proteasome association of USP14. *EMBO J* **20**, 5187-5196
74. Ziv, I., Matiuhin, Y., Kirkpatrick, D. S., Erpapazoglou, Z., Leon, S., Pantazopoulou, M., Kim, W., Gygi, S. P., Haguenauer-Tsapis, R., Reis, N., Glickman, M. H., and Kleifeld, O. (2011) A perturbed ubiquitin landscape distinguishes between ubiquitin in trafficking and in proteolysis. *Mol Cell Proteomics* **10**, M111 009753
75. Bredesen, D. E. (2009) Neurodegeneration in Alzheimer's disease: caspases and synaptic element interdependence. *Mol Neurodegener* **4**, 27
76. D'Amelio, M., Cavallucci, V., Middei, S., Marchetti, C., Pacioni, S., Ferri, A., Diamantini, A., De Zio, D., Carrara, P., Battistini, L., Moreno, S., Bacci, A., Ammassari-Teule, M., Marie, H., and Cecconi, F. (2011) Caspase-3 triggers early synaptic dysfunction in a mouse model of Alzheimer's disease. *Nat Neurosci* **14**, 69-76

77. Suzuki, Y., Nakabayashi, Y., and Takahashi, R. (2001) Ubiquitin-protein ligase activity of X-linked inhibitor of apoptosis protein promotes proteasomal degradation of caspase-3 and enhances its anti-apoptotic effect in Fas-induced cell death. *Proc Natl Acad Sci U S A* **98**, 8662-8667
78. Choi, Y. E., Butterworth, M., Malladi, S., Duckett, C. S., Cohen, G. M., and Bratton, S. B. (2009) The E3 ubiquitin ligase cIAP1 binds and ubiquitinates caspase-3 and -7 via unique mechanisms at distinct steps in their processing. *J Biol Chem* **284**, 12772-12782
79. Nakamura, T., Tu, S., Akhtar, M. W., Sunico, C. R., Okamoto, S., and Lipton, S. A. (2013) Aberrant protein s-nitrosylation in neurodegenerative diseases. *Neuron* **78**, 596-614
80. Nakamura, T., Wang, L., Wong, C. C., Scott, F. L., Eckelman, B. P., Han, X., Tzitzilonis, C., Meng, F., Gu, Z., Holland, E. A., Clemente, A. T., Okamoto, S., Salvesen, G. S., Riek, R., Yates, J. R., 3rd, and Lipton, S. A. (2010) Transnitrosylation of XIAP regulates caspase-dependent neuronal cell death. *Mol Cell* **39**, 184-195
81. Glenner, G. G., Wong, C. W., Quaranta, V., and Eanes, E. D. (1984) The amyloid deposits in Alzheimer's disease: their nature and pathogenesis. *Appl Pathol* **2**, 357-369
82. Goedert, M., Wischik, C. M., Crowther, R. A., Walker, J. E., and Klug, A. (1988) Cloning and sequencing of the cDNA encoding a core protein of the paired helical filament of Alzheimer disease: identification as the microtubule-associated protein tau. *Proc Natl Acad Sci U S A* **85**, 4051-4055
83. Wischik, C. M., Novak, M., Thogersen, H. C., Edwards, P. C., Runswick, M. J., Jakes, R., Walker, J. E., Milstein, C., Roth, M., and Klug, A. (1988) Isolation of a fragment of tau derived from the core of the paired helical filament of Alzheimer disease. *Proc Natl Acad Sci U S A* **85**, 4506-4510
84. Perry, G., Friedman, R., Shaw, G., and Chau, V. (1987) Ubiquitin is detected in neurofibrillary tangles and senile plaque neurites of Alzheimer disease brains. *Proc Natl Acad Sci U S A* **84**, 3033-3036
85. Thinakaran, G., and Koo, E. H. (2008) Amyloid precursor protein trafficking, processing, and function. *J Biol Chem* **283**, 29615-29619
86. Bertram, L., Lill, C. M., and Tanzi, R. E. (2010) The genetics of Alzheimer disease: back to the future. *Neuron* **68**, 270-281
87. Hernandez, F., Gomez de Barreda, E., Fuster-Matanzo, A., Lucas, J. J., and Avila, J. (2010) GSK3: a possible link between beta amyloid peptide and tau protein. *Exp Neurol* **223**, 322-325
88. Kumar, P., Ambasta, R. K., Veereshwarayya, V., Rosen, K. M., Kosik, K. S., Band, H., Mestril, R., Patterson, C., and Querfurth, H. W. (2007) CHIP and HSPs interact with beta-APP in a proteasome-dependent manner and influence Abeta metabolism. *Hum Mol Genet* **16**, 848-864
89. Kaneko, M., Koike, H., Saito, R., Kitamura, Y., Okuma, Y., and Nomura, Y. (2010) Loss of HRD1-mediated protein degradation causes amyloid precursor protein accumulation and amyloid-beta generation. *J Neurosci* **30**, 3924-3932

90. Gong, B., Chen, F., Pan, Y., Arrieta-Cruz, I., Yoshida, Y., Haroutunian, V., and Pasinetti, G. M. (2010) SCFFbx2-E3-ligase-mediated degradation of BACE1 attenuates Alzheimer's disease amyloidosis and improves synaptic function. *Aging Cell* **9**, 1018-1031
91. Atkin, G., Hunt, J., Minakawa, E., Sharkey, L., Tipper, N., Tennant, W., and Paulson, H. L. (2014) F-box only protein 2 (Fbxo2) Regulates Amyloid Precursor Levels and Processing. *J Biol Chem*
92. El Ayadi, A., Stieren, E. S., Barral, J. M., and Boehning, D. (2012) Ubiquilin-1 regulates amyloid precursor protein maturation and degradation by stimulating K63-linked polyubiquitination of lysine 688. *Proc Natl Acad Sci U S A* **109**, 13416-13421
93. Stieren, E. S., El Ayadi, A., Xiao, Y., Siller, E., Landsverk, M. L., Oberhauser, A. F., Barral, J. M., and Boehning, D. (2011) Ubiquilin-1 is a molecular chaperone for the amyloid precursor protein. *J Biol Chem* **286**, 35689-35698
94. Miller, V. M., Nelson, R. F., Gouvion, C. M., Williams, A., Rodriguez-Lebron, E., Harper, S. Q., Davidson, B. L., Rebagliati, M. R., and Paulson, H. L. (2005) CHIP suppresses polyglutamine aggregation and toxicity in vitro and in vivo. *J Neurosci* **25**, 9152-9161
95. Williams, A. J., Knutson, T. M., Colomer Gould, V. F., and Paulson, H. L. (2009) In vivo suppression of polyglutamine neurotoxicity by C-terminus of Hsp70-interacting protein (CHIP) supports an aggregation model of pathogenesis. *Neurobiol Dis* **33**, 342-353
96. Li, J., Pauley, A. M., Myers, R. L., Shuang, R., Brashler, J. R., Yan, R., Buhl, A. E., Ruble, C., and Gurney, M. E. (2002) SEL-10 interacts with presenilin 1, facilitates its ubiquitination, and alters A-beta peptide production. *J Neurochem* **82**, 1540-1548
97. Proctor, C. J., and Gray, D. A. (2010) GSK3 and p53 - is there a link in Alzheimer's disease? *Mol Neurodegener* **5**, 7
98. Richet, E., Pooler, A. M., Rodriguez, T., Novoselov, S. S., Schmidtke, G., Groettrup, M., Hanger, D. P., Cheetham, M. E., and van der Spuy, J. (2012) NUB1 modulation of GSK3beta reduces tau aggregation. *Hum Mol Genet* **21**, 5254-5267
99. Kamitani, T., Kito, K., Fukuda-Kamitani, T., and Yeh, E. T. (2001) Targeting of NEDD8 and its conjugates for proteasomal degradation by NUB1. *J Biol Chem* **276**, 46655-46660
100. Kito, K., Yeh, E. T., and Kamitani, T. (2001) NUB1, a NEDD8-interacting protein, is induced by interferon and down-regulates the NEDD8 expression. *J Biol Chem* **276**, 20603-20609
101. Kumar, S., Yoshida, Y., and Noda, M. (1993) Cloning of a cDNA which encodes a novel ubiquitin-like protein. *Biochem Biophys Res Commun* **195**, 393-399
102. Duda, D. M., Borg, L. A., Scott, D. C., Hunt, H. W., Hammel, M., and Schulman, B. A. (2008) Structural insights into NEDD8 activation of cullin-RING ligases: conformational control of conjugation. *Cell* **134**, 995-1006

103. Chen, Y., Neve, R. L., and Liu, H. (2012) Neddylation dysfunction in Alzheimer's disease. *J Cell Mol Med* **16**, 2583-2591
104. Dil Kuazi, A., Kito, K., Abe, Y., Shin, R. W., Kamitani, T., and Ueda, N. (2003) NEDD8 protein is involved in ubiquitinated inclusion bodies. *J Pathol* **199**, 259-266
105. Petrucelli, L., Dickson, D., Kehoe, K., Taylor, J., Snyder, H., Grover, A., De Lucia, M., McGowan, E., Lewis, J., Prihar, G., Kim, J., Dillmann, W. H., Browne, S. E., Hall, A., Voellmy, R., Tsuboi, Y., Dawson, T. M., Wolozin, B., Hardy, J., and Hutton, M. (2004) CHIP and Hsp70 regulate tau ubiquitination, degradation and aggregation. *Hum Mol Genet* **13**, 703-714
106. Dickey, C. A., Yue, M., Lin, W. L., Dickson, D. W., Dunmore, J. H., Lee, W. C., Zehr, C., West, G., Cao, S., Clark, A. M., Caldwell, G. A., Caldwell, K. A., Eckman, C., Patterson, C., Hutton, M., and Petrucelli, L. (2006) Deletion of the ubiquitin ligase CHIP leads to the accumulation, but not the aggregation, of both endogenous phospho- and caspase-3-cleaved tau species. *J Neurosci* **26**, 6985-6996
107. Hardingham, G. E., and Bading, H. (2010) Synaptic versus extrasynaptic NMDA receptor signalling: implications for neurodegenerative disorders. *Nat Rev Neurosci* **11**, 682-696
108. Shankar, G. M., Bloodgood, B. L., Townsend, M., Walsh, D. M., Selkoe, D. J., and Sabatini, B. L. (2007) Natural oligomers of the Alzheimer amyloid-beta protein induce reversible synapse loss by modulating an NMDA-type glutamate receptor-dependent signaling pathway. *J Neurosci* **27**, 2866-2875
109. Talantova, M., Sanz-Blasco, S., Zhang, X., Xia, P., Akhtar, M. W., Okamoto, S., Dziewczapolski, G., Nakamura, T., Cao, G., Pratt, A. E., Kang, Y. J., Tu, S., Molokanova, E., McKercher, S. R., Hires, S. A., Sason, H., Stouffer, D. G., Buczynski, M. W., Solomon, J. P., Michael, S., Powers, E. T., Kelly, J. W., Roberts, A., Tong, G., Fang-Newmeyer, T., Parker, J., Holland, E. A., Zhang, D., Nakanishi, N., Chen, H. S., Wolosker, H., Wang, Y., Parsons, L. H., Ambasudhan, R., Masliah, E., Heinemann, S. F., Pina-Crespo, J. C., and Lipton, S. A. (2013) Abeta induces astrocytic glutamate release, extrasynaptic NMDA receptor activation, and synaptic loss. *Proc Natl Acad Sci U S A* **110**, E2518-2527
110. Jurd, R., Thornton, C., Wang, J., Luong, K., Phamluong, K., Kharazia, V., Gibb, S. L., and Ron, D. (2008) Mind bomb-2 is an E3 ligase that ubiquitinates the N-methyl-D-aspartate receptor NR2B subunit in a phosphorylation-dependent manner. *J Biol Chem* **283**, 301-310
111. Kato, A., Rouach, N., Nicoll, R. A., and Bredt, D. S. (2005) Activity-dependent NMDA receptor degradation mediated by retrotranslocation and ubiquitination. *Proc Natl Acad Sci U S A* **102**, 5600-5605
112. Maestre, C., Delgado-Esteban, M., Gomez-Sanchez, J. C., Bolanos, J. P., and Almeida, A. (2008) Cdk5 phosphorylates Cdh1 and modulates cyclin B1 stability in excitotoxicity. *EMBO J* **27**, 2736-2745
113. Syme, C. D., Blanch, E. W., Holt, C., Jakes, R., Goedert, M., Hecht, L., and Barron, L. D. (2002) A Raman optical activity study of rheomorphism

in caseins, synucleins and tau. New insight into the structure and behaviour of natively unfolded proteins. *Eur J Biochem* **269**, 148-156
114. Kruger, R., Kuhn, W., Muller, T., Woitalla, D., Graeber, M., Kosel, S., Przuntek, H., Epplen, J. T., Schols, L., and Riess, O. (1998) Ala30Pro mutation in the gene encoding alpha-synuclein in Parkinson's disease. *Nat Genet* **18**, 106-108
115. Riess, O., Jakes, R., and Kruger, R. (1998) Genetic dissection of familial Parkinson's disease. *Mol Med Today* **4**, 438-444
116. Shimura, H., Schlossmacher, M. G., Hattori, N., Frosch, M. P., Trockenbacher, A., Schneider, R., Mizuno, Y., Kosik, K. S., and Selkoe, D. J. (2001) Ubiquitination of a new form of alpha-synuclein by parkin from human brain: implications for Parkinson's disease. *Science* **293**, 263-269
117. McNaught, K. S., and Jenner, P. (2001) Proteasomal function is impaired in substantia nigra in Parkinson's disease. *Neurosci Lett* **297**, 191-194
118. McNaught, K. S., Bjorklund, L. M., Belizaire, R., Isacson, O., Jenner, P., and Olanow, C. W. (2002) Proteasome inhibition causes nigral degeneration with inclusion bodies in rats. *Neuroreport* **13**, 1437-1441
119. McNaught, K. S., and Olanow, C. W. (2006) Proteasome inhibitor-induced model of Parkinson's disease. *Ann Neurol* **60**, 243-247
120. Lindersson, E., Beedholm, R., Hojrup, P., Moos, T., Gai, W., Hendil, K. B., and Jensen, P. H. (2004) Proteasomal inhibition by alpha-synuclein filaments and oligomers. *J Biol Chem* **279**, 12924-12934
121. Petrucelli, L., O'Farrell, C., Lockhart, P. J., Baptista, M., Kehoe, K., Vink, L., Choi, P., Wolozin, B., Farrer, M., Hardy, J., and Cookson, M. R. (2002) Parkin protects against the toxicity associated with mutant alpha-synuclein: proteasome dysfunction selectively affects catecholaminergic neurons. *Neuron* **36**, 1007-1019
122. Lucking, C. B., Durr, A., Bonifati, V., Vaughan, J., De Michele, G., Gasser, T., Harhangi, B. S., Meco, G., Denefle, P., Wood, N. W., Agid, Y., and Brice, A. (2000) Association between early-onset Parkinson's disease and mutations in the parkin gene. *N Engl J Med* **342**, 1560-1567
123. Khan, N. L., Graham, E., Critchley, P., Schrag, A. E., Wood, N. W., Lees, A. J., Bhatia, K. P., and Quinn, N. (2003) Parkin disease: a phenotypic study of a large case series. *Brain* **126**, 1279-1292
124. Shimura, H., Hattori, N., Kubo, S., Mizuno, Y., Asakawa, S., Minoshima, S., Shimizu, N., Iwai, K., Chiba, T., Tanaka, K., and Suzuki, T. (2000) Familial Parkinson disease gene product, parkin, is a ubiquitin-protein ligase. *Nat Genet* **25**, 302-305
125. Hardy, J. (2003) Impact of genetic analysis on Parkinson's disease research. *Mov Disord* **18 Suppl 6**, S96-98
126. Lu, X. H., Fleming, S. M., Meurers, B., Ackerson, L. C., Mortazavi, F., Lo, V., Hernandez, D., Sulzer, D., Jackson, G. R., Maidment, N. T., Chesselet, M. F., and Yang, X. W. (2009) Bacterial artificial chromosome transgenic mice expressing a truncated mutant parkin exhibit age-dependent hypokinetic motor deficits, dopaminergic neuron degeneration, and

accumulation of proteinase K-resistant alpha-synuclein. *J Neurosci* **29**, 1962-1976
127. Fallon, L., Belanger, C. M., Corera, A. T., Kontogiannea, M., Regan-Klapisz, E., Moreau, F., Voortman, J., Haber, M., Rouleau, G., Thorarinsdottir, T., Brice, A., van Bergen En Henegouwen, P. M., and Fon, E. A. (2006) A regulated interaction with the UIM protein Eps15 implicates parkin in EGF receptor trafficking and PI(3)K-Akt signalling. *Nat Cell Biol* **8**, 834-842
128. Iwakura, Y., Piao, Y. S., Mizuno, M., Takei, N., Kakita, A., Takahashi, H., and Nawa, H. (2005) Influences of dopaminergic lesion on epidermal growth factor-ErbB signals in Parkinson's disease and its model: neurotrophic implication in nigrostriatal neurons. *J Neurochem* **93**, 974-983
129. van Bergen En Henegouwen, P. M. (2009) Eps15: a multifunctional adaptor protein regulating intracellular trafficking. *Cell Commun Signal* **7**, 24
130. Valente, E. M., Abou-Sleiman, P. M., Caputo, V., Muqit, M. M., Harvey, K., Gispert, S., Ali, Z., Del Turco, D., Bentivoglio, A. R., Healy, D. G., Albanese, A., Nussbaum, R., Gonzalez-Maldonado, R., Deller, T., Salvi, S., Cortelli, P., Gilks, W. P., Latchman, D. S., Harvey, R. J., Dallapiccola, B., Auburger, G., and Wood, N. W. (2004) Hereditary early-onset Parkinson's disease caused by mutations in PINK1. *Science* **304**, 1158-1160
131. Abou-Sleiman, P. M., Healy, D. G., Quinn, N., Lees, A. J., and Wood, N. W. (2003) The role of pathogenic DJ-1 mutations in Parkinson's disease. *Ann Neurol* **54**, 283-286
132. Greene, J. C., Whitworth, A. J., Kuo, I., Andrews, L. A., Feany, M. B., and Pallanck, L. J. (2003) Mitochondrial pathology and apoptotic muscle degeneration in Drosophila parkin mutants. *Proc Natl Acad Sci U S A* **100**, 4078-4083
133. Vincow, E. S., Merrihew, G., Thomas, R. E., Shulman, N. J., Beyer, R. P., MacCoss, M. J., and Pallanck, L. J. (2013) The PINK1-Parkin pathway promotes both mitophagy and selective respiratory chain turnover in vivo. *Proc Natl Acad Sci U S A* **110**, 6400-6405
134. Yoshii, S. R., Kishi, C., Ishihara, N., and Mizushima, N. (2011) Parkin mediates proteasome-dependent protein degradation and rupture of the outer mitochondrial membrane. *J Biol Chem* **286**, 19630-19640
135. Das, C., Hoang, Q. Q., Kreinbring, C. A., Luchansky, S. J., Meray, R. K., Ray, S. S., Lansbury, P. T., Ringe, D., and Petsko, G. A. (2006) Structural basis for conformational plasticity of the Parkinson's disease-associated ubiquitin hydrolase UCH-L1. *Proc Natl Acad Sci U S A* **103**, 4675-4680
136. Sabatini, D. M., Erdjument-Bromage, H., Lui, M., Tempst, P., and Snyder, S. H. (1994) RAFT1: a mammalian protein that binds to FKBP12 in a rapamycin-dependent fashion and is homologous to yeast TORs. *Cell* **78**, 35-43

137. Hoeffer, C. A., and Klann, E. (2010) mTOR signaling: at the crossroads of plasticity, memory and disease. *Trends Neurosci* **33**, 67-75
138. Hay, N., and Sonenberg, N. (2004) Upstream and downstream of mTOR. *Genes Dev* **18**, 1926-1945
139. Ghosh, P., Wu, M., Zhang, H., and Sun, H. (2008) mTORC1 signaling requires proteasomal function and the involvement of CUL4-DDB1 ubiquitin E3 ligase. *Cell Cycle* **7**, 373-381
140. Quy, P. N., Kuma, A., Pierre, P., and Mizushima, N. (2013) Proteasome-dependent activation of mammalian target of rapamycin complex 1 (mTORC1) is essential for autophagy suppression and muscle remodeling following denervation. *J Biol Chem* **288**, 1125-1134
141. Costa-Mattioli, M., and Monteggia, L. M. (2013) mTOR complexes in neurodevelopmental and neuropsychiatric disorders. *Nat Neurosci* **16**, 1537-1543
142. Hussain, S., Feldman, A. L., Das, C., Ziesmer, S. C., Ansell, S. M., and Galardy, P. J. (2013) Ubiquitin hydrolase UCH-L1 destabilizes mTOR complex 1 by antagonizing DDB1-CUL4-mediated ubiquitination of raptor. *Mol Cell Biol* **33**, 1188-1197
143. Cartier, A. E., Ubhi, K., Spencer, B., Vazquez-Roque, R. A., Kosberg, K. A., Fourgeaud, L., Kanayson, P., Patrick, C., Rockenstein, E., Patrick, G. N., and Masliah, E. (2012) Differential effects of UCHL1 modulation on alpha-synuclein in PD-like models of alpha-synucleinopathy. *PLoS One* **7**, e34713
144. Liu, Y., Fallon, L., Lashuel, H. A., Liu, Z., and Lansbury, P. T., Jr. (2002) The UCH-L1 gene encodes two opposing enzymatic activities that affect alpha-synuclein degradation and Parkinson's disease susceptibility. *Cell* **111**, 209-218
145. Imai, Y., Soda, M., Hatakeyama, S., Akagi, T., Hashikawa, T., Nakayama, K. I., and Takahashi, R. (2002) CHIP is associated with Parkin, a gene responsible for familial Parkinson's disease, and enhances its ubiquitin ligase activity. *Mol Cell* **10**, 55-67
146. Nair, V. D., McNaught, K. S., Gonzalez-Maeso, J., Sealfon, S. C., and Olanow, C. W. (2006) p53 mediates nontranscriptional cell death in dopaminergic cells in response to proteasome inhibition. *J Biol Chem* **281**, 39550-39560
147. Mei, J., and Niu, C. (2010) Alterations of Hrd1 expression in various encephalic regional neurons in 6-OHDA model of Parkinson's disease. *Neurosci Lett* **474**, 63-68
148. Lowe, J. (1994) New pathological findings in amyotrophic lateral sclerosis. *J Neurol Sci* **124 Suppl**, 38-51
149. Walling, A. D. (1999) Amyotrophic lateral sclerosis: Lou Gehrig's disease. *Am Fam Physician* **59**, 1489-1496
150. Andersen, P. M., and Al-Chalabi, A. (2011) Clinical genetics of amyotrophic lateral sclerosis: what do we really know? *Nat Rev Neurol* **7**, 603-615
151. Rosen, D. R., Siddique, T., Patterson, D., Figlewicz, D. A., Sapp, P., Hentati, A., Donaldson, D., Goto, J., O'Regan, J. P., Deng, H. X., and et al.

(1993) Mutations in Cu/Zn superoxide dismutase gene are associated with familial amyotrophic lateral sclerosis. *Nature* **362**, 59-62
152. Gitcho, M. A., Baloh, R. H., Chakraverty, S., Mayo, K., Norton, J. B., Levitch, D., Hatanpaa, K. J., White, C. L., 3rd, Bigio, E. H., Caselli, R., Baker, M., Al-Lozi, M. T., Morris, J. C., Pestronk, A., Rademakers, R., Goate, A. M., and Cairns, N. J. (2008) TDP-43 A315T mutation in familial motor neuron disease. *Ann Neurol* **63**, 535-538
153. Mishra, A., Maheshwari, M., Chhangani, D., Fujimori-Tonou, N., Endo, F., Joshi, A. P., Jana, N. R., and Yamanaka, K. (2013) E6-AP association promotes SOD1 aggresomes degradation and suppresses toxicity. *Neurobiol Aging* **34**, 1310 e1311-1323
154. Miyazaki, K., Fujita, T., Ozaki, T., Kato, C., Kurose, Y., Sakamoto, M., Kato, S., Goto, T., Itoyama, Y., Aoki, M., and Nakagawara, A. (2004) NEDL1, a novel ubiquitin-protein isopeptide ligase for dishevelled-1, targets mutant superoxide dismutase-1. *J Biol Chem* **279**, 11327-11335
155. Kunst, C. B., Mezey, E., Brownstein, M. J., and Patterson, D. (1997) Mutations in SOD1 associated with amyotrophic lateral sclerosis cause novel protein interactions. *Nat Genet* **15**, 91-94
156. Niwa, J., Ishigaki, S., Hishikawa, N., Yamamoto, M., Doyu, M., Murata, S., Tanaka, K., Taniguchi, N., and Sobue, G. (2002) Dorfin ubiquitylates mutant SOD1 and prevents mutant SOD1-mediated neurotoxicity. *J Biol Chem* **277**, 36793-36798
157. Sone, J., Niwa, J., Kawai, K., Ishigaki, S., Yamada, S., Adachi, H., Katsuno, M., Tanaka, F., Doyu, M., and Sobue, G. (2010) Dorfin ameliorates phenotypes in a transgenic mouse model of amyotrophic lateral sclerosis. *J Neurosci Res* **88**, 123-135
158. Buratti, E., and Baralle, F. E. (2001) Characterization and functional implications of the RNA binding properties of nuclear factor TDP-43, a novel splicing regulator of CFTR exon 9. *J Biol Chem* **276**, 36337-36343
159. Buratti, E., and Baralle, F. E. (2010) The multiple roles of TDP-43 in pre-mRNA processing and gene expression regulation. *RNA Biol* **7**, 420-429
160. Neumann, M., Sampathu, D. M., Kwong, L. K., Truax, A. C., Micsenyi, M. C., Chou, T. T., Bruce, J., Schuck, T., Grossman, M., Clark, C. M., McCluskey, L. F., Miller, B. L., Masliah, E., Mackenzie, I. R., Feldman, H., Feiden, W., Kretzschmar, H. A., Trojanowski, J. Q., and Lee, V. M. (2006) Ubiquitinated TDP-43 in frontotemporal lobar degeneration and amyotrophic lateral sclerosis. *Science* **314**, 130-133
161. Igaz, L. M., Kwong, L. K., Lee, E. B., Chen-Plotkin, A., Swanson, E., Unger, T., Malunda, J., Xu, Y., Winton, M. J., Trojanowski, J. Q., and Lee, V. M. (2011) Dysregulation of the ALS-associated gene TDP-43 leads to neuronal death and degeneration in mice. *J Clin Invest* **121**, 726-738
162. Janssens, J., and Van Broeckhoven, C. (2013) Pathological mechanisms underlying TDP-43 driven neurodegeneration in FTLD-ALS spectrum disorders. *Hum Mol Genet* **22**, R77-87
163. Hebron, M. L., Lonskaya, I., Sharpe, K., Weerasinghe, P. P., Algarzae, N. K., Shekoyan, A. R., and Moussa, C. E. (2013) Parkin ubiquitinates Tar-

DNA binding protein-43 (TDP-43) and promotes its cytosolic accumulation via interaction with histone deacetylase 6 (HDAC6). *J Biol Chem* **288**, 4103-4115
164. Polymenidou, M., Lagier-Tourenne, C., Hutt, K. R., Huelga, S. C., Moran, J., Liang, T. Y., Ling, S. C., Sun, E., Wancewicz, E., Mazur, C., Kordasiewicz, H., Sedaghat, Y., Donohue, J. P., Shiue, L., Bennett, C. F., Yeo, G. W., and Cleveland, D. W. (2011) Long pre-mRNA depletion and RNA missplicing contribute to neuronal vulnerability from loss of TDP-43. *Nat Neurosci* **14**, 459-468
165. Olzmann, J. A., and Chin, L. S. (2008) Parkin-mediated K63-linked polyubiquitination: a signal for targeting misfolded proteins to the aggresome-autophagy pathway. *Autophagy* **4**, 85-87
166. Ross, C. A. (1995) When more is less: pathogenesis of glutamine repeat neurodegenerative diseases. *Neuron* **15**, 493-496
167. Orr, H. T. (2012) Polyglutamine neurodegeneration: expanded glutamines enhance native functions. *Curr Opin Genet Dev* **22**, 251-255
168. Robertson, A. L., Bate, M. A., Androulakis, S. G., Bottomley, S. P., and Buckle, A. M. (2011) PolyQ: a database describing the sequence and domain context of polyglutamine repeats in proteins. *Nucleic Acids Res* **39**, D272-276
169. Myers, R. H., MacDonald, M. E., Koroshetz, W. J., Duyao, M. P., Ambrose, C. M., Taylor, S. A., Barnes, G., Srinidhi, J., Lin, C. S., Whaley, W. L., and et al. (1993) De novo expansion of a (CAG)n repeat in sporadic Huntington's disease. *Nat Genet* **5**, 168-173
170. Snell, R. G., MacMillan, J. C., Cheadle, J. P., Fenton, I., Lazarou, L. P., Davies, P., MacDonald, M. E., Gusella, J. F., Harper, P. S., and Shaw, D. J. (1993) Relationship between trinucleotide repeat expansion and phenotypic variation in Huntington's disease. *Nat Genet* **4**, 393-397
171. Chong, S. S., Almqvist, E., Telenius, H., LaTray, L., Nichol, K., Bourdelat-Parks, B., Goldberg, Y. P., Haddad, B. R., Richards, F., Sillence, D., Greenberg, C. R., Ives, E., Van den Engh, G., Hughes, M. R., and Hayden, M. R. (1997) Contribution of DNA sequence and CAG size to mutation frequencies of intermediate alleles for Huntington disease: evidence from single sperm analyses. *Hum Mol Genet* **6**, 301-309
172. Walker, F. O. (2007) Huntington's disease. *Lancet* **369**, 218-228
173. DiFiglia, M., Sapp, E., Chase, K. O., Davies, S. W., Bates, G. P., Vonsattel, J. P., and Aronin, N. (1997) Aggregation of huntingtin in neuronal intranuclear inclusions and dystrophic neurites in brain. *Science* **277**, 1990-1993
174. Cattaneo, E., Zuccato, C., and Tartari, M. (2005) Normal huntingtin function: an alternative approach to Huntington's disease. *Nat Rev Neurosci* **6**, 919-930
175. Parsons, M. P., Kang, R., Buren, C., Dau, A., Southwell, A. L., Doty, C. N., Sanders, S. S., Hayden, M. R., and Raymond, L. A. (2013) Bidirectional control of postsynaptic density-95 (PSD-95) clustering by huntingtin. *J Biol Chem*

176. Milnerwood, A. J., Gladding, C. M., Pouladi, M. A., Kaufman, A. M., Hines, R. M., Boyd, J. D., Ko, R. W., Vasuta, O. C., Graham, R. K., Hayden, M. R., Murphy, T. H., and Raymond, L. A. (2010) Early increase in extrasynaptic NMDA receptor signaling and expression contributes to phenotype onset in Huntington's disease mice. *Neuron* **65**, 178-190
177. Gladding, C. M., Sepers, M. D., Xu, J., Zhang, L. Y., Milnerwood, A. J., Lombroso, P. J., and Raymond, L. A. (2012) Calpain and STriatal-Enriched protein tyrosine phosphatase (STEP) activation contribute to extrasynaptic NMDA receptor localization in a Huntington's disease mouse model. *Hum Mol Genet* **21**, 3739-3752
178. Okamoto, S., Pouladi, M. A., Talantova, M., Yao, D., Xia, P., Ehrnhoefer, D. E., Zaidi, R., Clemente, A., Kaul, M., Graham, R. K., Zhang, D., Vincent Chen, H. S., Tong, G., Hayden, M. R., and Lipton, S. A. (2009) Balance between synaptic versus extrasynaptic NMDA receptor activity influences inclusions and neurotoxicity of mutant huntingtin. *Nat Med* **15**, 1407-1413
179. Kalchman, M. A., Graham, R. K., Xia, G., Koide, H. B., Hodgson, J. G., Graham, K. C., Goldberg, Y. P., Gietz, R. D., Pickart, C. M., and Hayden, M. R. (1996) Huntingtin is ubiquitinated and interacts with a specific ubiquitin-conjugating enzyme. *J Biol Chem* **271**, 19385-19394
180. Venkatraman, P., Wetzel, R., Tanaka, M., Nukina, N., and Goldberg, A. L. (2004) Eukaryotic proteasomes cannot digest polyglutamine sequences and release them during degradation of polyglutamine-containing proteins. *Mol Cell* **14**, 95-104
181. Holmberg, C. I., Staniszewski, K. E., Mensah, K. N., Matouschek, A., and Morimoto, R. I. (2004) Inefficient degradation of truncated polyglutamine proteins by the proteasome. *EMBO J* **23**, 4307-4318
182. Raspe, M., Gillis, J., Krol, H., Krom, S., Bosch, K., van Veen, H., and Reits, E. (2009) Mimicking proteasomal release of polyglutamine peptides initiates aggregation and toxicity. *J Cell Sci* **122**, 3262-3271
183. Suhr, S. T., Senut, M. C., Whitelegge, J. P., Faull, K. F., Cuizon, D. B., and Gage, F. H. (2001) Identities of sequestered proteins in aggregates from cells with induced polyglutamine expression. *J Cell Biol* **153**, 283-294
184. Seo, H., Sonntag, K. C., Kim, W., Cattaneo, E., and Isacson, O. (2007) Proteasome activator enhances survival of Huntington's disease neuronal model cells. *PLoS One* **2**, e238
185. Jia, H., Kast, R. J., Steffan, J. S., and Thomas, E. A. (2012) Selective histone deacetylase (HDAC) inhibition imparts beneficial effects in Huntington's disease mice: implications for the ubiquitin-proteasomal and autophagy systems. *Hum Mol Genet* **21**, 5280-5293
186. Yang, H., Zhong, X., Ballar, P., Luo, S., Shen, Y., Rubinsztein, D. C., Monteiro, M. J., and Fang, S. (2007) Ubiquitin ligase Hrd1 enhances the degradation and suppresses the toxicity of polyglutamine-expanded huntingtin. *Exp Cell Res* **313**, 538-550
187. Zucchelli, S., Marcuzzi, F., Codrich, M., Agostoni, E., Vilotti, S., Biagioli, M., Pinto, M., Carnemolla, A., Santoro, C., Gustincich, S., and Persichetti, F. (2011) Tumor necrosis factor receptor-associated factor 6 (TRAF6)

associates with huntingtin protein and promotes its atypical ubiquitination to enhance aggregate formation. *J Biol Chem* **286**, 25108-25117
188. Lu, B., Al-Ramahi, I., Valencia, A., Wang, Q., Berenshteyn, F., Yang, H., Gallego-Flores, T., Ichcho, S., Lacoste, A., Hild, M., Difiglia, M., Botas, J., and Palacino, J. (2013) Identification of NUB1 as a suppressor of mutant Huntington toxicity via enhanced protein clearance. *Nat Neurosci* **16**, 562-570
189. Subramaniam, S., Sixt, K. M., Barrow, R., and Snyder, S. H. (2009) Rhes, a striatal specific protein, mediates mutant-huntingtin cytotoxicity. *Science* **324**, 1327-1330
190. Steffan, J. S., Agrawal, N., Pallos, J., Rockabrand, E., Trotman, L. C., Slepko, N., Illes, K., Lukacsovich, T., Zhu, Y. Z., Cattaneo, E., Pandolfi, P. P., Thompson, L. M., and Marsh, J. L. (2004) SUMO modification of Huntingtin and Huntington's disease pathology. *Science* **304**, 100-104
191. Choo, Y. S., Johnson, G. V., MacDonald, M., Detloff, P. J., and Lesort, M. (2004) Mutant huntingtin directly increases susceptibility of mitochondria to the calcium-induced permeability transition and cytochrome c release. *Hum Mol Genet* **13**, 1407-1420
192. Mealer, R. G., Murray, A. J., Shahani, N., Subramaniam, S., and Snyder, S. H. (2013) Rhes, a Striatal-Selective Protein Implicated in Huntington Disease, Binds Beclin-1 and Activates Autophagy. *J Biol Chem*
193. de Pril, R., Fischer, D. F., Roos, R. A., and van Leeuwen, F. W. (2007) Ubiquitin-conjugating enzyme E2-25K increases aggregate formation and cell death in polyglutamine diseases. *Mol Cell Neurosci* **34**, 10-19
194. Lee, S. J., Choi, J. Y., Sung, Y. M., Park, H., Rhim, H., and Kang, S. (2001) E3 ligase activity of RING finger proteins that interact with Hip-2, a human ubiquitin-conjugating enzyme. *FEBS Lett* **503**, 61-64
195. Garcia-Arencibia, M., Hochfeld, W. E., Toh, P. P., and Rubinsztein, D. C. (2010) Autophagy, a guardian against neurodegeneration. *Semin Cell Dev Biol* **21**, 691-698
196. Metcalf, D. J., Garcia-Arencibia, M., Hochfeld, W. E., and Rubinsztein, D. C. (2012) Autophagy and misfolded proteins in neurodegeneration. *Exp Neurol* **238**, 22-28
197. Nixon, R. A. (2013) The role of autophagy in neurodegenerative disease. *Nat Med* **19**, 983-997
198. Hochfeld, W. E., Lee, S., and Rubinsztein, D. C. (2013) Therapeutic induction of autophagy to modulate neurodegenerative disease progression. *Acta Pharmacol Sin* **34**, 600-604
199. Adachi, H., Waza, M., Tokui, K., Katsuno, M., Minamiyama, M., Tanaka, F., Doyu, M., and Sobue, G. (2007) CHIP overexpression reduces mutant androgen receptor protein and ameliorates phenotypes of the spinal and bulbar muscular atrophy transgenic mouse model. *J Neurosci* **27**, 5115-5126
200. Lee, J. S., Seo, T. W., Yi, J. H., Shin, K. S., and Yoo, S. J. (2013) CHIP has a protective role against oxidative stress-induced cell death through specific regulation of Endonuclease G. *Cell Death Dis* **4**, e666

201. Perez, R. G., Squazzo, S. L., and Koo, E. H. (1996) Enhanced release of amyloid beta-protein from codon 670/671 "Swedish" mutant beta-amyloid precursor protein occurs in both secretory and endocytic pathways. *J Biol Chem* **271**, 9100-9107

Chapter Two: F-box only protein 2 (Fbxo2) Regulates Amyloid Precursor Protein Levels and Processing

ABSTRACT

The Amyloid Precursor Protein (APP) is an integral membrane glycoprotein whose cleavage products, particularly Amyloid-β, accumulate in Alzheimer's Disease (AD). APP is present at synapses and is thought to play a role in both the formation and plasticity of these critical neuronal structures. Despite the central role suggested for APP in AD pathogenesis, the mechanisms regulating APP in neurons and its processing into cleavage products remain incompletely understood. F-box only protein 2 (Fbxo2), a neuron-enriched ubiquitin ligase substrate adaptor that preferentially binds high-mannose glycans on glycoproteins, was previously implicated in APP processing by facilitating the degradation of the APP-cleaving beta-secretase, beta-site-APP-cleaving enzyme (BACE1). Here we sought to determine whether Fbxo2 plays a similar role for other glycoproteins in the amyloid processing pathway. We present in vitro and in vivo evidence that APP is itself a substrate for Fbxo2. APP levels were decreased in the presence of Fbxo2 in non-neuronal cells, and increased in both cultured hippocampal neurons and brain tissue from Fbxo2 knockout mice. The processing of APP into its cleavage products was also increased in hippocampi and cultured hippocampal neurons lacking Fbxo2. In hippocampal slices, this

increase in cleavage products was accompanied by a significant reduction in APP at the cell surface. Taken together, these results suggest that Fbxo2 regulates APP levels and processing in the brain and may play a role in modulating AD pathogenesis.

INTRODUCTION

Alzheimer's Disease (AD) is the most common neurodegenerative disorder. Its progressive brain pathology robs patients of memory and cognitive abilities through complex mechanisms that remain unclear. Abnormalities in the processing of Amyloid Precursor Protein (APP) are thought to play a central role in AD pathogenesis (1), largely based on the fact that mutations in APP and the APP cleavage enzyme gamma secretase cause early-onset familial AD and replicate key disease features in animal models, including the accumulation of Amyloid Beta (Aβ) peptide (2). Generated from proteolytic processing of APP (3), Aβ is the major component of the characteristic amyloid plaques that accumulate in AD. Aβ has also been shown to alter synaptic function and decrease synapse numbers (4). Indeed, the loss of synaptic connections more closely correlates with cognitive deficits observed in AD patients than does the loss of neurons and cortical thinning observed later in AD (5).

The regulation of APP expression and processing is critically important to the development and progression of AD. APP is sequentially cleaved by a series of secretase enzymes through a complex process linked to neuronal metabolism

and activity (6). Factors that increase the amount of APP available for cleavage inversely correlate with the age of onset of dementia and AD-like pathology (7). For example, patients with trisomy 21, a triplication of the chromosome harboring the APP gene, develop early onset dementia with characteristic AD pathology, which is not observed in patients with partial trisomy excluding the APP gene (8). Genetic studies in animal models further support the notion that increased APP expression or processing, either through gene duplication or mutation, can lead to early onset dementia with AD-like pathologies (9).

The correlation of APP levels and APP processing to AD pathogenesis underscores the importance of understanding how neurons regulate APP levels and subcellular localization. The importance of APP, moreover, extends beyond its disease link: APP also plays numerous roles in neuronal function and development. Synapse formation and localization, maintenance of dendritic spines, neurite outgrowth, synaptic plasticity, and neuronal survival are all influenced by APP (10-14). Cleavage of APP is regulated by neuronal activity, and its cleavage products in turn seem to regulate neuronal activity, although the precise function of this feedback remains uncertain (15).

The current study seeks to define pathways that regulate APP levels in neurons, focusing on Fbxo2, a brain-enriched, ubiquitin ligase adaptor subunit that specifically recognizes glycoproteins containing high mannose glycans (16). As a type 1 transmembrane glycoprotein, APP is synthesized in the cytoplasm and

translocated into the endoplasmic reticulum (ER) where it achieves native folding and becomes glycosylated. Properly folded and glycosylated APP then transits from the ER to the Golgi apparatus for further modification, and is eventually delivered to the plasma membrane. APP is known to undergo rapid and constant bulk turnover (17); the extensive, newly synthesized APP that is continually produced by neurons must be appropriately governed for protein quality control purposes. ER-associated-degradation (ERAD) is a normal cellular process by which uncomplexed or improperly modified proteins are removed from the ER and degraded by the ubiquitin proteasome system (UPS). The ERAD ubiquitin ligase HRD1 has already been shown to play a role in clearing mutant or misfolded APP from the ER (18). Knocking down this ligase increases APP levels and promotes Aβ generation. Whether HRD1 is the only ubiquitin ligase that mediates APP clearance from the ER remains uncertain.

For several reasons, Fbxo2 is an attractive candidate to contribute to APP. First, it is a neuron-enriched ubiquitin ligase substrate adaptor protein that binds glycoproteins containing high mannose N-linked glycans and facilitates their degradation through ERAD (19). Second, Fbxo2 was recently shown to decrease levels of the beta secretase enzyme, BACE1, which is essential for Aβ generation, in an N-linked glycan-dependent manner (20). Over-Expression of Fbxo2 resulted in decreased BACE1 levels, in turn diminishing Aβ production. And third, levels of Fbxo2 are decreased in AD patient brains, raising the

intriguing possibility that age-related reduction in Fbxo2 levels might accelerate the amyloid process (20).

Although substrate specificity is conferred by ubiquitin ligases and their adaptors, an individual ligase can have numerous substrates. Here, using cell based studies and *Fbxo2* knockout (*Fbxo2* -/-) mice, we show that Fbxo2 also regulates additional glycoproteins beyond BACE1 in the amyloid precursor pathway, specifically APP itself and the alpha secretase enzyme, ADAM10. Our results suggest that the loss of Fbxo2 results in dysregulation of glycoprotein homeostasis in neurons with implications for APP processing.

EXPERIMENTAL PROCEDURES

Animals – Fbxo2 -/- mice were previously generated through targeted deletion of the first five of six exons encoding Fbxo2. These mice were backcrossed to a C57BL/6J background and exhibited no abnormalities in brain size, weight, development, or adult gross brain structure, though they developed cochlear degeneration (21).

DNA Constructs, HEK Cell Culture, and Lysate Preparation – HEK-293 cells were cultured and maintained as previously described (22). For expression in HEK-293 cells, constructs for full-length APP (produced by D. Selkoe, Addgene plasmid 30154), Myc-Adam10 (produced by R. Derynck, Addgene plasmid 31717), BACE1 (Origene, clone SC115547) or Fbxo2 (gift of K. Glenn, Univ.

Iowa) were transfected with Lipofectamine 2000 (Invitrogen) as per manufacturer's directions. 48 hours after transfection, cells were collected in hot denaturing lysis buffer containing 2% SDS and 100mM DTT. Lysates were boiled for five minutes, centrifuged, and loaded onto 4-15 or 4-20% gradient SDS-PAGE gels (Biorad).

Brain Extraction/Lysis – For western blot experiments, animals were anesthetized with ketamine/xylazine and cardiac perfused with pre-warmed phosphate-buffered saline (PBS). Mice were then decapitated and their brains removed. When required, hippocampi were rapidly dissected under a dissecting microscope. Tissues were then lysed in hot SDS (2%) lysis buffer with 100mM DTT in a dounce homogenizer, centrifuged, and boiled for five minutes. Protein concentrations were determined using a quantification kit (Macerey-Nagel, Duren, Germany) and equal amounts were loaded and run on 4-15 or 4-20% SDS-PAGE gels. For ELISA experiments, brains or hippocampi were lysed in cold RIPA buffer with protease and phosphatase inhibitors (Roche) in a dounce homogenizer, centrifuged, and kept on ice for immediate analysis.

Western Blotting – Proteins were immunoblotted using antibodies against APP (22C11, Millipore) or its C-terminal fragments (polyclonal anti-APP cytoplasmic domain G369 antibody, a gift from S Gandy), Fbxo2 (a gift from K. Glenn, Univ. Iowa, directed against an amino-terminal domain of Fbxo2), Myc (Santa Cruz),

BACE1 (gift from R Vassar), Transferrin Receptor (Invitrogen), Caspase-3 (Cell Signaling) or GAPDH (Millipore).

ELISAs – RIPA buffer-homogenized lysates and collected media were analyzed using ELISA kits according to the manufacturer's instruction. For brain tissue, Aβ42 (high sensitivity, Wako) and sAPPα (IBL) kits were used. For collected media from neurons, soluble APP (sAPPα) (IBL), Aβ40 (Invitrogen), and Aβ42 (Novex/Life Technologies) were used.

Immunohistochemistry of frozen brain sections – Briefly, mice were processed as for brain extraction, but were perfused with 4% paraformaldehyde in PBS following the PBS flush. Upon removal, brains were post-fixed, rinsed, and cryopreserved. Once frozen, they were cut into 12 micron sections and preserved at minus eighty degrees until use. Alexafluor 488 (Invitrogen) was used to visualize 22C11 staining and sections were imaged on a Nikon A1 confocal microscope. All lower intensity images were collected at the same laser, offset, and detection intensity regardless of brain region. Higher intensity images were generated by increasing the brightness equally for all pixels in all images in Fiji Image J. Z-stack images were collected through equal stack dimensions. Images were cropped using Photoshop CS3 (Adobe). Heat maps were generated in Fiji Image J with the Rainbow RGB lookup table. The CA1 region of hippocampus and the portion of visual cortex (V1/V2) directly lateral and superior

to CA1 were imaged. Three mice at the six month time point were used for imaging.

Acute Slice Biotinylation – Surface levels of proteins were compared to total amounts as previously described (23). Briefly, mice were anesthetized and their brains removed. Hippocampi were rapidly dissected in ice cold, oxygenated artificial cerebrospinal fluid (ACSF). 350 µm slices were then cut using a MacIlwain Tissue Chopper, and alternating sections from both hippocampi were placed into cold, oxygenated ACSF with or without EZ-Link Sulfo-NHS-LC-biotin (Pierce). After 45 minutes, slices were washed in artificial cerebrospinal fluid (ACSF) and any unbound biotin was quenched by incubating the slices in lysine. Following additional washes, the non-biotinylated slices were homogenized in SDS (2%) lysis buffer with 100 mM DTT using a dounce homogenizer. Lysates were then boiled and centrifuged and retained at -80º C as the “total” fraction. Slices with biotin were lysed in buffer containing 1% TX-100, 0.1% SDS, 1 mM EDTA, 50 mM NaCl, 20 mM Tris, pH 7.5, with protease inhibitors (Roche) in a glass homogenizer. Biotinylated proteins were then precipitated by the addition of Streptavidin Resin (Pierce) and overnight incubation at 4º C on a rotating platform. Precipitates were then collected by first centrifuging to separate supernatant from resin, then boiling the resin in SDS (2%) lysis buffer with 100mM DTT. The resulting “surface” fraction was retained at minus eighty degrees until being analyzed. 30 µg of protein from each “total” fraction was run alongside 2 µg of enriched “surface” protein.

Hippocampal Neuron Culture and Immunofluorescence – Hippocampal neurons were obtained and cultured from pups 3 days postnatal, maintained, and immunostained as previously described (24). All neurons were analyzed at 14 days in vitro (DIV14). Antibodies against APP (22C11, Millipore), Vesicular Glutamate Transporter (Vglut) (Millipore), Spinophilin (Millipore), PSD-95 (Abcam), and Binding Protein (BiP) (Abcam) were visualized using AlexaFluor 488, 568 or 647 secondary antibodies (Invitrogen). Confocal z-stack images were collected using an A-1 confocal microscope (Nikon) at the University of Michigan Microscopy and Image Analysis Laboratory.

Quantification and Statistical Analysis – Immunoblot results were scanned into Adobe Photoshop and measured using ImageJ software. Prism 6 software (GraphPad) was used for statistical analysis and to generate graphs. Immunofluorescence data was analyzed using ImageJ as previously described (25).

RESULTS

Fbxo2 has been implicated in the clearance of BACE1 (20). To determine whether Fbxo2 facilitates the degradation of other key glycoproteins in the amyloid processing pathway, we expressed constructs encoding full-length APP or a Myc epitope-tagged form of the alpha-secretase ADAM10 in HEK cells together with empty vector or FLAG-tagged Fbxo2 (Fig7). BACE1, already

established as an in vitro substrate for Fbxo2, was included as a positive control (Fig7, c). Co-expression of Fbxo2 resulted in a marked decrease in steady-state levels of each co-expressed substrate as measured by western blot. The antibodies for APP and ADAM10 detect bands for both immature, high mannose glycan-bearing and mature, complex glycan-bearing forms of the protein on western blot. Levels of APP are significantly decreased when co-expressed with Fbxo2 (Fig7, a). A similar reduction is seen when Fbxo2 is co-expressed with ADAM10, with the immature form of ADAM10 being further reduced (Fig7, b)(26). These ADAM10 results are consistent with the canonical view of the role of Fbxo2 in ERAD, as immature forms of these proteins still carry high mannose glycans (the major ligand for Fbxo2), which are later processed to complex glycans in the Golgi apparatus.

As Fbxo2 is a brain-enriched protein (27), we next sought to determine whether these APP pathway components, identified here as Fbxo2 substrates in heterologous, non-neuronal cell systems, are also physiologically relevant in neuronal cells. Cultured neurons isolated from wild-type and *Fbxo2* knockout mice previously generated in our lab offer three distinct advantages for addressing this question: First, we are able to measure endogenous proteins without the confounding factor of transient over-expression; second, media collected from cultures provides a feasible and practical way to assess the processing of APP into its secreted cleavage products; and third, neurons are more easily visualized in culture than in vivo, allowing for a better assessment of

any potential differences in the localization of APP. Primary cultures of hippocampal neurons were prepared from mice at postnatal day 3. Cultured neurons lacking Fbxo2 differed markedly from wild-type neurons in several respects. Compared to levels in wild-type cultured neurons, total APP levels were elevated in *Fbxo2 -/-* neurons as revealed by Western blot (Fig 8, a). ELISA assessment of media collected from *Fbxo2 -/-* neuronal cultures revealed more than double the levels of secreted Aβ40, Aβ42 and sAPPα (Fig 8, b). The ratio of Aβ40 to Aβ42 remained unchanged, with both metabolites increasing proportionately (Fig 8, b). Neither ADAM10 nor BACE1 levels differed between wild-type and Fbxo2 knockout neurons (data not shown).

We next examined the distribution of the increased APP observed in Fbxo2 null neurons (Fig 9). Quantitative immunofluorescence showed that while APP levels were higher throughout *Fbxo2 -/-* neurons, APP accumulated to a greater degree in dendrites than in soma (Figure 9, a, d). Immunoreactive APP puncta were observed along dendrites with greater frequency and size than in wild-type controls. Consistent with previous studies describing APP trafficking to synapses (28), APP puncta in dendrites colocalized with the pre- and post-synaptic markers Vglut and Spinophilin (Fig 9 a, b). Remarkably, the amount of synaptic marker-positive puncta, additionally measured with the postsynaptic scaffolding protein PSD95, was significantly increased in neurons lacking Fbxo2 (Fig 9, c, d). BiP, an ER-resident protein whose accumulation is indicative of ER stress, was not increased in knockout neurons (Fig 9, d). Caspase 3, a cytosolic protein whose

cleavage is believed to play a role in apoptosis, was also assessed by western blot (Fig 9, d). No difference in the level of uncleaved caspase-3 was observed between wild-type and knockout neurons, and no cleaved Caspase 3 was detected for either genotype. These results suggest that the loss of Fbxo2 does not cause pathological consequences for neuronal health, nor does it universally affect protein expression.

Having identified several changes in APP handling in cultured neurons, we next assessed these changes in the intact brain. Examination of brains from wild-type and *Fbxo2* knockout mice at several ages revealed age-dependent differences. We observed a significant increase in endogenous APP levels in *Fbxo2* knockout mouse brain at three and six months of age as measured by western blot from whole brain lysates (Fig 10, a). The time course of this difference is consistent with the onset of murine Fbxo2 expression during the first month of age. We next sought to visualize the difference in APP expression between wild-type and knockout mice. In cortex at six months, anti-APP immunofluorescence confocal imaging revealed that both the cell bodies of cortical neurons and the surrounding neuropil are more strongly labeled in knockout cortex than in control cortex (Fig 11, a). Image brightness was equally increased (Figure 11, c) to help visualize the comparatively less-bright staining in wild-type mice. Whereas in vitro we observed a shift toward higher dendritic expression, in vivo we observe increased expression throughout the cell bodies and neuronal projections of the cortex.

ELISA experiments were used to assess whether the increased steady-state levels of APP seen in *Fbxo2* knockout mice corresponded to an increase in cleavage products. No change in the amyloid cleavage products Aβ42 and sAPPα was observed at the level of whole brain (Fig 10, b, c). However, since amyloid cleavage products are rapidly removed from the brain through enzymatic degradation, glial uptake, and cerebrospinal fluid (CSF) clearance (29), attempts to quantify secreted amyloid cleavage products by measuring brain tissue lysates can be confounded by these factors, making it difficult to gauge fully the extent of the role played by Fbxo2 in brain tissue. No differences were observed at three or six months of age in the levels of APP C-terminal fragments (CTFs) C99, C89, or C83 (Fig 10, d). It is possible that knockout mice have no difficulty limiting these fragments to appropriate levels.

The previous study linking Fbxo2 to the regulation of BACE1 employed transient shifts in Fbox2 levels, either through heterologous cell expression or over-expression in mice (20). As shown earlier in Fig1, we similarly used transient expression to demonstrate facilitated degradation of BACE1 by Fbxo2 and to identify ADAM 10 as an additional Fbxo2 substrate. When *Fbxo2* is constitutively knocked out in the mouse, however, we did not detect any alteration in endogenous BACE1 or ADAM10 levels (Fig 10, e, f).

Fbxo2 is expressed throughout the brain, but at higher levels in forebrain and midbrain than in hindbrain (27). AD preferentially affects specific brain regions including the hippocampus (30). To test whether the effects of *Fbxo2* knockout on APP pathway components were more pronounced in this disease-relevant region, hippocampi were dissected and similarly assessed for APP levels. At three and six months of age, there was no statistical difference in total APP observed between *Fbxo2*+/+ and *Fbxo2 -/-* in the hippocampus (Fig 12, a). Consistent with our western blot data, anti-APP immunofluorescence of the hippocampus did not reveal a significant difference between wild-type and knockout mice (Fig 12, e). There was, however, a significant increase in hippocampal levels of Aβ42 at three months of age in *Fbxo2 -/-* mice and a non-statistically significant trend toward increased sAPPα (Fig 12, c). The observation that the whole brain of *Fbxo2 -/-* mice carries more uncleaved APP (Fig 10, a) while the hippocampus carries more APP cleavage products may reflect regional differences in neuronal activity and amyloid processing, as previously described (15). In such a scenario, we might expect to see this change reflected in increased levels of CTFs of APP in *Fbxo2* knockout mouse hippocampus. We did not, however, observe differences in the levels of CTFs between wild-type and knockout hippocampi at three or six months (Fig 12, d), despite a level of amyloid beta in knockout hippocampus at three months which is 50% greater than it is in wild-type hippocampus. Taken together, these data suggest that there are region-specific responses to the effects of eliminating Fbxo2.

Aβ is primarily generated from APP that has been endocytosed from the cell surface and transported to the trans-Golgi network where it is cleaved by BACE1 (11,31-33). Alterations to surface APP levels have been shown to affect Aβ production (31,33). To determine whether the increase in amyloid cleavage products observed in three-month-old hippocampus corresponds to a decrease in surface APP, we performed in vivo biotinylation of acute hippocampal slices from three-month old mice, a technique that allows one to estimate the cell surface versus intracellular pools of APP or other protein of interest. In contrast to the lack of change in total hippocampal APP, the amount of surface APP in the hippocampus of Fbxo2 -/- mice was indeed significantly decreased compared to wild-type controls (Fig 13, b). The Transferrin Receptor (TfR) was used as a control glycoprotein known to have some surface expression, and no difference in the amount of surface TfR was observed between genotypes. These results suggest that although total levels of APP appear unaltered in the hippocampus of Fbxo2 knockout mice, the handling of APP with respect to its surface localization is significantly different, which may reflect increased processing into Aβ.

DISCUSSION

Here we describe a broader role for Fbxo2 than previously recognized in handling glycoprotein turnover relevant to APP processing. The constant demand for newly produced APP in neurons requires optimal protein quality control, and ERAD provides an effective means of clearing unwanted, immature glycoproteins still bearing high-mannose glycans. As a brain-enriched ubiquitin

ligase adaptor subunit, Fbxo2 binds to such glycans on immature glycoproteins and facilitates their ubiquitin-dependent degradation. In the current study, we combined cell-based and animal models to show that Fbxo2 contributes to the regulation of both the steady-state levels of APP and its cleavage products.

Our results in cell-based, transient expression models support previous work (20) implicating Fbxo2 in handling BACE1 and extend Fbxo2 activity to two other critical amyloid pathway glycoproteins, APP and ADAM10. There are, however, important differences between our cell-based findings and our results in *Fbxo2* knockout mice that underscore the importance of combining in vitro and vivo studies when seeking to define the role of a ubiquitin pathway protein like Fbxo2. Over-Expression in transient systems may elicit protein behaviors and protein-protein interactions not readily observed under normal, or more physiological, conditions. The fact that we do not see changes in BACE1 in *Fbxo2* knockout mice does not necessarily conflict with the previously findings by Gong et al (20). Their studies employed transient changes to Fbxo2 levels in vivo and in vitro, and similarly, our transient over-expression studies in heterologous cell models strongly support the view that Fbxo2 facilitates the degradation of BACE1. The same is true for our transient expression studies showing Fbxo2 activity toward ADAM10. Under more physiologic conditions with endogenous ADAM10 and BACE1, however, no such effects are observed in *Fbxo2* knockout mice. We suggest that the lifelong deprivation from Fbxo2 occurring in *Fbxo2 -/-* mice expressing endogenous levels of BACE1 and ADAM10 may elicit redundant

cellular mechanisms by which these proteins are regulated, resulting in only a partial effect of Fbxo2 absence on APP levels and no observed effect on BACE1 or ADAM10 levels in vivo. In the future, conditional *Fbxo2* knockout models could be utilized to address the discrepancy between previous in vitro data and the in vivo data presented here.

Our results suggest APP may be processed more extensively in *Fbxo2* -/- hippocampus than in wild type hippocampus, as there is an increased amount of Aβ compared to cortex with a decreased amount of total APP. In opposition to this idea, we were unable to detect an increase in APP C-terminal fragments in cortex or hippocampus at three or six months. While this seems counter-intuitive for the time point at which increased Aβ is observed, the processes by which these fragments are cleared are not entirely understood, although they may involve autophagic mechanisms. In *Fbxo2* knockout mice, presumably any excess in CTFs above the normal amount found in wild-type mice are cleared through a non-*Fbxo2* dependent manner as they no longer contain glycans.

There is brain region selectivity regarding the effect of Fbxo2 absence on the steady-state levels of APP as revealed by immunohistochemistry. In the cortex, imaging reveals strong staining for APP within neurons and throughout the neuropil. In the hippocampus, however, the signal is markedly less than that observed in the cortex, consistent with our finding that in *Fbxo2 -/-* mice, full-length APP is increased in whole brain but not in the hippocampus per se. With

no apparent difference in the level of Fbxo2 expression between cortex and hippocampus of wild type mice, it remains to be determined why the loss of this protein would result in differing effects on a substrate in distinct brain regions.

Given the absence of changes to BACE1 and ADAM10 levels in *Fbxo2* knockout mice, the apparent increased cleavage of APP in the hippocampus of knockout mice becomes more difficult to explain. If, in the absence of Fbxo2, APP bypasses ERAD and transits from the ER to the cell surface where it is subsequently endocytosed and cleaved, then we would anticipate that the ratio of surface to total APP might remain the same while seeing an increase in total cleavage products. Essentially both APP and its cleavage products would increase, as observed in our cultured hippocampal neurons. In *Fbxo2* knockout hippocampal neurons, however, the intracellular pool of APP and the cleavage products are both increased, presumably at the expense of the surface pool. What might cause the surface pool of APP to become more rapidly depleted in *Fbxo2* knockout mice remains to be determined. Conceivably, the absence of Fbxo2 drives excess APP to the neuronal cell surface, but into a different subregion of the plasma membrane or in an altered conformational state that allows it to be endocytosed and cleaved at a greater rate. Further analysis of *Fbxo2* -/- mice may reveal whether, for example, there is preferential distribution of surface APP to lipid rafts, allowing for more rapid processing into Aβ (34). Alternatively, the loss of Fbxo2 may permit the continued existence of a pool of improperly complexed or folded APP which is not properly trafficked to the

surface and is preferentially retained in cortical neurons over hippocampal neurons.

It is important to recognize that Fbxo2 may have functions beyond ERAD. It is expressed throughout neurons including near synapses, far from the bulk of ER in neurons. The only known binding preference of Fbxo2 is for high mannose N-linked glycans on glycoproteins, which traditionally are modified during passage through the secretory pathway, losing their high mannose status in the process (35). There is, however, precedence for cell surface expression of high mannose forms of another known Fbxo2 substrate, the NMDA receptor subunit GRIN1 (36): all GRIN1 in neurons is susceptible to cleavage by EndoH, which cleaves high mannose N-linked glycans but not the complex glycans present on most glycoproteins after processing in the Golgi apparatus (37). Accordingly, even at the synaptic membrane GRIN1 remains a potential substrate for Fbxo2. The post-translational modifications to which APP is subjected are complex, and it remains uncertain whether immature (i.e. high mannose glycan-bearing) forms of APP exist in the cell beyond the ER. If APP retains high mannose forms of N-linked glycans on the cell surface, then Fbxo2 could play a role in regulating the endocytosis of APP through ubiquitination. An effect on differential trafficking of APP - namely, the retention of APP in specific cellular compartments - has been attributed to Ubiquilin 1 (UBQLN1): polyubiquitination by UBQLN1 sequesters APP in the Golgi (38). Given this observation, we examined the relative distribution of APP in ER and Golgi of neurons in *Fbxo2 -/-* and wild-type mice

and found no differences in the pattern of expression (data not shown). While these data suggest that altered sequestration of APP in the ER and Golgi does not occur, sequestration elsewhere in the secretory pathway or other vesicular bodies cannot be ruled out.

Our analysis of cultured hippocampal neurons suggests that neuronal connectivity is altered in the absence of Fbxo2. The marked changes in number and intensity of synaptic puncta in Fbxo2 knockout neurons are especially intriguing. It is unlikely these data represent a universal increase in protein expression in the absence of Fbxo2, as the levels of two tested proteins that are not expected to interact with Fbxo2, BiP and Caspase-3, are unchanged. However, whether these additional synapses function normally remains unknown. The presence of presynaptic terminals directly opposed to these postsynaptic markers suggests they are not “silent” synapses. But there may be other compensatory mechanisms by which these additional synapses are regulated. Future studies will be required to examine the composition and contribution of these synapses. If these additional synaptic connections are indeed active, their activity may feed back onto APP processing. Intriguingly, both Aβ and sAPPα possess dose-dependent neuromodulatory functions (14).

It is somewhat puzzling that cultured neurons from *Fbxo2 -/-* mice maintain more synapses in the presence of elevated Aβ, which has been shown to eliminate synapses (4). It is not known how many substrates Fbxo2 has, but with regard to

synaptic dynamics two may be of particular importance: Beta Integrin 1 (16) and GRIN1 (36). Beta Integrin 1 is a membrane receptor that supports cell adhesion and responds to cues from surrounding cells. GRIN1 mediates the formation of NMDA receptors, which have profound effects on plasticity and structural change at the synapse. Both of these Fbxo2 substrates can significantly affect synapse formation, assembly, and maintenance. Therefore, we consider it unlikely that all or even most of the synaptic changes in Fbxo2 null neurons and brain can be attributed to altered APP alone.

In summary, our findings implicate Fbxo2 as a potentially important upstream regulator of key elements of neuronal health and function – APP processing and synaptic connectivity – that are also central to the pathogenesis of AD and perhaps other neurodegenerative diseases.

FIGURE LEGENDS

Figure 7. Fbxo2 expression leads to decreased levels of key glycoproteins in the amyloid pathway

(a) APP levels are decreased in the presence of Fbxo2. HEK293 cells expressing full-length APP together with empty vector (EV) or vector encoding Fbxo2 were collected 48 hours after transfection. Lysates were examined by western blot with antibodies recognizing APP (22C11), Fbxo2, or GAPDH (upper panel). The mature, complex glycan-bearing form is denoted at ~130kD, and the immature, high mannose glycan-bearing form at ~110kD. Results of triplicate experiments

were quantified (lower panel). (b) ADAM10 levels are decreased when Fbxo2 is co-expressed. Fbxo2 and ADAM10 were co-expressed as in panel a., and levels of ADAM10 were measured by anti-myc antibody (upper panel) and quantified (lower panel). The mature form of ADAM10 is observed at ~60kD and the immature form at ~85kD. (c) Fbxo2 expression leads to decreased BACE1. As in panel a., BACE1 and Fbxo2 were coexpressed and BACE1 levels were assessed by western blot using an anti-BACE1 antibody (upper panel) and quantified (lower panel). This antibody detects a single band of ~60kD corresponding to mature BACE1. Shown in lower panels are mean values from triplicate experiments. Error Bars = S.E. *, $p<0.05$; ** $p<0.01$; **** $p<0.0001$; (unpaired t test).

Figure 8. Dysregulated APP processing and levels in *Fbxo2 -/-* neurons
(a) Increased APP in cultured *Fbxo2* null neurons. Cultured hippocampal neurons from p3 wild type and knockout pups, DIV 14, were lysed and APP levels measured by western blot. Representative results from four dishes per genotype are presented (left panel). A significant increase in APP was observed and quantified (right panel); three replicates from different culture preparations were measured to control for potential prep-to-prep differences. (b) Loss of Fbxo2 results in a doubling of secreted APP cleavage products. Neuronal culture media was exchanged and then collected four days later and assessed by ELISA for secreted APP products. Each measured product was approximately doubled in the knockout neurons, with the ratio of Aβ40 to Aβ42 remaining

unchanged (lower left panel). As in panel (a) representative quantification of quadruplicate samples from a single preparation are presented; three different preparations showed similar results. Error Bars S.E. *, *** p<0.001; **** p<0.0001 (unpaired t test).

Figure 9. Loss of Fbxo2 results in increased APP, altered APP localization and increased synaptic markers in cultured hippocampal neurons

(a) APP is increased and distributed differently in *Fbxo2* null neurons. DIV 14 hippocampal neurons were fixed, permeabilized, and immunostained for APP and synaptic markers. Representative confocal images of wild-type and knockout neurons reveal increased overall APP compared to wild type controls, with a greater increase in dendritic than somatic immunoreactivity. APP-immunoreactive puncta (arrows in a, b) were observed to co-localize with the presynaptic marker Vglut (a) and with the postsynaptic marker Spinophilin (b). Levels of Vglut, Spinophilin, BiP, and PSD-95 (c) were also assessed and quantified, shown in (d). Caspase 3 (d) was measured by western blot as in Figure 8. Quantification of immunofluorescence was performed in six to eight neurons per genotype. For somatic and dendritic analysis, three to six dendritic segments of 100 um per neuron and six neurons per genotype were measured. Error Bars = S.E. ** p<0.01; *** p<0.001; (unpaired t test). Scale bar = 25um.

Figure 10. Increased levels of APP, but not Amyloid-β, in *Fbxo2* -/- brain.

(a) The absence of Fbxo2 increases APP levels in whole brain. APP levels in brain lysates from wild-type and *Fbxo2* null mice were assessed by western blot. Representative immunoblot results from three mice of each genotype at six months are shown (left panel). APP levels were quantified and normalized at three time points, with an n of three animals per genotype at each time point (right panel). Error Bars S.E. *, $p<0.05$ (unpaired t-test). (b) and (c), APP cleavage products are not increased in whole brain of *Fbxo2* null mice. ELISA assays for Aβ42 (b) and sAPPα (c) were performed on protein homogenates from whole brains of three mice per genotype at the indicated time points. (d) Levels of APP C-terminal fragments were measured in triplicate at three and six months by western blot. Results for three month time point are presented (left panel) and results for both time points were quantified relative to loading control and total APP (right panel). (e,f) ADAM10 (e) and BACE1 (f) expression are not changed in the absence of Fbxo2. Data shown represent quantification of three animals per genotype at three months. Additional time points were examined and no differences were observed.

Figure 11. Increased levels of APP in *Fbxo2* -/- brain.

APP immunoreactivity is increased in the cortex of Fbxo2 null mice. (a) Confocal microscopy shows increased levels of APP in *Fbxo2* -/- mice (column a, lower row) compared to wild-type mice (upper row). From left to right, results from cortices are shown at 10x (a) and then in the denoted inset at 60x with a 2x optical zoom, at relatively lower (b) and higher brightness (c). (d) A heat map at

the far right illustrates differences in pixel intensity. Scale bar = 50um (a) and 20um (b).

Figure 12. Unchanged APP levels, but increased Amyloid-β, in *Fbxo2* -/- hippocampus.

(a) Loss of Fbxo2 does not alter full length APP levels in the hippocampus. Hippocampi from wild-type and *Fbxo2* null mice were dissected, lysed, and examined by western blot at three and six months of age. Representative immunoblots from six months are shown (left panel) and quantified in three animals per genotype at three and six months (right panel). (b) APP cleavage products are increased in the hippocampus of *Fbxo2* null mice. ELISAs show a significant increase in Aβ42 (b) at three months and suggest a nonstatistically significant increase in sAPPα (c). Results from three mice per genotype per time point were quantified. Error Bars = S.E. *, $p<0.05$ (unpaired t-test). (d) APP C-terminal fragment levels were also measured in triplicate at three and six months by western blot. Results from three month time point are shown (left panel) and quantified relative to loading control and total APP for both time points (right panel). (e) APP immunoreactivity is unaltered in the hippocampus of *Fbxo2* null mice. Confocal microscopy reveals no difference in the levels of APP in *Fbxo2* -/- mice (right panels) compared to wild-type mice (left panels). From left to right, results from the CA1 region of hippocampi are shown at 10x, and then in the denoted inset at 60x with a 2x optical zoom.

Figure 13. Decreased Surface Localization of APP in Hippocampi of *Fbxo2* -/- mice

(a) Schematic of biotinylation procedure to assess surface APP levels in hippocampal slices. Acute hippocampal slices were incubated with oxygenated artificial cerebrospinal fluid (ACSF) with or without biotin for 45 minutes, washed, blocked with lysine, lysed and homogenized, after which labeled surface proteins were affinity purified with streptavidin beads (see Experimental Procedures). (b) Surface levels of APP are reduced in the absence of Fbxo2. Acute slices were processed as above and total and surface fractions were examined by western blot for APP, GAPDH, or the transferrin receptor as a control glycoprotein with surface expression. Representative results from a single animal of each genotype are shown (left panel). Three animals per genotype from three months of age were examined and the results quantified (right panel). Error Bars = S.E. ** $p<0.01$ (unpaired t test).

Figure 7

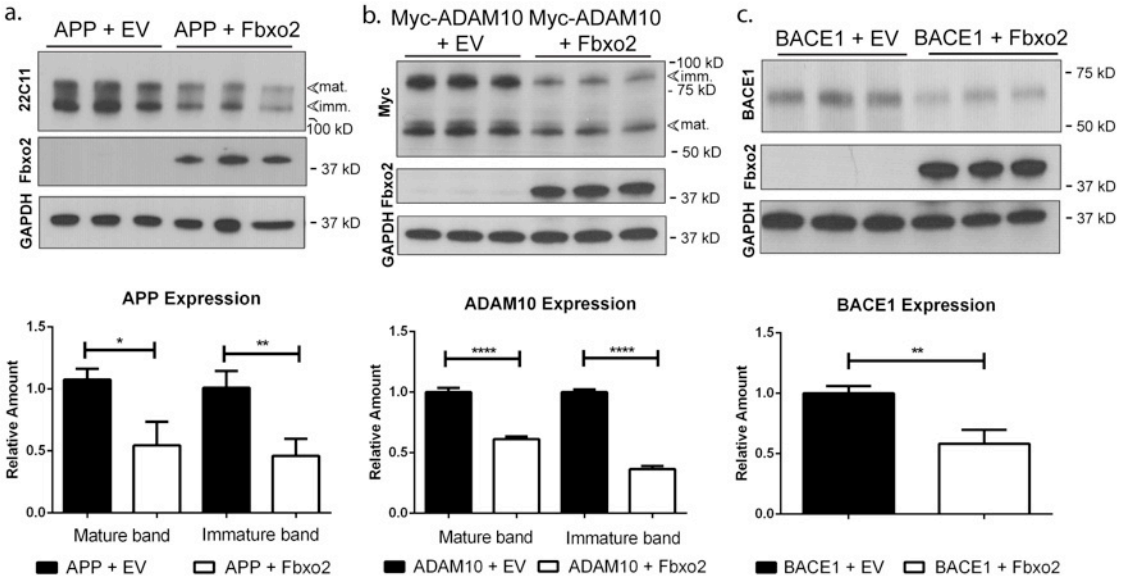

Figure 7. Fbxo2 expression leads to decreased levels of key glycoproteins in the amyloid pathway

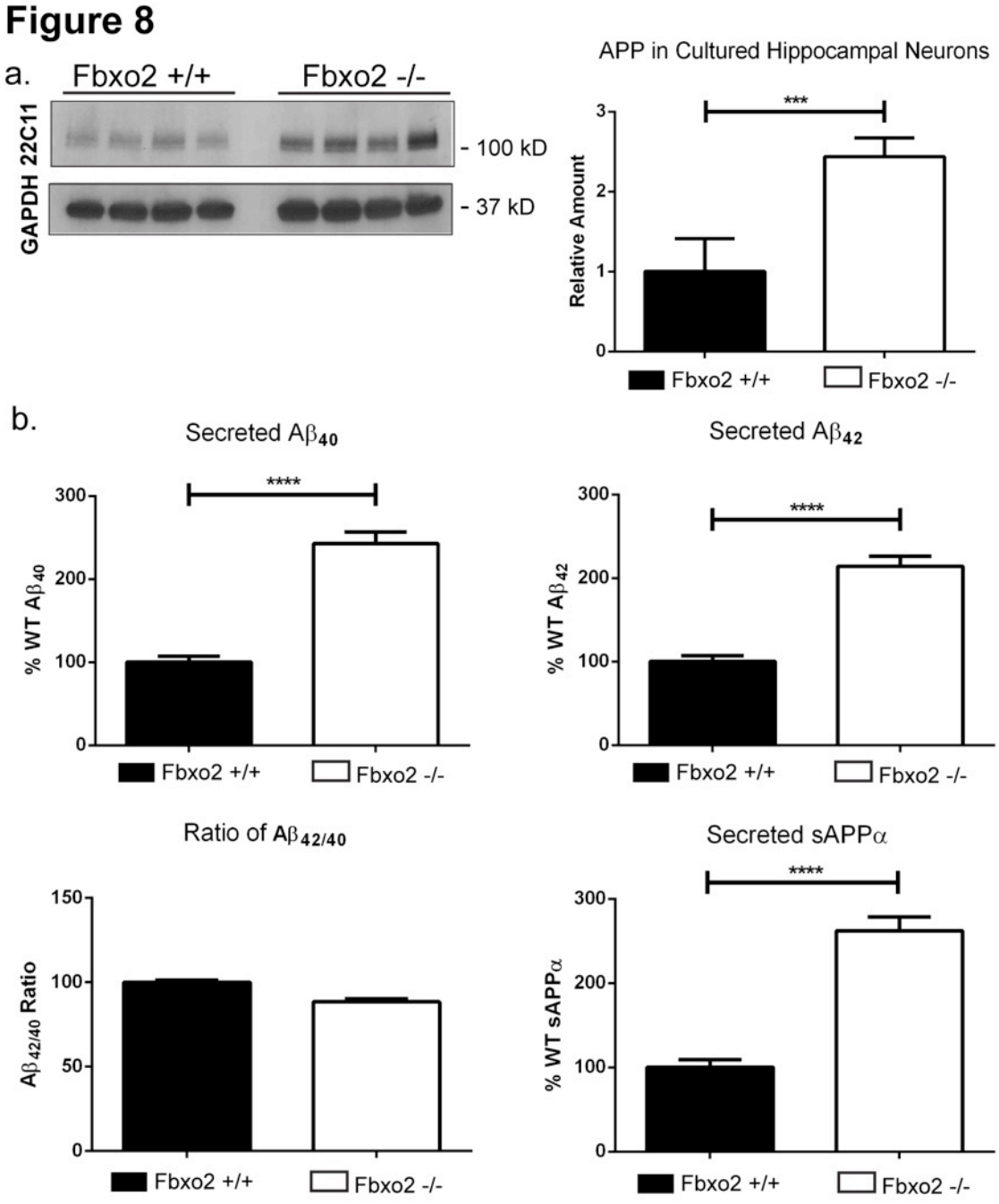

Figure 8. Dysregulated APP processing and levels in *Fbxo2 -/-* neurons

Figure 9

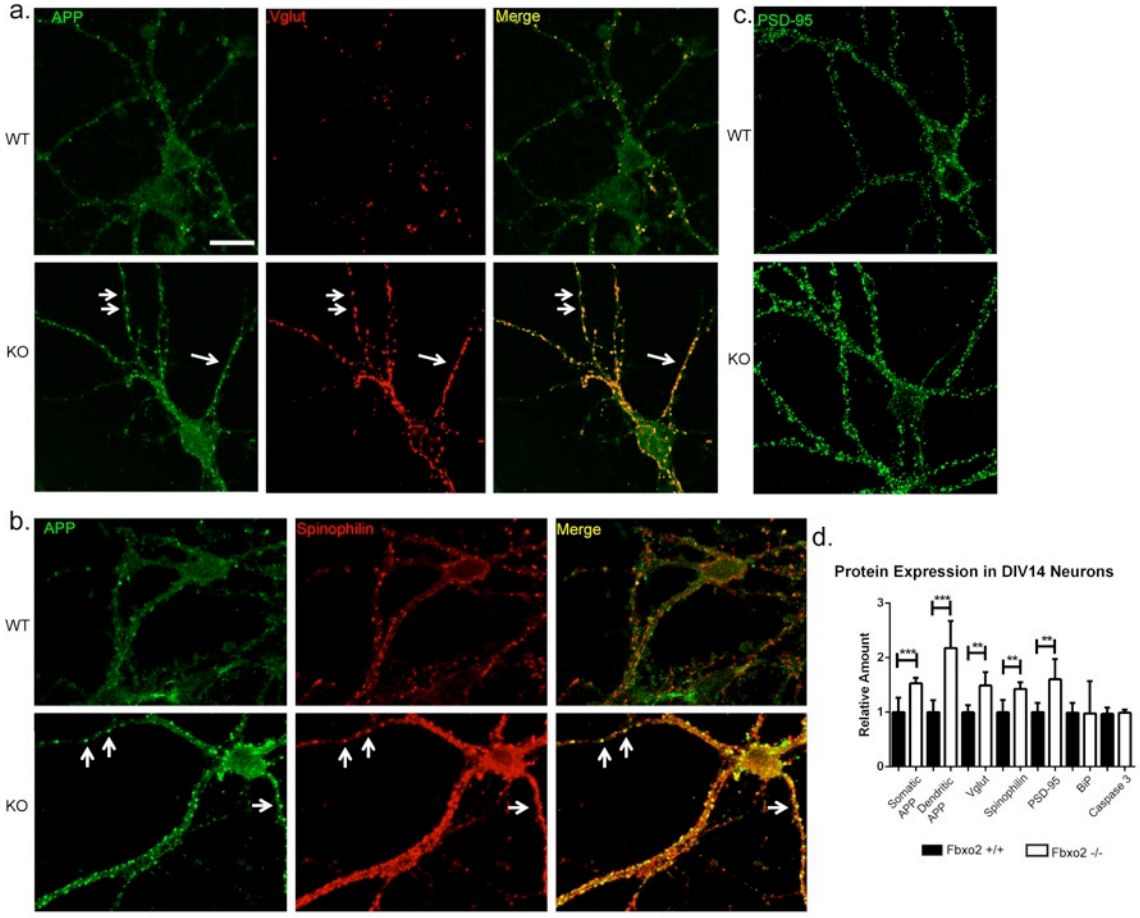

Figure 9. Loss of Fbxo2 results in increased APP, altered APP localization and increased synaptic markers in cultured hippocampal neurons

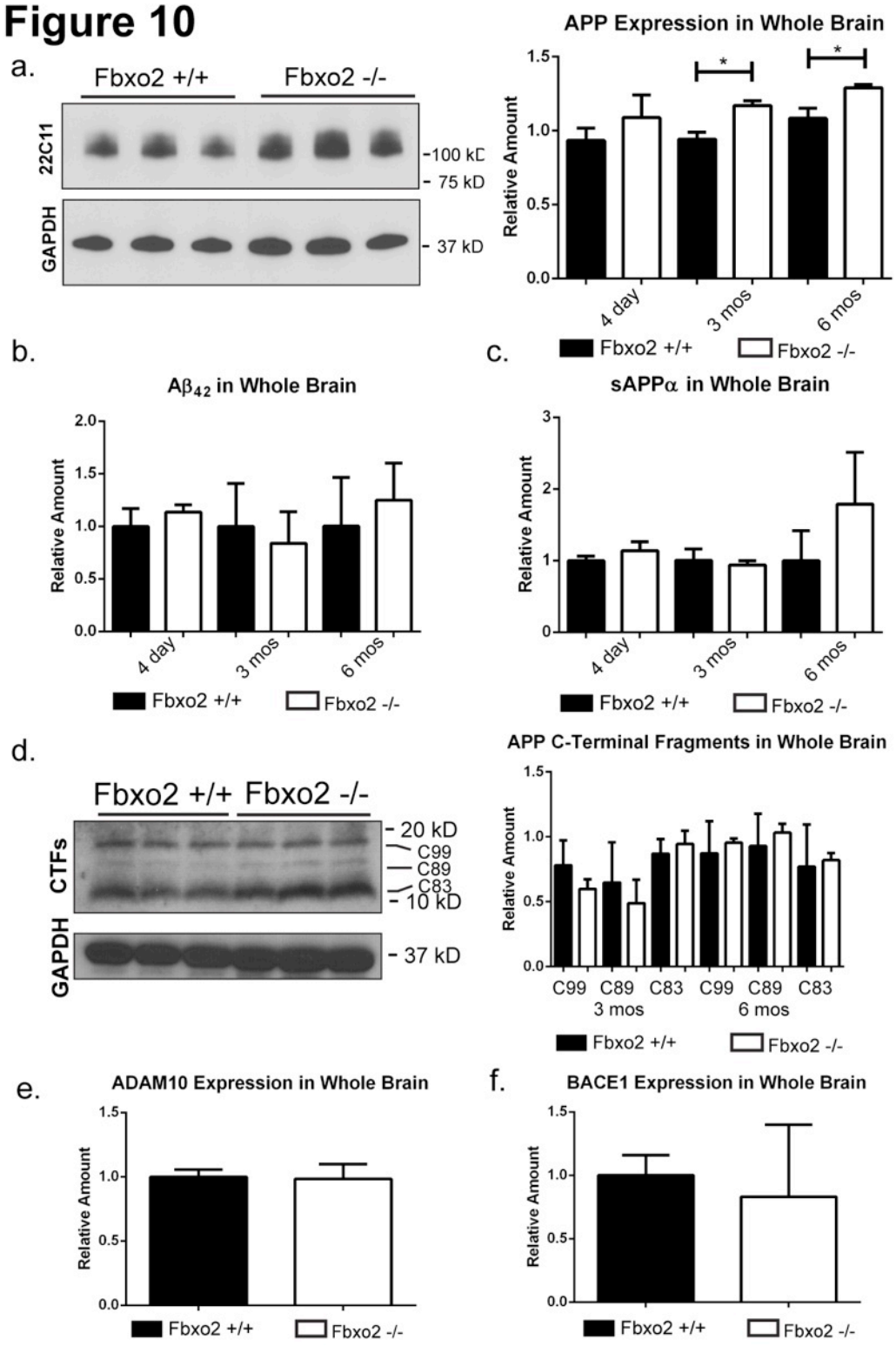

Figure 10. Increased levels of APP, but not Amyloid-β, in *Fbxo2* -/- brain.

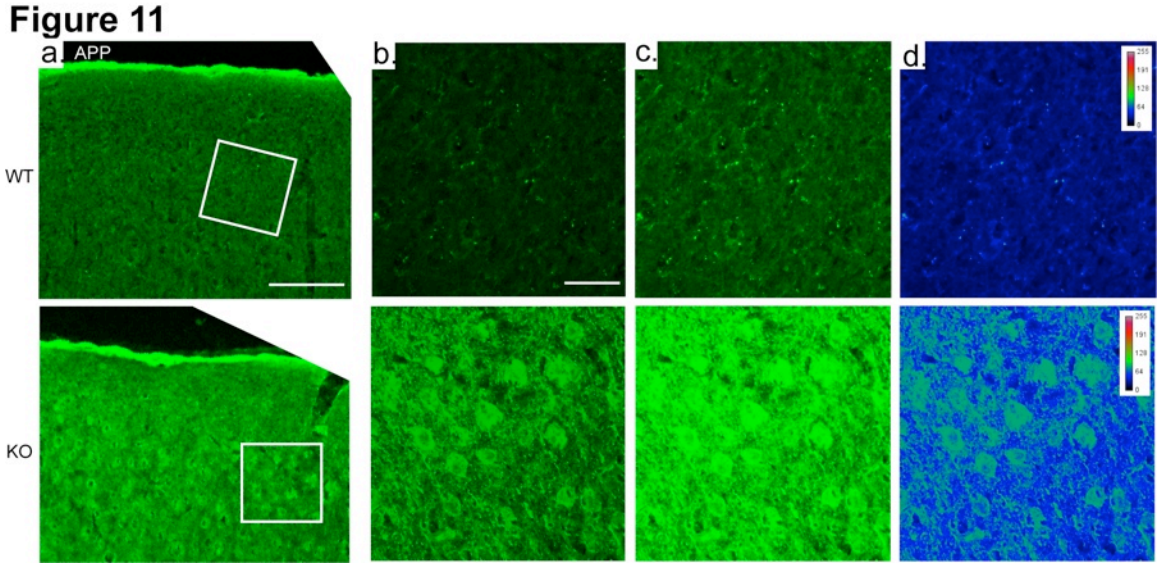

Figure 11. Increased levels of APP in *Fbxo2* -/- brain.

Figure 12

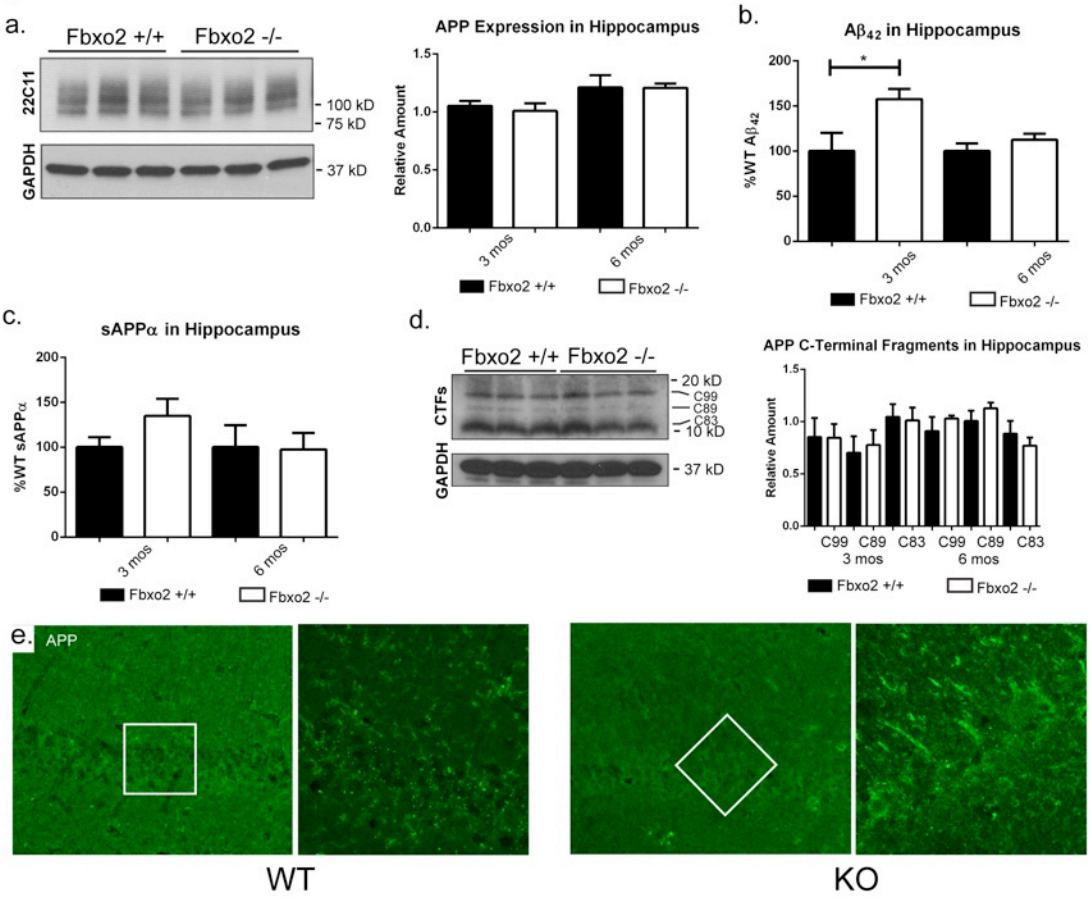

Figure 12. Unchanged APP levels, but increased Amyloid-β, in *Fbxo2* -/- hippocampus.

Figure 13

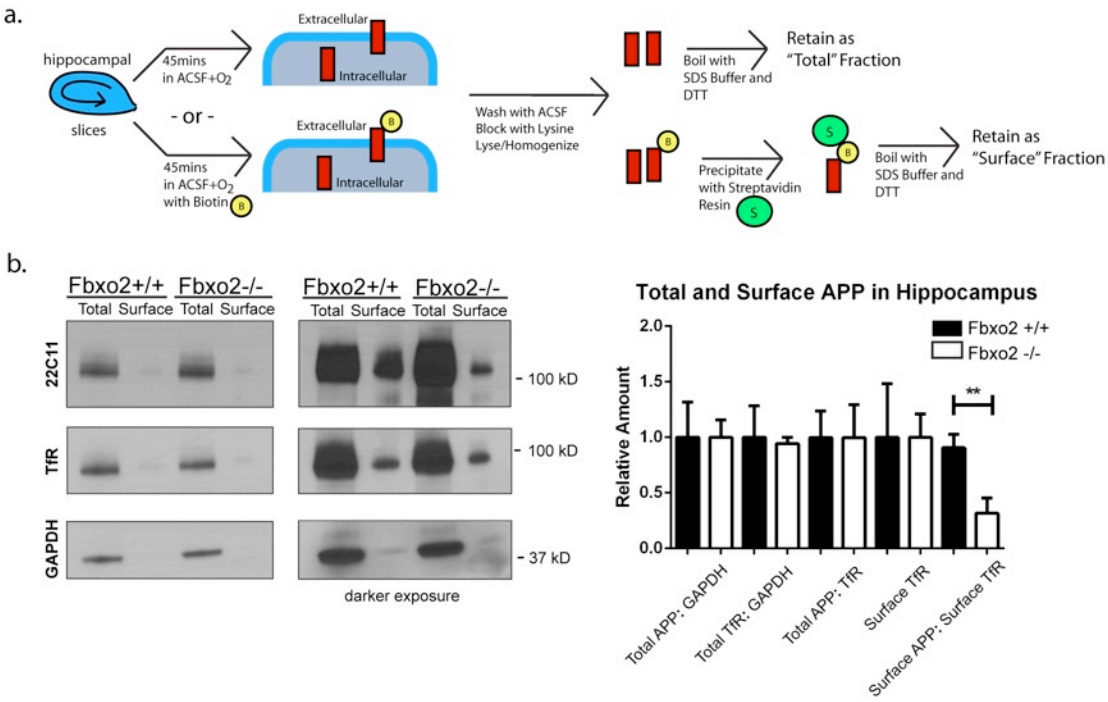

Figure 13. Decreased Surface Localization of APP in Hippocampi of *Fbxo2* -/- mice

REFERENCES

1. De Strooper, B., Vassar, R., and Golde, T. (2010) The secretases: enzymes with therapeutic potential in Alzheimer disease. *Nat Rev Neurol* **6**, 99-107
2. Bertram, L., Lill, C. M., and Tanzi, R. E. (2010) The genetics of Alzheimer disease: back to the future. *Neuron* **68**, 270-281
3. Thinakaran, G., and Koo, E. H. (2008) Amyloid precursor protein trafficking, processing, and function. *J Biol Chem* **283**, 29615-29619
4. Purro, S. A., Dickins, E. M., and Salinas, P. C. (2012) The secreted Wnt antagonist Dickkopf-1 is required for amyloid beta-mediated synaptic loss. *J Neurosci* **32**, 3492-3498
5. Palop, J. J., Chin, J., and Mucke, L. (2006) A network dysfunction perspective on neurodegenerative diseases. *Nature* **443**, 768-773
6. Citron, M. (2010) Alzheimer's disease: strategies for disease modification. *Nat Rev Drug Discov* **9**, 387-398
7. Brouwers, N., Sleegers, K., Engelborghs, S., Bogaerts, V., Serneels, S., Kamali, K., Corsmit, E., De Leenheir, E., Martin, J. J., De Deyn, P. P., Van Broeckhoven, C., and Theuns, J. (2006) Genetic risk and transcriptional variability of amyloid precursor protein in Alzheimer's disease. *Brain* **129**, 2984-2991
8. Millan Sanchez, M., Heyn, S. N., Das, D., Moghadam, S., Martin, K. J., and Salehi, A. (2012) Neurobiological elements of cognitive dysfunction in down syndrome: exploring the role of APP. *Biol Psychiatry* **71**, 403-409
9. Rovelet-Lecrux, A., Hannequin, D., Raux, G., Le Meur, N., Laquerriere, A., Vital, A., Dumanchin, C., Feuillette, S., Brice, A., Vercelletto, M., Dubas, F., Frebourg, T., and Campion, D. (2006) APP locus duplication causes autosomal dominant early-onset Alzheimer disease with cerebral amyloid angiopathy. *Nat Genet* **38**, 24-26
10. Tyan, S. H., Shih, A. Y., Walsh, J. J., Maruyama, H., Sarsoza, F., Ku, L., Eggert, S., Hof, P. R., Koo, E. H., and Dickstein, D. L. (2012) Amyloid precursor protein (APP) regulates synaptic structure and function. *Mol Cell Neurosci* **51**, 43-52
11. De Strooper, B., and Annaert, W. (2000) Proteolytic processing and cell biological functions of the amyloid precursor protein. *J Cell Sci* **113 (Pt 11)**, 1857-1870
12. Mattson, M. P. (1997) Cellular actions of beta-amyloid precursor protein and its soluble and fibrillogenic derivatives. *Physiol Rev* **77**, 1081-1132
13. Cousins, S. L., Hoey, S. E., Anne Stephenson, F., and Perkinton, M. S. (2009) Amyloid precursor protein 695 associates with assembled NR2A- and NR2B-containing NMDA receptors to result in the enhancement of their cell surface delivery. *J Neurochem* **111**, 1501-1513
14. Puzzo, D., Privitera, L., Fa, M., Staniszewski, A., Hashimoto, G., Aziz, F., Sakurai, M., Ribe, E. M., Troy, C. M., Mercken, M., Jung, S. S., Palmeri, A., and Arancio, O. (2011) Endogenous amyloid-beta is necessary for hippocampal synaptic plasticity and memory. *Ann Neurol* **69**, 819-830

15. Bero, A. W., Yan, P., Roh, J. H., Cirrito, J. R., Stewart, F. R., Raichle, M. E., Lee, J. M., and Holtzman, D. M. (2011) Neuronal activity regulates the regional vulnerability to amyloid-beta deposition. *Nat Neurosci* **14**, 750-756
16. Yoshida, Y., Chiba, T., Tokunaga, F., Kawasaki, H., Iwai, K., Suzuki, T., Ito, Y., Matsuoka, K., Yoshida, M., Tanaka, K., and Tai, T. (2002) E3 ubiquitin ligase that recognizes sugar chains. *Nature* **418**, 438-442
17. Morales-Corraliza, J., Mazzella, M. J., Berger, J. D., Diaz, N. S., Choi, J. H., Levy, E., Matsuoka, Y., Planel, E., and Mathews, P. M. (2009) In vivo turnover of tau and APP metabolites in the brains of wild-type and Tg2576 mice: greater stability of sAPP in the beta-amyloid depositing mice. *PLoS One* **4**, e7134
18. Kaneko, M., Koike, H., Saito, R., Kitamura, Y., Okuma, Y., and Nomura, Y. (2010) Loss of HRD1-mediated protein degradation causes amyloid precursor protein accumulation and amyloid-beta generation. *J Neurosci* **30**, 3924-3932
19. Nelson, R. F., Glenn, K. A., Miller, V. M., Wen, H., and Paulson, H. L. (2006) A novel route for F-box protein-mediated ubiquitination links CHIP to glycoprotein quality control. *J Biol Chem* **281**, 20242-20251
20. Gong, B., Chen, F., Pan, Y., Arrieta-Cruz, I., Yoshida, Y., Haroutunian, V., and Pasinetti, G. M. (2010) SCFFbx2-E3-ligase-mediated degradation of BACE1 attenuates Alzheimer's disease amyloidosis and improves synaptic function. *Aging Cell* **9**, 1018-1031
21. Nelson, R. F., Glenn, K. A., Zhang, Y., Wen, H., Knutson, T., Gouvion, C. M., Robinson, B. K., Zhou, Z., Yang, B., Smith, R. J., and Paulson, H. L. (2007) Selective cochlear degeneration in mice lacking the F-box protein, Fbx2, a glycoprotein-specific ubiquitin ligase subunit. *J Neurosci* **27**, 5163-5171
22. Miller, V. M., Nelson, R. F., Gouvion, C. M., Williams, A., Rodriguez-Lebron, E., Harper, S. Q., Davidson, B. L., Rebagliati, M. R., and Paulson, H. L. (2005) CHIP suppresses polyglutamine aggregation and toxicity in vitro and in vivo. *J Neurosci* **25**, 9152-9161
23. Thomas-Crusells, J., Vieira, A., Saarma, M., and Rivera, C. (2003) A novel method for monitoring surface membrane trafficking on hippocampal acute slice preparation. *J Neurosci Methods* **125**, 159-166
24. Aakalu, G., Smith, W. B., Nguyen, N., Jiang, C., and Schuman, E. M. (2001) Dynamic visualization of local protein synthesis in hippocampal neurons. *Neuron* **30**, 489-502
25. Iliff, A. J., Renoux, A. J., Krans, A., Usdin, K., Sutton, M. A., and Todd, P. K. (2013) Impaired activity-dependent FMRP translation and enhanced mGluR-dependent LTD in Fragile X premutation mice. *Hum Mol Genet* **22**, 1180-1192
26. Escrevente, C., Morais, V. A., Keller, S., Soares, C. M., Altevogt, P., and Costa, J. (2008) Functional role of N-glycosylation from ADAM10 in processing, localization and activity of the enzyme. *Biochim Biophys Acta* **1780**, 905-913

27. Glenn, K. A., Nelson, R. F., Wen, H. M., Mallinger, A. J., and Paulson, H. L. (2008) Diversity in tissue expression, substrate binding, and SCF complex formation for a lectin family of ubiquitin ligases. *J Biol Chem* **283**, 12717-12729
28. Kamenetz, F., Tomita, T., Hsieh, H., Seabrook, G., Borchelt, D., Iwatsubo, T., Sisodia, S., and Malinow, R. (2003) APP processing and synaptic function. *Neuron* **37**, 925-937
29. Wang, Y. J., Zhou, H. D., and Zhou, X. F. (2010) Modified immunotherapies against Alzheimer's disease: toward safer and effective amyloid clearance. *J Alzheimers Dis* **21**, 1065-1075
30. Frisoni, G. B., Ganzola, R., Canu, E., Rub, U., Pizzini, F. B., Alessandrini, F., Zoccatelli, G., Beltramello, A., Caltagirone, C., and Thompson, P. M. (2008) Mapping local hippocampal changes in Alzheimer's disease and normal ageing with MRI at 3 Tesla. *Brain* **131**, 3266-3276
31. Choy, R. W., Cheng, Z., and Schekman, R. (2012) Amyloid precursor protein (APP) traffics from the cell surface via endosomes for amyloid beta (Abeta) production in the trans-Golgi network. *Proc Natl Acad Sci U S A* **109**, E2077-2082
32. Andersen, O. M., Reiche, J., Schmidt, V., Gotthardt, M., Spoelgen, R., Behlke, J., von Arnim, C. A., Breiderhoff, T., Jansen, P., Wu, X., Bales, K. R., Cappai, R., Masters, C. L., Gliemann, J., Mufson, E. J., Hyman, B. T., Paul, S. M., Nykjaer, A., and Willnow, T. E. (2005) Neuronal sorting protein-related receptor sorLA/LR11 regulates processing of the amyloid precursor protein. *Proc Natl Acad Sci U S A* **102**, 13461-13466
33. Hoe, H. S., Fu, Z., Makarova, A., Lee, J. Y., Lu, C., Feng, L., Pajoohesh-Ganji, A., Matsuoka, Y., Hyman, B. T., Ehlers, M. D., Vicini, S., Pak, D. T., and Rebeck, G. W. (2009) The effects of amyloid precursor protein on postsynaptic composition and activity. *J Biol Chem* **284**, 8495-8506
34. Rushworth, J. V., and Hooper, N. M. (2010) Lipid Rafts: Linking Alzheimer's Amyloid-beta Production, Aggregation, and Toxicity at Neuronal Membranes. *Int J Alzheimers Dis* **2011**, 603052
35. Helenius, A., and Aebi, M. (2004) Roles of N-linked glycans in the endoplasmic reticulum. *Annu Rev Biochem* **73**, 1019-1049
36. Kato, A., Rouach, N., Nicoll, R. A., and Bredt, D. S. (2005) Activity-dependent NMDA receptor degradation mediated by retrotranslocation and ubiquitination. *Proc Natl Acad Sci U S A* **102**, 5600-5605
37. Huh, K. H., and Wenthold, R. J. (1999) Turnover analysis of glutamate receptors identifies a rapidly degraded pool of the N-methyl-D-aspartate receptor subunit, NR1, in cultured cerebellar granule cells. *J Biol Chem* **274**, 151-157
38. El Ayadi, A., Stieren, E. S., Barral, J. M., and Boehning, D. (2012) Ubiquilin-1 regulates amyloid precursor protein maturation and degradation by stimulating K63-linked polyubiquitination of lysine 688. *Proc Natl Acad Sci U S A* **109**, 13416-13421

Chapter Three: The Role of F-box Only Protein 2 (Fbxo2) in Synaptic Dynamics

ABSTRACT

NMDA receptors play an essential role in some forms of synaptic plasticity, learning, and memory. In addition, dysregulation of these receptors has been implicated in Alzheimer's Disease, schizophrenia, and epilepsy. Previously, it was reported that NMDA receptor-mediated synaptic currents are reduced in cultured neurons in an activity-dependent manner that requires the ubiquitin ligase adaptor subunit, F-box Only Protein 2 (Fbxo2). Each NMDA receptor is formed as a heterotetramer of obligatory GluN1 and variable GluN2 subunits. Fbxo2 facilitates the ubiquitination of GluN1 in cultured neurons, but the physiologic relevance of this regulation in vivo remains unclear. Whether Fbxo2 also can regulate GluN2 subunits in vivo and whether that control is subtype-specific are unknown. GluN2A and GluN2B are the most highly expressed GluN2 subunits in the mammalian hippocampus, a region strongly associated with memory and cognition. Although topologically similar, GluN2A and 2B confer different kinetic properties, downstream effects, and pharmacologic-sensitivities. Here, we use an *Fbxo2* knockout mouse to show that GluN1 and GluN2A, but not GluN2B, are substrates for Fbxo2 in vivo, and that the loss of Fbxo2 results in greater surface localization of GluN1. Widespread increases in the synaptic markers PSD-95

and Vglut1 are also observed in the absence of Fbxo2. We report that these synaptic changes do not manifest as electrophysiologic differences or alterations in dendritic spine density in *Fbxo2* knockout mice, but result instead in a pronounced increase in axo-dendritic shaft synapses. Taken together, these findings suggest that Fbxo2 controls the abundance and localization of select NMDA receptor subunits in the brain and may influence synapse formation and maintenance.

INTRODUCTION

NMDA receptors have profound effects on normal and pathologic processes in mammalian neurons (1). The formation of spatial memories requires NMDA receptors (2), which also play a crucial part in the formation and retention of contextual fear memories (3). Calcium conducted through NMDA receptors plays an important part in synaptic plasticity in the cortex and hippocampus. This same calcium conductance, however, also links NMDA receptors to neuronal dysfunction and glutamate-induced excitotoxicity in stroke (4) and in neurodegenerative diseases such as Huntington's Disease (5) and Alzheimer's Disease (6-8). Dysregulation of NMDA receptors through pharmacologic antagonism in humans can result in impaired cognition and schizophrenia-like symptoms (9) and down-regulation of NMDA receptor subunit GluN1 by auto-immune disease in humans induces both cognitive deficits and encephalitis, and in some patients, psychosis (10). How NMDA receptors are regulated under normal and pathological conditions remains an area of extensive investigation.

Fortunately, the effects of NMDA receptor dysregulation in humans are also partially observed in animal models, allowing for in-depth study of receptor structure and function in vivo.

NMDA receptors are formed as heterotetramers containing both GluN1 and GluN2 subunits. GluN1 is necessary for receptor function and present in all NMDA receptors; it can be coupled with various GluN2 subunits, which regulate the kinetics and gating of receptor function (11). During brain development, GluN2 subunits play a role in targeting receptors to synaptic or extra-synaptic sites at the plasma membrane, with GluN2A-containing receptors preferentially targeted to synaptic sites in adulthood and GluN2B-containing receptors targeted to extrasynaptic sites (12). Activation of these two classes of NMDA receptors at their respective locations has profoundly different downstream effects on neuronal health and function: synaptic NMDA receptor activation supports neuroprotection and extrasynaptic activation promotes pro-apoptotic pathways (13). GluN2A and 2B-containing NMDA receptors are the most widely expressed types within the mammalian hippocampus(14), and as such mediate the majority of NMDA receptor-dependent functions associated with that brain region, including learning and memory (2,15).

As transmembrane glycoproteins, GluN1 and N2 subunits are synthesized in the endoplasmic reticulum (ER). Each subunit contains an endoplasmic reticulum retention signal, which becomes inactivated only when each subunit complexed

with its corresponding partner (16). GluN1 is produced at higher levels than GluN2, sufficient to create two pools: the first GluN1 pool forms a complex with GluN2 subunits and is trafficked to the plasma membrane, where its turnover half-life is roughly thirty hours (17). The second pool is in excess of GluN2 levels and thus is not complexed with GluN2 subunits; it has been proposed to serve as a reserve pool available for times when rapid upregulation of NMDA receptors is required. This pool of unassembled GluN1 subunits is retained in the ER and is short-lived, lasting only three hours (17).

A ubiquitin ligase adaptor subunit, the Fbox-containing protein Fbox2, has been shown to play an important role in the turnover of GluN1 in cultured hippocampal neurons (18). In a model of chemically induced long-term depression, over-expression of a dominant-negative form of Fbxo2 prevented the reduction of NMDA-mediated currents (18). Fbxo2 is an E3 ligase substrate adaptor protein that preferentially binds high mannose glycans (19). High-mannose glycans are added to the N-terminal region of GluN1 (18) in the ER but appear to remain on the subunit regardless of the location of GluN1 within the cell (17).

The trafficking of NMDA receptors remains incompletely understood. It has been suggested that complexed NMDA receptors bind to scaffolding proteins that are then trafficked to the plasma membrane, bypassing the normal Golgi apparatus (20,21). NMDA receptor subunit mRNA has also been observed in dendrites, raising the possibility that NMDA receptor subunits can be locally synthesized in

distal neuronal processes (22). Whether the same trafficking machinery is present for GluN subunits produced in dendrites is not known. Extensive post-translational modifications to GluN subunits have been described for the modulation of NMDA receptor-mediated functions and trafficking, including multiple phosphorylation events (23). NMDA receptors are both able to influence and be influenced by synaptic activity, but many of the fundamental details of their governance and turnover remain unanswered.

Here, we use cell-based model systems and *Fbxo2* knockout mice to show that Fbxo2 is able to facilitate the degradation of NMDA receptor subunits, but does so selectively in the brain. Furthermore, we find that the loss of *Fbxo2* affects subunit localization and significantly increases the formation of synaptic connections.

EXPERIMENTAL PROCEDURES

Animals - Fbxo2 -/- mice were generated via the targeted deletion of the first five of six exons encoding Fbxo2. Mice were backcrossed onto a C57BL/6J background strain. Following examination, there were no reported abnormalities in brain size, weight, development, or adult gross brain structure. However, the cochleae of Fbxo2 knockout mice demonstrate degeneration (24).

DNA Constructs, HEK Cell Culture, and Cell Lysate Preparation – HEK-293 cell cultures were prepared and kept as previously described (24). Transfection of

constructs for GFP-Glun1, Glun2A, GluN2B (gifts from W. Rebeck, Georgetown University), or Fbxo2 (gift of K. Glenn, Univ. Iowa) was carried out using Lipofectamine 2000 (Invitrogen) following the manufacturer's directions. 48 hours post-transfection, cells were lysed in hot denaturing buffer containing 2% SDS and 100mM DTT. Cell homogenates were boiled for five minutes, centrifuged, and loaded onto 4-15 or 4-20% gradient SDS-PAGE gels (Biorad). Cultured neurons were also processed in this manner for western blotting experiments.

Brain Extraction/Lysis – To prepare samples for immunoblotting, animals were anesthetized using ketamine/xylazine, followed by cardiac perfusion with pre-warmed phosphate-buffered saline (PBS). Brains were dissected out following decapitation. As necessary, hippocampi were rapidly removed under a dissecting microscope. Using a dounce homogenizer, brain tissues were then homogenized in hot SDS (2%) lysis buffer with 100mM DTT, centrifuged, and boiled for five minutes. A protein quanitifcation kit (Macerey-Nagel, Duren, Germany) was used to measure the samples. Equal protein amounts were electrophoresed on 4-15 or 4-20% SDS-PAGE gels.

Western Blotting – Proteins were immunoblotted using antibodies against GluN1 (Millipore) or its extracellular epitope (Alomone), GluN2A (Alomone), GluN2B (Alomone), GluR1 (Millipore), Fbxo2 (a gift from K. Glenn, Univ. Iowa, directed against the PEST domain of Fbxo2), Transferrin Receptor (Invitrogen), or GAPDH (Millipore).

Deglycosylation of NMDA subunits – The glycosylation of GluN2A and GluN2B was assessed as previously described (17) with one modification: to increase substrate-to-enzyme ratio, GluN2 subunits were immunoprecipitated from separate hippocampal membrane fractions prior to incubation with glycolytic enzymes using antibodies directed against GluN2A (Invitrogen) or GluN2B (Invitrogen) conjugated to Protein G beads (Invitrogen). Enzymes were added directly to pelleted beads following 24-hour precipitation in reaction buffer. Reaction products were then examined by western blotting as described above.

Immunohistochemistry of frozen brain sections – Mice were processed as above, but were perfused with 4% paraformaldehyde in PBS following the PBS flush. Upon extraction, brains were post-fixed in 4% paraformaldehyde, rinsed in PBS, and cryopreserved. After freezing, brains were cut into 12 micron sections and stored at -80 ◦C until use. Antibodies against GluN1 (Millipore), GluN2A (Invitrogen), PSD-95 (Abcam), Vglut1 (Millipore), VGAT(Millipore), and Spinophilin (Millipore) were visualized with AlexaFluor 488, 568 or 647 secondary antibodies (Invitrogen). Z-stack images were collected A-1 confocal microscope (Nikon) at the University of Michigan Microscopy and Image Analysis Laboratory through equal stack dimensions. Images were cropped using Photoshop CS3 (Adobe). The portion of visual cortex (V1/V2) directly lateral and superior to region CA1 of the hippocampus along with CA1 were selected for imaging. Three male mice of each genotype at the six month time point were examined.

Immuofluorescent intensities were analyzed using Fiji Image J software.

Hippocampal Neuron Culture and Immunofluorescence – Hippocampal neurons cultured from 3 day postnatal male and female pups, plated at 80,000 cells per dish onto glass-bottom dishes (Mattek), and were maintained and processed for immunocytochemistry as previously described (25,26). Neurons were stained or harvested for western blotting at 14 days in vitro (DIV14). Antibodies against GluN1 (Millipore), GluN2A (Alomone), GluN2B (Alomone), PSD-95 (Abcam), Vglut1 (Millipore), VGAT(Millipore), Spinophilin (Millipore), were visualized using AlexaFluor 488, 568 or 647 secondary antibodies (Invitrogen). Confocal images were obtained using an A-1 confocal microscope (Nikon) at the University of Michigan Microscopy and Image Analysis Laboratory.

Proteolysis of Surface Proteins – The surface expression of GluN1 in hippocampal neuron cultures at DIV14 was assessed as previously described (27,28). Briefly, neurons were incubated with or without Chymotrypsin (Sigma) for 10 minutes at 37◦C and then lysed and analyzed by western blot.

Cell-Surface ELISA – Surface levels of GluN1 among cultured neurons at DIV14 in the presence or absence of 50 μM Bicuculine (Sigma) for 48 hours was accomplished using a previously described method (29) and an antibody directed against the extracellular loop of GluN1 (Alomone). For each condition in these experiments, 320,000 neurons were plated into each well of clear-bottom six-well

dishes (Corning) and maintained as above.

Acute Slice Biotinylation – Comparison of total protein amounts to surface levels was accomplished as previously described (26,30). In brief, male mice were anesthetized and their hippocampi rapidly removed in ice cold, oxygenated artificial cerebrospinal fluid (ACSF). 350 μm hippocampal slices were cut using a MacIlwain Tissue Chopper, and alternate sections from both hippocampi were incubated in cold, oxygenated ACSF in the presence or absence of EZ-Link Sulfo-NHS-LC-biotin (Pierce) for 45 minutes. Slices were then washed in ACSF and incubated briefly in lysine to quench any unbound biotin. Slices were washed again in ACSF, and the slices incubated without biotin were processed for western blotting as described above and retained at -80 ◦C as the “total” fraction. Biotinlyated slices were lysed in precipitation buffer containing 1% TX-100, 0.1% SDS, 1 mM EDTA, 50 mM NaCl, 20 mM Tris, pH 7.5, with protease inhibitors (Roche) in a glass homogenizer. Streptavidin Resin (Pierce) was then added and biotinylated proteins were then precipitated overnight at 4◦C with rotation. The resultant precipitates were centrifuged to separate the resin from the supernatant, and the resin was resuspended in SDS (2%) lysis buffer with 100mM DTT and boiled. This “surface” fraction was kept at -80◦C until being immunoblotted. Lanes containing 25 μg and 2.5 μg of “total” protein were run on the same gel as 2.5 μg of “surface” protein.

Preparation of Acute Hippocampal Slices for Electrophysiology – Animals were

placed under deep halothane anesthesia before decapitation. Coronal sections (300 μm) were cut on a VT1000S vibratome (Leica) in ice cold sucrose cutting solution saturated with 95% O2/5% CO2 containing (in mM): 206 sucrose, 26 NaHCO3, 2.8 KCl, 1.25 NaH2PO4, 1 CaCl2, 3 MgCl2, 0.4 ascorbic acid, and 25 d-glucose. Hippocampal slices were then allowed to recover for at least 1 hour at room temperature in a holding chamber containing artificial cerebrospinal fluid (ACSF) saturated with 95% O2/5% CO2 containing (in mM): 125 NaCl, 25 NaHCO3, 2.5 KCl, 1.25 NaH2PO4, 2 CaCl2, 1 MgCl2, 0.4 ascorbic acid, and 25 d-glucose. All recordings were made in a submerged chamber perfused continuously with oxygenated ACSF at elevated temperature (30-32°C).

Electrophysiology of Synaptic Transmission in the Hippocampus – Extracellular recordings of field excitatory postsynaptic potentials (fEPSP) were made in the stratum radiatum of CA1 with a differential amplifier (DP-301, Warner Instruments) using borosilicate glass (Sutter Instruments) to make pipettes with a P-97 Flaming-Brown pipette puller (Sutter Instruments) with a tip resistance of ~1 MΩ filled with ACSF. Recordings were digitized using an Axon Instruments 1440A Digidata A/D converter and stored on a Dell desktop computer running pClamp 10.2 (Axon Instruments). Field EPSPs were evoked by stimulating the Schaffer collateral afferent fibers with bipolar platinum electrodes (square pulse, 100 μs in duration). An input/output curve was first generated in ACSF by delivering test stimuli every 10 s with increasing stimulus intensity (from 0 to 0.5 mA). To isolate the NMDA-mediated component of the fEPSP response, ACSF

containing 6-cyano-7-nitroquinoxaline-2,3-dione (CNQX, 50 μM; Sigma-Aldrich) was then washed into the bath while continuously monitoring the fEPSP amplitude at the half-max stimulus intensity (once every 30 s). As expected, the amplitude of the fEPSP significantly decreased in the presence of CNQX; when there was no further decrease in fEPSP amplitude, another input/output curve was generated (as above) in the presence of CNQX. The amplitude of the fiber volley and the fEPSP were quantified relative to baseline. Statistical comparisons between conditions were made using a repeated-measures ANOVA.

Electrophysiology of Miniature Synaptic Currents and Long-Term Potentiation – ACSF-filled glass electrodes (resistance <1 MΩ) were positioned in the stratum radiatum of area CA1 for extracellular recording. Synaptic responses were evoked by stimulating Schaffer collaterals with 0.1 ms pulses with a bipolar tungsten electrode (WPI Inc., Sarasota, FL) once every 15 s. The stimulation intensity was systematically increased to determine the maximal field excitatory post-synaptic potential (fEPSP) slope and then adjusted to yield 40-60% of the maximal (fEPSP) slope. Experiments with maximal fEPSPs of less than 0.5 mV or with substantial changes in the fiber volley were rejected. After recording of a stable baseline for 15 min, LTP was induced by one 1 s/100Hz stimulus train. Field EPSPs were recorded (AxoClamp 2B amplifier, Axon Instruments, Foster City, CA), filtered at 1 kHz, digitized at 10 kHz (Axon Digidata 1200), and stored for off-line analysis (Clampfit 9). Initial slopes of fEPSPs were expressed as percentages of baseline averages. In summary graphs, each point represents the

average of 4 consecutive responses. The time-matched, normalized data were averaged across experiments and expressed as means±SEM. For statistical analysis, the last 5 min in each measurement were average and normalized to the average of the baseline preceding LTP induction before comparison with the corresponding control values.

Whole-cell recordings from pyramidal neurons in CA1 with a holding potential at -70 mV provided mEPSCs. Patch pipettes (3~6 MΩ), were pulled from KG-33 glass capillaries (1.1 mm I.D., 1.7 mm O.D., Garner Glass Company, Claremont, CA) on a Flaming-Brown electrode puller (P-97, Sutter Instruments Co., Novato, CA) and filled with internal solution (in mM: 125 K-Gluconate, 20 KCl, 10 NaCl, 2 Mg-ATP, 0.3 Na-GTP, 2.5 QX314, 10 PIPES, 0.2 EGTA, pH 7.3 adjusted with KOH). Slices were perfused with ACSF. GABAA receptor currents were blocked with 50 μM picrotoxin (Sigma), NMDAR currents with 10 μM APV (Sigma), and Na+ channel currents with 1 μM tetrodotoxin (TTX, Sigma). Recordings were made using an Axopatch 200B amplifier (Axon Instruments, Foster City, CA), filtered at 1 kHz, digitized at 10 kHz via an Axon Digidata 1322A, and stored for off-line analysis.

Dendritic Spine Labeling – Acute hippocampal slices were prepared as above, and then immediately fixed using 2% paraformaldehyde in PBS (31). Following fixation, slices were rinsed and labeled with DiI (Invitrogen) for 24 hours. They were then mounted using Prolong Gold antifade reagent (Invitrogen) and visualized as above. Z-stack images were reconstructed and dendrites were

modeled in a semi-automated manner using Imaris software as previously described (32). Dendritic segments from stratum radiatum of four male mice per genotype were analyzed, totaling 60 dendritic segments per genotype. Data were compiled using Excel (Microsoft) and analyzed using Prism 6 software (GraphPad).

Transmission Electron Microscopy – Mice were anesthetized and flushed as above, then fixed with 2.5% Glutaraldehyde in 0.1 M Sorensen's buffer. Hippocampi were then dissected out under a dissecting scope and then immersion fixed overnight at four degrees. Hippocampi were then trimmed to 1mm x 1mm blocks, rinsed in Sorensen's buffer, then post-fixed for one hour in one percent osmium tetroxide in the same buffer, and rinsed again in fresh Sorensen's buffer. The tissue was then dehydrated in ascending concentrations of ethanol, transitioned through propylene oxide, and embedded in Epon epoxy resin. Semi-thin sections were stained with toluidine blue for tissue identification. Selected regions of interest were ultra-thin sectioned 70 nm in thickness, mounted on copper mesh grids (Ted Pella), and post stained with uranyl acetate and lead citrate. Sections were imaged using a Philips CM100 electron microscope at 60 KV. Images were recorded digitally using a Hamamatsu ORCA-HR digital camera system, operated using AMT software (Advanced Microscopy Techniques Corp., Danvers, MA). 4 male animals per genotype were examined, totaling 500μm of dendritic segments from stratum radiatum of hippocampus. Shaft synapses were counted by three separate lab members,

blind to genotype, and there was no statistically significant difference between their counts.

Quantification and Statistical Analysis – Immunoblot results were scanned using Adobe Photoshop and analyzed using ImageJ software. Prism 6 software (GraphPad) was used for statistical analysis and to make graphs. Immunofluorescence data was analyzed using ImageJ as previously described (26,33).

RESULTS

Fbxo2 has been shown to facilitate the degradation of the NMDA receptor subunits GluN1 in cultured neurons (18) and GluN2A in transfected non-neuronal cells (34). To investigate whether Fbxo2 similarly participates in the clearance of the NMDA receptor subunit GluN2B, we transiently expressed plasmids encoding these proteins in HEK293 cells together with either FLAG-tagged Fbxo2 or empty vector (Fig 14). Whereas levels of GluN1 and GluN2A were markedly reduced when co-expressed with Fbxo2 (Fig 14, a), consistent with prior studies (18,34), GluN2B levels were decreased by approximately 50% (Fig 14, c).

As NMDA receptors are nervous-system-specific and Fbxo2 is brain-enriched, we sought to move beyond the over-expression of neuronal proteins in non-neuronal cells to examine the physiological significance of Fbxo2 for GluN1,

N2A, and N2B in vivo in the nervous system. Utilizing *Fbxo2* knockout mice generated in our lab (24), we observed that GluN1 levels are almost 300% of those in wild-type mice at three months of age, and 150-200% at six and nine months of age (Fig 15, a). GluN2A levels are also consistently increased in the absence of Fbxo2, at around 150% of wild-type controls from three through nine months of age (Fig 15, b). In contrast, Fbxo2 does not appear to regulate the levels of GluN2B in vivo, which remain unchanged in *Fbxo2* knockout brains for all ages examined (Fig 15, c).

As a ubiquitin ligase subunit that binds substrates, Fbxo2 preferentially targets glycoproteins that contain high-mannose glycans (19). High mannose N-linked oligosaccharides on glycoproteins are typically processed to a complex (not high mannose) form as a protein transits through the Golgi apparatus (35). However, it has been suggested that NMDA receptor subunits are not trafficked through this canonical system, instead making use of alternative methods for transport from the endoplasmic reticulum to the cell surface (21). Bypassing the Golgi would allow the high-mannose glycans placed on NMDA receptor subunits in the ER to be retained even as these receptors arrive at the cell surface. As a result, NMDA receptor subunits would remain sensitive to Endoglycosidase H (Endo H), which selectively cleaves high-mannose glycans on glycoproteins. This has been previously shown to be the case for GluN1 (17), raising two intriguing possibilities: 1) that the differential regulation of GluN2A and GluN2B observed in the *Fbxo2* knockout brain reflects a difference in the retention of high-mannose

glycans on different NMDA receptor subunits; and 2) that even at the synapse, NMDA receptor subunits remain potential candidates for regulation by Fbxo2.

To investigate the first of these, it was critical to determine whether these subunits are similarly Endo H sensitive. To do so, hippocampi were removed from six month old mice, and a membrane fraction was prepared. GluN2A and GluN2B were then immunoprecipitated from separate samples and the resultant product was treated with Endo H, PNGaseF (which cleaves all N-linked glycans), or left untreated. These proteins were then examined by western blot. We observed similar Endo H sensitivity, for both GluN2A and 2B, evident as a decrease in molecular weight (Fig 15, d and e). The entire population of both receptor subunits remained Endo H sensitive at one or more oligosaccharides, suggesting that all GluN2A and 2B subunits associated with neuronal membranes retain the requisite high-mannose glycans for recognition by Fbxo2. Both subunits showed further reduction in molecular weight when treated with PNGaseF, suggesting the presence of additional, complex glycans. Given the abundance of post-translational modifications reported for GluN2 receptor subunits, GluN2B levels are likely governed by other mechanisms independent of Fbxo2. The E3 ligase Mind bomb-2, for example, has previously been shown to regulate GluN2B levels in a phosphorylation-dependent manner (36).

To explore the possibility of whether Fbxo2 plays a role in determining the NMDA receptor content at synapses, we first sought to visualize the distribution of

increased GluN1 and GluN2A in Fbxo2 knockout mice. To do so, we performed confocal immunofluorescence microscopy on six-month old mouse brain. In cortex (Fig 16, a) and CA1 of hippocampus (Fig 16, b), we observed increased amounts of GluN1 both in cell bodies and throughout the neuropil. Elevated GluN2A appeared predominantly throughout the neuropil. We did not observe subregional differences between cortex and hippocampus in the extent of these increases.

Increased levels of NMDA receptor subunits could represent an increase in receptor levels at the plasma membrane or the retention of subunits in intracellular pools. Previously, pharmacologic elevation of NMDA receptor subunit levels was shown to increase NMDA synaptic currents and enhance postsynaptic plasticity (37). Over-expression of GluN2A and GluN2B has also been shown to cause the formation of increased synaptic NMDA receptors (38,39), but whether the robust increase in endogenous subunit proteins observed in the absence of Fbxo2 would yield similar results remains unclear. To address whether these increased endogenous NMDAR subunit proteins were present on the cell surface and at synapses, several lines of investigation were used. First, we hypothesized that a substantial increase in NMDAR receptor content at synapses would involve a concomitant increase in the extent of post-synaptic architecture necessary to stabilize those receptors. PSD-95 has been shown to anchor GluN2A-containing receptors at synaptic sites on the cell surface (40). Additionally, presynaptic markers might also increase as a response to additional

post-synaptic content. We previously reported an increase in PSD-95 and Vglut1 in cultured hippocampal neurons from mice lacking Fbxo2 (26), and therefore inquired whether this same phenomenon was present in vivo. Using confocal immunofluorescence microscopy of six-month old mice, we examined the CA1 region of the hippocampus. In *Fbxo2* knockout mice, PSD-95 and Vglut1 levels were 175-200% of wild-type controls (Fig 17, a and b). We did not, however, observe a significant difference in the levels of spinophilin, a protein enriched in dendritic spines, nor in the levels of the vesicular GABA transporter (VGAT) present at synapses of inhibitory interneurons. Despite the increase in pre- and post-synaptic markers, we also did not observe a difference in the levels of the AMPA receptor subunit GluR-1 (Fig 17, c and d). NMDA receptor function is voltage-dependent with AMPA receptors playing the role of a depolarizing agent for the postsynaptic cell. Several substrates identified for Fbxo2 have been implicated in synapse formation and stability, including Beta Integrin 1 (19), the Amyloid Precursor Protein (26,41), and NMDA receptors themselves (42). With such heightened levels, colocalization of GluN immunoreactivity with that of synaptic markers appeared to be extensive at this scale. However, as the question of GluN1‘s surface and synaptic localization was central to understanding the consequences of Fbxo2’s absence, we elected to more carefully examine protein distribution and colocalization with greater detail by using cultured hippocampal neurons. Cultured neurons provide a practical means to biochemically assess the handling of proteins within living neurons and greater visual resolution of protein localization than in vivo studies.

To more effectively examine the distribution of NMDA receptors and their surface presentation in neurons, we cultured hippocampal neurons from P2 wild-type and knockout pups. At DIV 14, these neurons showed similar differences in GluN1 and N2A levels, but a decrease in GluN2B levels (Fig 18, a). As previously reported, Fbxo2 is expressed as early as DIV 3 in this system (26).

Fbxo2 has been described previously for its role in clearing proteins through ER-associated degradation (ERAD) (34), and not for regulating the surface levels of substrate proteins. However, the work of Bredt. et al demonstrated the persistence of NMDA currents when Fbxo2 function was repressed (18) - suggesting that the NMDA receptors no longer being handled by Fbxo2 were retained on the cell surface. To elucidate this point, we next sought to address whether the increase in GluN1 levels in our *Fbxo2* knockout neurons corresponded to subunits expressed on the neuronal cell surface or retained intracellularly in the absence of Fbxo2. Exogenously applied chymotrypsin will cleave the extracellular domain of transmembrane proteins present on the surface of neurons. Using this technique, we were able to measure by western blot the amount of GluN1 in untreated cultures versus the amount remaining after chymotrypsin cleavage, with the chymotrypsin-resistant fraction representing GluN1 <u>not</u> present on the cell surface. In treated cultures, after chymotrypsin treatment a lower molecular weight GluN1 band of ~ 50kD was observed, which presumably represents the intracellular portion of the receptor left following

surface cleavage. Despite an increase in GluN1 to nearly 150% that of wild-type controls, in *Fbxo2* knockout neurons only ~10% of GluN1 is chymotrypsin-resistant, significantly less than in wild-type controls (Fig 18, b). These results suggest that nearly all the increased GluN1 present in the absence of Fbxo2 reaches the cell surface.

We next inquired whether we could observe changes in the ability of *Fbxo2* knockout neurons to remove GluN1 from the cell surface. In their studies, Bredt et al. drove the activity-dependent down-regulation of synaptic NMDA receptors by using a model of long-term depression (LTD) evoked by bicuculline treatment (18). Exposure to bicuculline for 48 hours has been shown to cause the internalization of NMDA receptors. Using an antibody against the extracellular loop of GluN1 yielded weak signal, so we used larger cultures in a cell-surface-based-ELISA reporter assay to measure the amount of internalization in treated versus untreated cultures. Whereas approximately half of the surface receptors in wild-type neurons were removed following bicuculline treatment, approximately all of the surface receptors in knockout neurons remained on the surface, as evident by equal surface immunoreactivity between treated and untreated cultures of *Fbxo2* knockout neurons (Fig 18, c). These results are consistent with previously reported observations, and suggest a persistence of NMDA receptors at the cell surface following loss or disruption of Fbxo2.

The finding that increased GluN1 is present on the cell surface does not reveal

whether that surface GluN1 is present at synapses. To elucidate this question, the colocalization of GluN1 and synaptic markers was observed using confocal immunofluorescence microscopy. GluN1 levels were increased throughout *Fbxo2* knockout neurons, most notably at numerous, large GluN1-positive puncta in dendrites (Figure 19, a, arrows). These puncta colocalize with the synaptic marker Vglut1 (Figure 19, a), suggesting that increased receptor levels are present at synapses. In accordance with our western blot data, GluN2A levels are increased in cultured neurons and GluN2B levels appear decreased (Fig 19, b and c).

Having observed greater surface localization of GluN1 in vitro, we sought to determine whether this change also occurred in vivo. Neither chymotrypsin cleavage nor cell-surface-based-ELISA is compatible with in vivo studies, so instead we employed surface biotinylation of acute hippocampal slices, previously used to measure surface proteins in vivo (26,30). We focused on the hippocampus because of its functional importance and because it is a discrete subcortical region that can be readily and reproducibly isolated by dissection, adding to its value as a model system for these studies. Following biotinylation and immunoprecipitation, *Fbxo2* knockout mice showed a marked increase in surface GluN1 and GluN2A: approximately 200% of that observed in wild-type controls (Fig 20). By contrast, levels of the Transferrin Receptor, which was used as a loading control for the surface fraction were not altered in *Fbxo2* knockout mice.

With the greater levels of cell surface NMDA receptor subunits and increased synaptic marker proteins in *Fbxo2* knockout mice, we predicted that NMDA-mediated current in acute hippocampal slices would also be increased in knockout mice. However, field recordings from region CA1 of hippocampus of 3-6 month old *Fbxo2* knockout mice did not reveal any difference in basal transmission (Figure 21, a, filled circles) or in NMDA-mediated current recorded in the presence of AMPA-receptor blocker CNQX (Fig 21, a, open circles). Moreover, no difference was observed in the size of fiber volleys evoked for each genotype (Fig 21, b), and plotting the fiber volley data against the field excitatory post-synaptic potentials (EPSPs) revealed no difference between genotypes (figure 21, c). The frequency, amplitude, and decay of spontaneous miniature excitatory post-synaptic currents (EPSCs) did not differ between genotype (Fig 22, b, c, d). Long-term potentiation (LTP) evoked by 100Hz stimulation was also equal in amplitude and persistence out to 60 min for mice with and without *Fbxo2* (Fig 22, e and f).

The output measured in each of these experiments hinges upon functional receptors on the post-synapse. Our findings are consistent with the interpretation that the increased NMDA receptors of *Fbxo2* knockout mice are not functional and do not participate in synaptic transmission. The lack of a concomitant increase in GluR1 levels (reported in Fig. 17, c) suggests one mechanism (the absence of sufficient AMPA receptors) by which additional synapses in *Fbxo2*

knockout mice are kept silent. However, these recordings were performed in low or zero Mg2+, a non-physiologic condition that circumvents the voltage-dependent block of NMDA receptors. Still, numerous other potential mechanisms exist for the modulation of NMDA receptor activity including regulation by Protein Kinase A (43), Protein Kinase C (44,45), and Src kinase (46), among many others.

As a potential confounding factor to the interpretation of these studies, we discovered that following incubation in ACSF for several hours, the difference in GluN1 levels between wild-type and *Fbxo2* knockout mice is ameliorated (Fig 23, a). This is an important observation because slices used for electrophysiology experiments are cut and typically allowed to recover for one hour, then recorded from over a period of hours, such that slices may remain incubated in ACSF anywhere from 1 to 5 hours following recovery. To address the timing of this equalizing phenomenon with GluN1, we re-examined those slices used for the "total" fraction in our biotinylation experiments, which were similarly cut but were incubated for only one hour prior to lysis. These slices show a consistent difference in GluN1 between genotypes (Fig 23, b), suggesting that it takes several hours for the equilibration of NMDA receptor subunit protein content to occur. Importantly, no apparent difference was observed between slices recorded at the earliest point in each session and those recorded hours later, further suggesting that the increased GluN1 content of *Fbxo2* knockout mice is not electrophysiologically active.

Given the absence of obvious electrophysiological consequences of increased GluN1 and N2A in *Fbxo2* knockout brain, we recognized that it was critically important to assess the morphological impact of increased NMDA receptor subunits, as well as increased pre- and post-synaptic marker proteins, on the structures essential for synaptic transmission. To do so, we cut thick sections of region CA1 which were then fixed, labeled with DiI, and imaged by confocal microscopy. Dendrites were then reconstructed in three-dimensions and spines were measured and counted in a semi-automated manner (example images Fig 24, a and b). Using this method, we observed no difference in the density of dendritic spines (Fig 24, c). A significant reduction in spine length was observed, however, with spines in *Fbxo2* knockout hippocampus reaching only 78% of the length seen in wild-type neurons (Fig 24, c). Much smaller, but statistically significant differences were observed in the diameter of the head and neck of spines: on average, knockout spine heads were 5% larger, and the necks 13% thinner (Fig 24, c). Overall, there was minimal difference in spine size and shape and no difference in density. Thus, the extensive changes in protein content evident in *Fbxo2* knockout mice do not appear to impair other mechanisms regulating spinogenesis and spine density.

With no apparent change in spine density or electrophysiological parameters in Fbxo2 knockout mice, the presence of increased synaptic markers would seem paradoxical. In an effort to explain this discrepancy, we examined the

ultrastructure of pyramidal cells in region CA1 by Transmission Electron Microscopy (TEM). At this greatly increased resolution, we observed a striking and significant difference in the architecture of dendrites from neurons lacking Fbxo2: a marked increase in axo-dendritic shaft synapses (Fig 25, a-f) in *Fbxo2* knockout hippocampus. These synapses demonstrated an electron-dense postsynaptic density, and were opposed to pre-synaptic terminals with apparent vesicles (Fig 25, insets b, d, and e). While these structures are rarely seen in wild-type dendrites (Fig 25, h and inset i)(47,48), we identified shaft synapses decorating *Fbxo2* knockout neurons at a density approaching that of spinous synapses (~50-90%; Fig 25, g). Shaft synapses were found both adjacent to dendritic spines (Fig 25, a and b) and at a distance from them (Fig 25, c-f). A subset of these structures appeared with a discontinuous (or perforated) postsynaptic density (Fig 25, e and d) but were still counted as a single synapse for the purposes of quantification. Taken together, these results suggest that the increased levels of synaptic markers correspond to additional axo-dendritic shaft synapses.

DISCUSSION

Here we have identified a role for Fbxo2 in regulating the levels of specific NMDA receptor subunits in vivo, namely GluN1 and GluN2A. We have found that the increased levels of these subunits in mice lacking Fbxo2 are accompanied by an enhancement of surface and synaptic localization. These changes were accompanied by elevated amounts of synaptic marker proteins,

but no change to the density of dendritic spines. These additional synapses did not appear to affect synaptic transmission, and through electron microscopy, were found localized along dendritic shafts.

The necessity of the presence on the substrate of high-mannose glycans in order for Fbxo2 to interact with and regulate it has been established previously for GluN1 (18) and additional proteins (19). But our findings with GluN2A and N2B suggest that in the hippocampus, the presence of these glycans is not the only factor determining regulation by Fbxo2. In *Fbxo2* knockout mice, we report increased levels of both pre- and post-synaptic markers but this increase is not accompanied by a change in spine density or electrophysiological properties in slice culture, suggesting that the increased synaptic markers may reflect silent synapses. Using fixed tissue, we provide evidence of heightened numbers of axo-dendritic excitatory shaft synapses, as well as greater surface localization of GluN1 and N2A within the hippocampus of knockout mice.

Many forms of neuronal plasticity require the degradation of existing synaptic proteins (49,50), while also placing demands on local machinery for new protein synthesis (51,52). Protein quality control pathways exist to ensure these demands are met with the appropriate complement of properly synthesized and correctly assembled proteins. Proteins synthesized in dendrites are processed in specialized ER near dendritic spines (53). With limited evidence for the presence of Golgi apparatus at these local sites (54), it is intriguing to speculate that GluN

subunits may not be the only synaptic proteins still bearing high-mannose glycans. As a brain-enriched ubiquitin ligase substrate adaptor protein linked to ERAD (34), Fbxo2 is an appealing target for studying the role of protein quality control pathways in responding to the unique proteostatic needs of neurons, especially given its localization at synaptic sites and throughout the neuronal cytoplasm (18). Intriguingly, Fbxo2 levels are reportedly decreased in Alzheimer's Disease (AD) patient brain tissue (55). Fbxo2 has already been linked to the regulation of the Amyloid Precursor Protein, the central causative protein in AD (26), and we now link it to a second factor proposed to play a role AD, the dysregulation of NMDA receptors. For these reasons, further studies will be needed to fully address the contribution of Fbxo2 reduction in AD pathogenesis.

In our present studies, the observed increase in surface localization of GluN1 and N2A in *Fbxo2* -/- mice is an effect beyond the straightforward elevation of substrate protein levels. This effect more likely results from one of two scenarios. First, Fbxo2 could affect the endocytosis of receptors through an ubiquitin-dependent signal on NMDA receptors; indeed such a mechanism has been described elsewhere for EGFR receptors (56,57). Alternatively, downstream of endocytosis Fbxo2 may play a key role in determining receptor fate. Receptors on the surface are regularly endocytosed and either recycled back to the surface or targeted for degradation (58). A role for Fbxo2 in this triage pathway is supported by the presence of high-mannose glycans on all membrane-associated GluN2 subunits, suggesting their continued capacity to interact with

Fbxo2. The fact that Fbxo2, an intracellular protein, binds substrates through their high mannose glycans, which reside on the extracellular face of surface glycoproteins, argues against a direct role for Fbxo2 in regulating endocytosis itself. The high-mannose glycans on GluN1, GluN2A and other synaptic glycoproteins targeted by Fbxo2 should remain inaccessible to Fbxo2 even after the initial steps of endocytosis. Thus we suggest that internalization of NMDAR must precede ubiquitination of GluN subunits by Fbxo2, much like the activity-dependent ubiquitination of GluA2 requires clathrin-mediated endocytosis of the receptor before ubiquitination can occur (59). Upon endocytosis, these formerly extracellular glycans would reside within endosomes, but a translocation apparatus analogous to the translocation apparatus that mediates ERAD could facilitate the presentation of N-terminal glycans to intracellular Fbxo2. Evidence for such an apparatus includes the identification of Sec61B, a core component of the ER translocation machinery, on endosomes (60,61). Alternatively, delivery of substrates to dendritic ER, followed by Sec61B-mediated presentation to the cytosol, remains a possibility. In this scenario, the kinetics of NMDA receptor recycling would remain the same whether Fbxo2 is present or not, but knockout neurons would develop an increased amount of receptors on the surface for want of counterbalancing degradation. The method of chemical LTD employed in our studies and used elsewhere requires a lengthy treatment, on the order of 48 hours, making it difficult to interpret whether endocytosis of NMDA receptors itself is impaired. More rapid internalization protocols could help to elucidate whether these receptors are properly internalized. We did attempt additional

pharmacologic treatments on shorter time scales but they did not elicit robust and consistent internalization of NMDA receptors in wild-type control neurons. Further studies employing subunits with pH-sensitive fluorescent tags could shed light on whether the kinetics of endo- and exocytosis of NMDA receptor subunits remains normal following the loss of Fbxo2.

If the levels of GluN1 and GluN2A depend on Fbxo2-mediated ubiquitination and subsequent degradation, it is nevertheless likely that many other mechanisms also contribute to the regulation of NMDAR levels and activity at the synapse. The contribution of those subunits to synaptic transmission and downstream NMDA receptor-mediated signaling in Fbxo2 knockout brains when joined as receptors is likely determined in the context of, and under the control of, numerous complex mechanisms governing homeostatic plasticity, in which Fbxo2 likely has little, if any, direct role. That we observe no change in spine density and no proportional change in head diameter suggest that in the absence of Fbxo2 the mechanisms responsible for regulating the morphology of spinous synapses continue to function (62-64). The loss of Fbxo2 does not interfere with these mechanisms, even though Fbxo2 does localize to spines (18).

Our findings raise an intriguing question: where, if not at spinous synapses, do these additional NMDA receptors in *Fbxo2* knockout mice reside? The plasma membrane is populated with pools of receptors that are believed to function as a reserve stock for rapid changes in receptor content at synapses (65-68).

Upwards of 65% of synaptic NMDA receptors are mobile and participate in exchange with extrasynaptic pools (69). It is unclear, however, what regulates the size of these reserve pools. GluN2A-containing receptors are preferentially targeted to synapses, but are also found in these reserve pools and can be laterally trafficked into synapses as needed (69). Because the amount of NMDA receptors at spinous synapses is tightly regulated and no alteration in synaptic transmission was observed, it stands to reason that the increased steady-state levels and surface localization of GluN1 and N2A in *Fbxo2* knockout mice represent an increase in the reserve pool of NMDA receptors.

On its own, however, this model of an increased reserve pool does not account for the significant increase we observe in synaptic markers. Previous studies involving the over-expression of GluN subunits have reported an increase in NMDA-mediated synaptic currents (38,39), but have not commented on whether these currents were accompanied by additional synaptic markers, as observed here in the absence of Fbxo2. The NMDA receptor interacts with PSD-95, which has been suggested to serve as a scaffold for additional trans-synaptic proteins (70,71). Perhaps if the pool of receptors and their interactors such as PSD-95 in the peripheral membrane reached sufficient density and complexity, that pool could recruit presynaptic branching and an opposed axonal terminal, thereby creating a shaft synapse. Together with our findings regarding the increased amounts and surface presentation of NMDA receptor subunits in the absence of Fbxo2, we propose that failure to clear NMDA subunits both from the ER and

upon activity-dependent endocytosis results in aberrant clustering in the peripheral membrane (Fig 26).

The mechanisms regulating the formation and removal of excitatory shaft synapses are not well characterized. Excitatory shaft synapses are relatively uncommon under normal physiologic conditions (47), but their formation can be rapidly induced following LTP in the hippocampus (47,72). Shaft synapse numbers can also increase following experiential and behavioral modifications of awake, behaving animals (73-75). As shaft synapses are opposed to presynaptic terminals, it seems likely that postsynaptic rearrangement and clustering of proteins is able to induce the recruitment of presynaptic terminals. However, the formation of shaft connections is not necessarily an intermediate step toward the creation of spines extending from the shaft, as has been suggested elsewhere (47,76). Spine outgrowth precedes synaptic connectivity (77) and studies of post-synaptically over-expressed EphB3 reveal an increase in shaft synapses with no effect on spinogenesis (78).

The mechanisms by which shaft synapses are removed are also unclear. They can be rapidly removed following tetanic stimulation (47,73) or persist for hours (72). The precise conditions that trigger the selective removal of shaft synapses are not known. Blockade of activity has been shown to cause the selective elimination of shaft, but not spinous, synapses; in contrast, epileptiform activity induces a reduction in spinous, but not shaft, synapses (79). "Removal" itself

may be a misnomer; it has been proposed that as a part of maintaining potentiation, the synaptic surface architecture of rapidly produced shaft synapses is redistributed to strengthen and enlarge selected spinous synapses (47). Whether this relocation makes use of lateral mobility or the removal and reinsertion of receptors is not known, and why no such increase in spine head size is observed in *Fbxo2* knockout mice remains uncertain. Because the loss of shaft synapses is governed by processes unknown to us, it is not currently possible to answer whether this still undefined process mediates the reduction in GluN1 levels observed in knockout animals following incubation in ACSF. Extensive remodeling of synaptic connections has been reported following preparation of acute slices (80). To bridge our morphological and electrophysiological findings, further studies will be required to address whether the additional amount of GluN1 lost during incubation after slice culture preparation represents a loss of shaft synapses in CA1.

The rapid induction of shaft synapses following over-expression of the post-synaptic protein EphB3 is marked by increased excitatory transmission in cultured neurons (78). It is conceivable that in vivo, an increase on the scale observed in Fbxo2 knockout mice would lead to epileptogenic activity, which could be fatal to animals. Therefore, the silencing of such synapses may be an essential, compensatory homeostatic response. It is possible that the localization of shaft synapses makes them more potent (81) and causes the loss of input selectivity, which could evoke a compensatory change in the length of dendritic

spines (82), as we observed (Fig 24). Alternatively, the difference in transmission through spines of different lengths may reflect multiple factors (83). Additional studies exploring the formation and turnover of shaft synapses will address their contribution to learning and memory.

FIGURE LEGENDS

Figure 14. Co-expression of Fbxo2 decreases levels of unassembled NMDA Receptor Subunits

(a) Co-expression with Fbxo2 reduces GluN1 levels. HEK293 cells expressing GFP-GluN1 together with vector encoding Fbxo2 or empty vector (EV) were harvested 48 hours after transfection, and lysates were examined by western blot with antibodies recognizing GluN1, Fbxo2, or GAPDH. *(b)* GluN2A and *(c)* GLuN2B levels are similarly decreased following co-expression with Fbxo2. Fbxo2 and GluN2A or GluN2B were co-expressed as in panel a, and subunit levels assessed by western blot with anti-GluN2A or anti-GluN2B antibody. Results shown are representative of triplicate experiments. *(d)* Quantification of results from panels *a-c*. Error Bars = S.E. *, $p<0.05$; ** $p<0.01$; **** $p<0.0001$; (unpaired t test).

Figure 15. Increased levels of GluN1 and GluN2A, but not GluN2B, in *Fbxo2 -/-* brain.

The absence of Fbxo2 increases (*a*) GluN1 and (*b*) GLuN2A subunit levels, but not (*c*) GluN2B subunit levels, in whole brain. Subunit levels in brain lysates from

wild-type and *Fbxo2* null mice were assessed by western blot, with representative immunoblots (upper panels) shown for three mice of each genotype at three months of age Subunit levels were quantified (lower panels) and normalized at four ages, with an n of three animals per genotype at each age. *(d)* GluN2A and *(e)* GluN2B associated with hippocampal membranes remain Endoglycosidase H sensitive. GluN2A or GluN2B was immunoprecipitated from hippocampal membrane fractions of 6-month old wild-type mice, then incubated with Endo H, PNGase F or (as control) PBS alone. Deglycosylation of GluN2A or GluN2B was then assessed by western blot with anti-GluN2A or GluN2B antibody, respectively. The observed sensitivity to Endo H, indicating the presence of retained high mannose glycans on GluN2A and GluN2B, was not altered in *Fbxo2* null mice. Error Bars = S.E. *, $p<0.05$ (unpaired t-test).

Figure 16. Immunofluorescence confirms increased GluN1 and GluN2A levels in *Fbxo2 -/-* brain.

Confocal immunofluorescence microscopy in *(a)* cortex and *(b)* CA1 region of hippocampus shows increased levels of GluN1 (left column) and GluN2A (center column) in 6 month old *Fbxo2* knockout mice (lower row) compared to wild-type mice (upper row).

Figure 17. Elevated levels of PSD-95 and Vglut1 in *Fbxo2 -/-* brain.

(a) PSD-95 and Vglut1 immunofluorescence are increased in the CA1 region of 6

month old *Fbxo2* null mice (lower row) versus wild type mice (upper row), while Spinophilin and VGAT levels are unchanged. *(b)* Quantification of immunofluorescence results from three mice per genotype. (unpaired t-test). *(c)* GluR1 levels in hippocampus of 6 month old wild-type and *Fbxo2* null mice was assessed by western blot using an anti-GluR1 antibody (left panel). Quantification of immunoblots from three mice per genotype (right panel) showed no change in GLuR1 levels. Error Bars = S.E. *, $p<0.05$

Figure 18. NMDA receptor levels and cell surface localization are increased in cultured *Fbxo2* -/- hippocampal neurons

(a) GluN1 and GluN2A levels are increased in cultured *Fbxo2* null neurons, whereas GluN2B levels are decreased. Cultured hippocampal neurons isolated from p3 wild type and *Fbxo2* null mice, DIV 14, were lysed and NMDA receptor subunit levels assessed by western blot. Representative results from three dishes per genotype are shown (left panels) and quantified (right panel). *(b)* Fbxo2 absence results in greater cell surface localization of GluN1. Intact neurons were treated with chymotrypsin for 15 minutes or left untreated, then lysed, and GluN1 levels were assessed by western blot. Representative immunoblot results from a single experiment are shown (left panel) and results from triplicate experiments were quantified (right panel). (*c*) the amount of surface GluN1 remaining after 48 hour exposure to 50uM bicuculline, as detected by cell-surface ELISA assay, is reduced to approximately 50% of those in untreated controls for wild-type neurons, but for *Fbxo2* knockout neurons, no

surface immunoreactivity is lost following treatment. Treated and untreated cultures were labeled with an antibody against the extracellular loop of GluN1, which was then labeled with Horse Radish Peroxidase(HRP)-conjugated secondary antibody. HRP cleavage of Tetramethylbenzidine in triplicate cultures per genotype per treatment was then detected and quantified. Error Bars S.E. *, p<0.05, ** p<0.005*** p<0.001; **** p<0.0001 (unpaired t test).

Figure 19. Greater GluN1 immunoreactivity colocalizes with the presynaptic marker VGlut1 in cultured hippocampal neurons

(a) GluN1 immunoreactivity in DIV 14 cultured hippocampal neurons was assessed by fluorescent confocal microscopy. Neurons were fixed, permeabilized, and immunostained for GluN1 (left column) and the synaptic marker Vglut1 (second column). GluN1 puncta (arrows) colocalize with Vglut1 puncta (second and third columns, arrows). Two representative neurons per genotype are shown. (*b*) Consistent with western blot results, GluN2A immunoreactivity is increased in cultured hippocampal neurons *(b)* and GluN2B is decreased *(c)*. Scale bar = 25um.

Figure 20. Enhanced Surface Localization of GluN1 and GluN2A in Hippocampi of Fbxo2 -/- mice

Acute hippocampal slices from six month old mice were incubated with oxygenated ACSF with or without biotin for 45 minutes, and processed to measure surface proteins (see Experimental Procedures). Surface levels of

GluN1 and GluN2A are nearly doubled in the absence of Fbxo2. Total and surface fractions were examined by western blot for GluN1, GluN2A, GAPDH, or the transferrin receptor as a control glycoprotein known to have some surface expression. Representative immunoblot results are shown from a single animal of each genotype (left panel). Slices from three animals per genotype were examined and the results quantified (right panel). Error Bars = S.E. ** $p<0.01$ (unpaired t test).

Figure 21. The loss of Fbxo2 does not alter hippocampal synaptic transmission *(a)* fEPSPs were measured in acute slices of hippocampi from wild-type and Fbxo2 knockout mice at the indicated stimulus intensities both in the presence and absence of CNQX (empty and filled circles, respectively) and quantified. Neither Ampa nor NMDA-mediated currents differed between genotype. Fiber volley amplitude *(b)* was similarly unchanged. No difference was observed when fEPSPs were plotted against fiber volley amplitude *(c)*.

Figure 22. The loss of Fbxo2 does not alter hippocampal synaptic miniature synaptic currents or LTP induction

(a) Examples of AMPAR mEPSCs from acute hippocampal slices from litter mate wild-type and knockout mice. Cumulative fraction (*b, left panel*) and histogram distribution (insert) of mEPSC amplitude are unchanged in knockout mice. The amplitude average (*b, right panel*) is comparable between wild-type and littermate-matched knockout mice. Cumulative fraction *(c, left panel*) and

histogram distribution (insert) of mEPSC frequency is not significantly changed in the absence of Fbxo2. The frequency average (*c, right panel*) is comparable between wild-type and knockout mice. Cumulative fraction *(d, left panel*) and histogram distribution (insert) of mEPSC decay tau is not significantly changed in knockout mice. The decay tau average (*d, right panel*) is comparable between wild-type and knockout mice. P values of 2-tailed student t-test are shown in each subpanel. *(e)* LTP is not affected in *Fbxo2* knockout mice. LTP was induced by a single tetanus (1 s/100 Hz; arrow in i.) in CA1 of acute hippocampal slices from *Fbxo2* knockout and littermate-matched wild-type control mice. Example fEPSPs recordings before (dashed lines) and 60 min after LTP induction (solid lines) from wild-type and knockout mice are shown. *(i)* Averages of the complete time courses are shown from wild-type and knockout mice. LTP is comparable in hippocampal slices from wild-type and knockout mice.

Figure 23. GluN1 levels are equilibrated following lengthy incubation in ACSF. *(a)* GluN1 levels are increased in hippocampi from six-month old *Fbxo2* null mice when rapidly lysed following excision. Following slicing and 5 hour incubation in ACSF in preparation for electrophysiology studies, GluN1 levels no longer differ between genotypes. (*b*) Immunoblot of slices lysed one hour after cutting still demonstrate elevated levels of GluN1 in *Fbxo2* knockout hippocampi consistent with those seen following immediate lysis (left panel). Western blot results from three mice per genotype per condition were quantified (right panel). Error Bars = S.E. *, $p<0.05$, ** $p<0.01$ (unpaired t test).

Figure 24. Dendritic Spine Density is not affected by the loss of Fbxo2

(a) Dendritic spines of CA1 pyramidal neurons from 6 month old mice were labeled with DiI and imaged by confocal laser microscopy, then reconstructed using Imaris software (see Experimental Procedures) as represented in an example of imaged spines (top panel) and their reconstruction (with dendrite reconstruction removed to aid visualization, lower panel) is shown. Scale bar = 5um. *(b)* Representative examples of wild-type and *Fbxo2* null dendrites are shown. Scale bar = 10um. (*c*) Quantification of dendritic spine density reveals no difference between genotypes (upper left panel). Spine length is decreased by 22% in the absence of Fbxo2 (upper right panel). Spine head diameter is increased by 5% (lower left panel) and spine neck diameter is decreased by 12% (lower right panel) in *Fbxo2* knockout mice. Quantified data represent approximately 6,000 spines from 60 dendritic segments per genotype. Error Bars S.D. **** $p<0.0001$ (unpaired t test).

Figure 25. Increased density of axo-dendritic shaft synapses in CA1 of *Fbxo2* -/- mice

Transmission Electron microscopy reveals increased dendritic shaft synapses in CA1 region of hippocampus from six month old *Fbxo2* null mice. Representative images show synapses on dendritic shafts (false-colored green) at sites adjacent to spinous synapses *(a and inset, b)* and along peripheral membranes (*c* and *e*, with respective insets *d* and *f*). Synapses were identified by the presence of an

electron-dense postsynaptic structure (arrows, *c*, *d*, *f*) opposed to a presynaptic terminal with visible, round, synaptic vesicles (labeled V, panels *b*, *d*, and *f.*) The increase in density of shaft synapses per animal was quantified (*g*) from 500um of dendritic length from 4 animals per genotype. Shaft synapses were also found less frequently in wild-type dendrites, as shown in *(h)* and inset *(i)*. Error Bars S.E. *, $p<0.05$ Scale bars = 500nm (*a,c,e, h*) and 250nm (*b, d, f, i*).

Figure 26. Proposed Model for the Altered Handling of NMDA receptors and Aberrant Formation of Axo-Dendritic Shaft Synapses in the Absence of Fbxo2 [1] Based on co-expression experiments with uncoupled receptor subunits and analysis of brain lysates, we propose that Fbxo2 may play a role in limiting the steady-state levels of newly-synthesized GluN1 and N2A in the ER. [2] As steady state levels increase, subunits complex together with scaffolding and transynaptic proteins and leave the ER to be trafficked to synapses. [3] Homeostatic mechanisms limit the number of NMDA receptors at a given synapse, shuttling unused receptor complexes to and from reserve pools at non-synaptic sites in the peripheral membrane. [4] As NMDA receptors are endocytosed in response to activity or as part of their normal lifespan, the option to degrade these receptors is lost in the absence of Fbxo2, cauing all receptors to recycle back to the surface, keeping the reserve pool large. [5] Given sufficient density of receptor complexes - with associated scaffolds and trans-synaptic proteins - recruits pre-synaptic branching to create axo-dendritic shaft synapses.

Figure 14

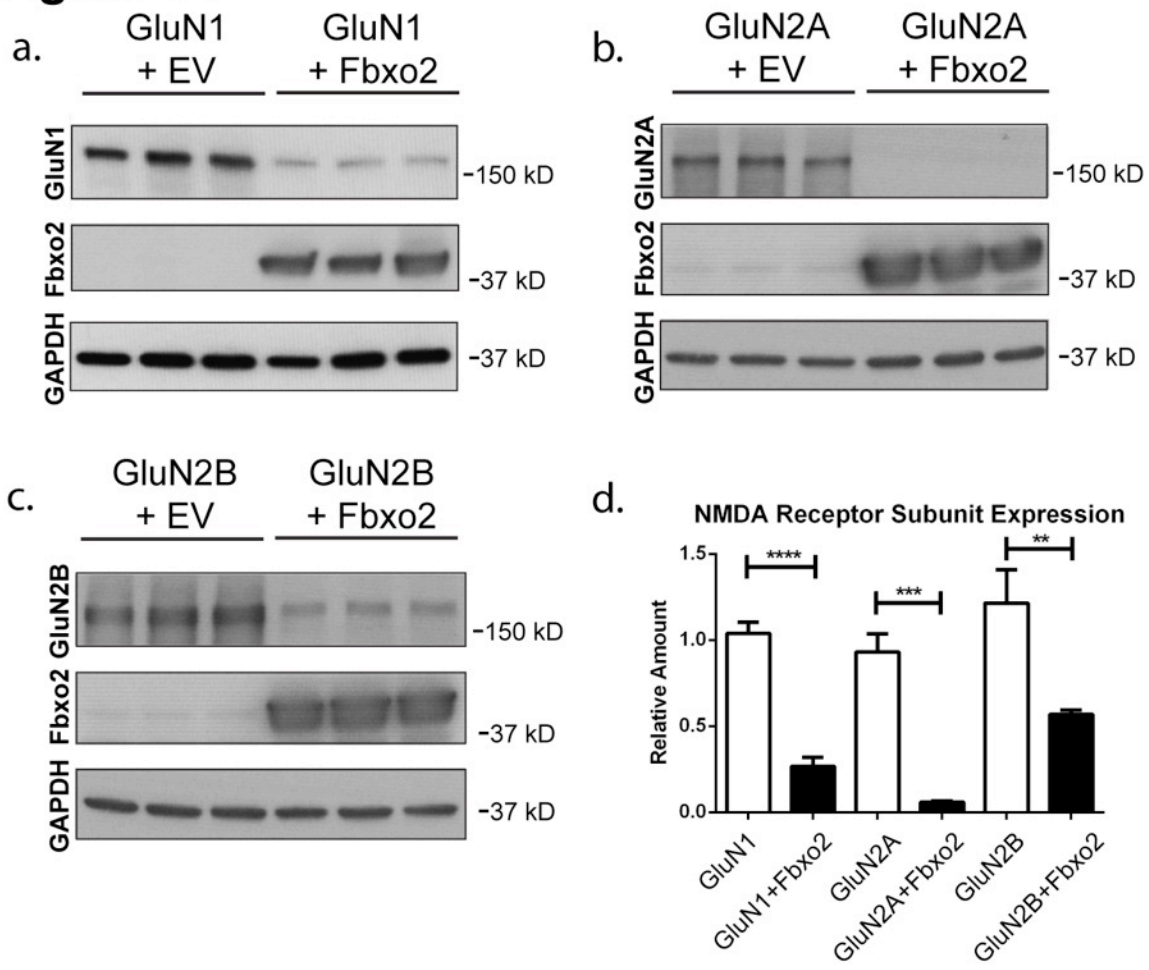

Figure 14. Co-expression of Fbxo2 decreases levels of unassembled NMDA Receptor Subunits

Figure 15

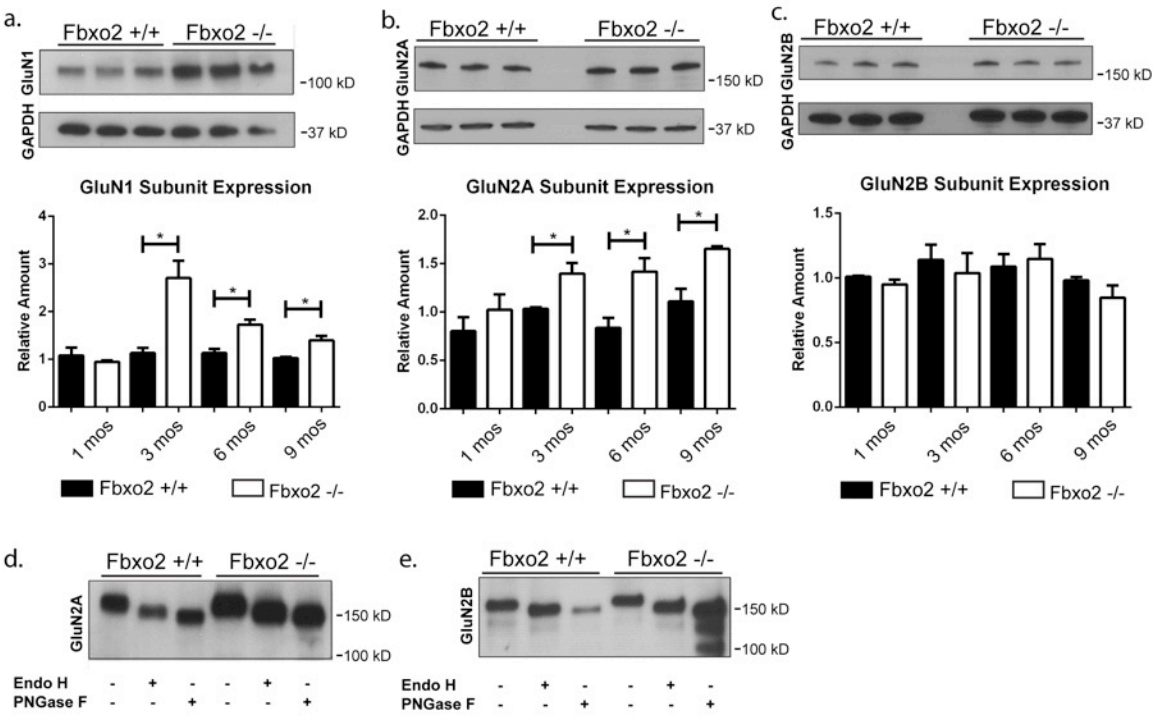

Figure 15. Increased levels of GluN1 and GluN2A, but not GluN2B, in *Fbxo2 -/-* brain.

Figure 16

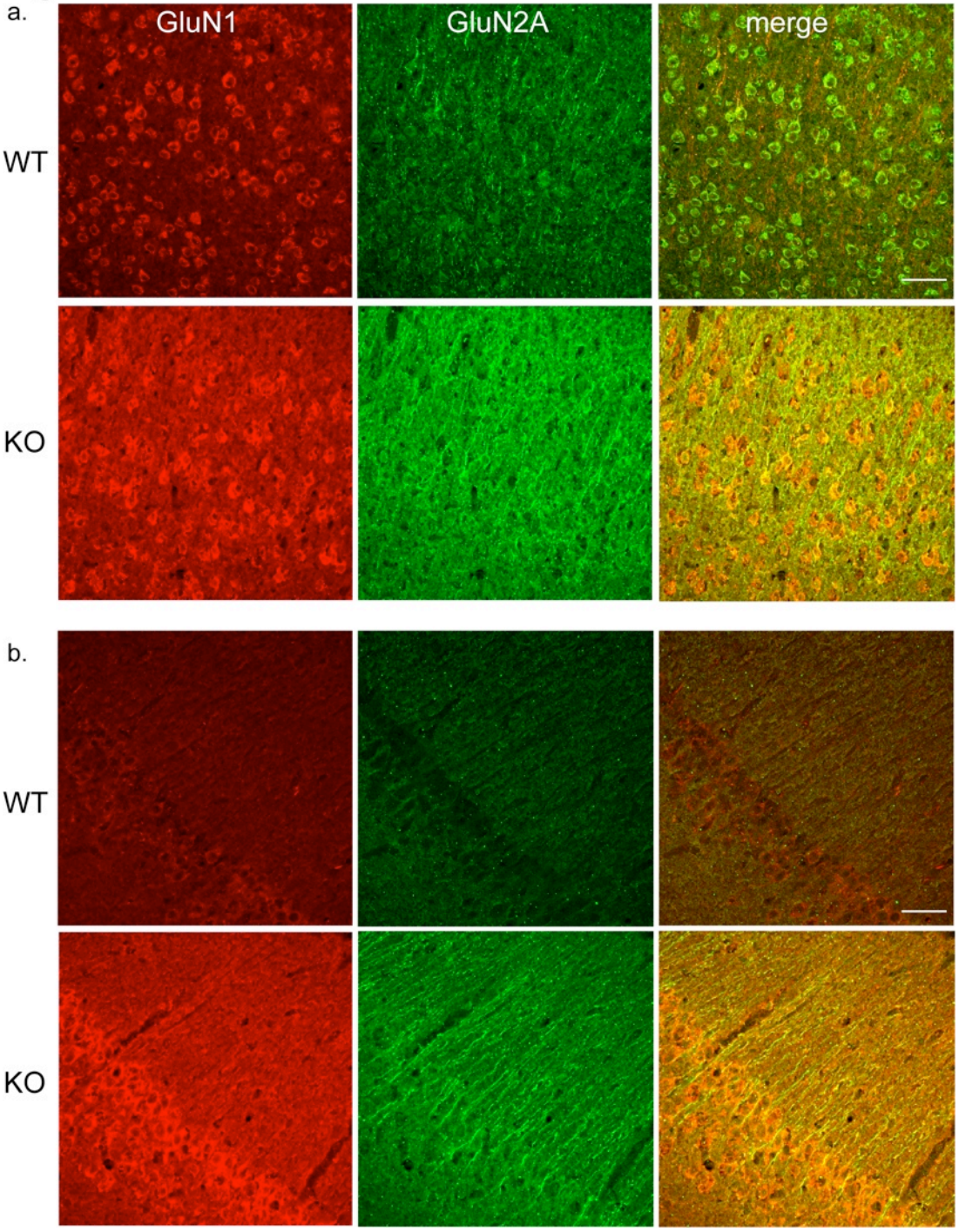

Figure 16. Immunofluorescence confirms increased GluN1 and GluN2A levels in *Fbxo2 -/-* brain.

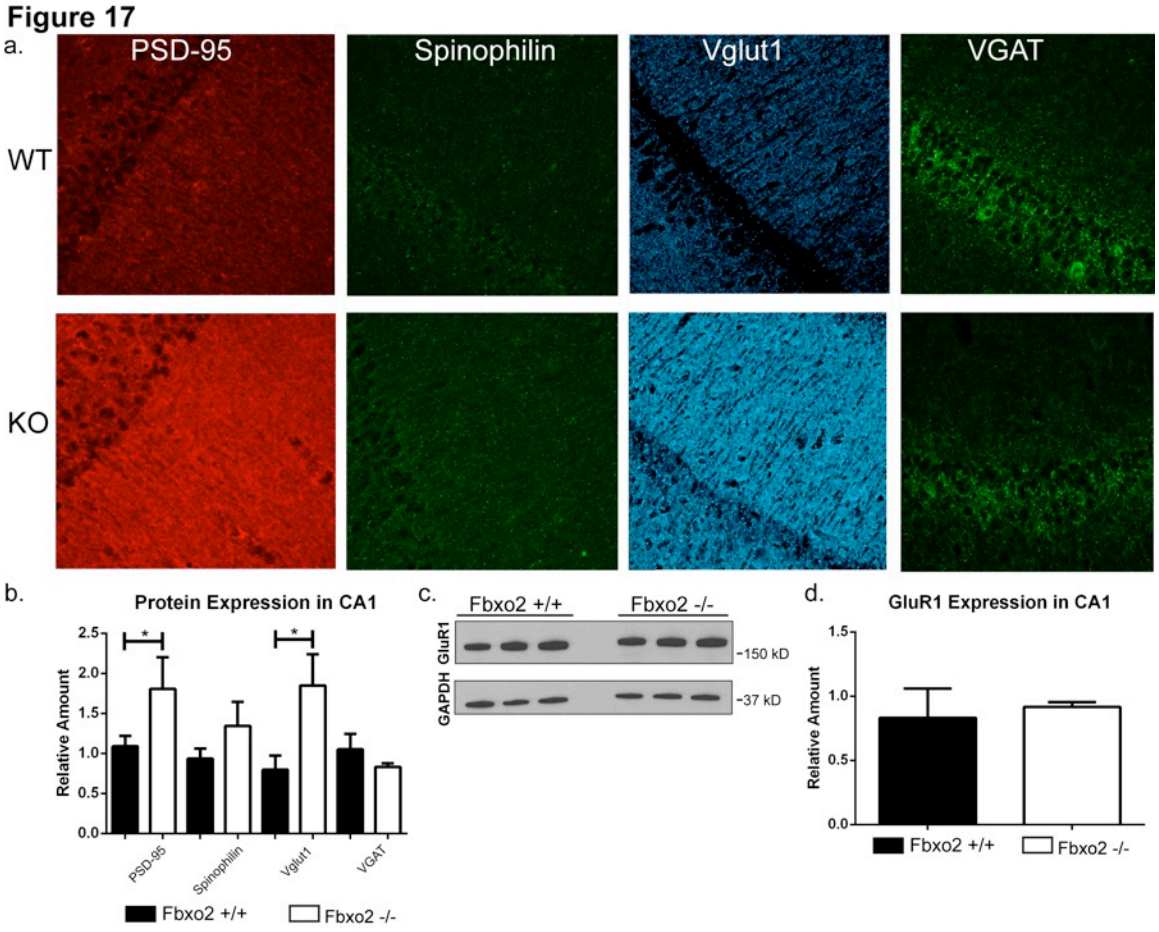

Figure 17. Elevated levels of PSD-95 and Vglut1 in *Fbxo2 -/-* brain.

Figure 18

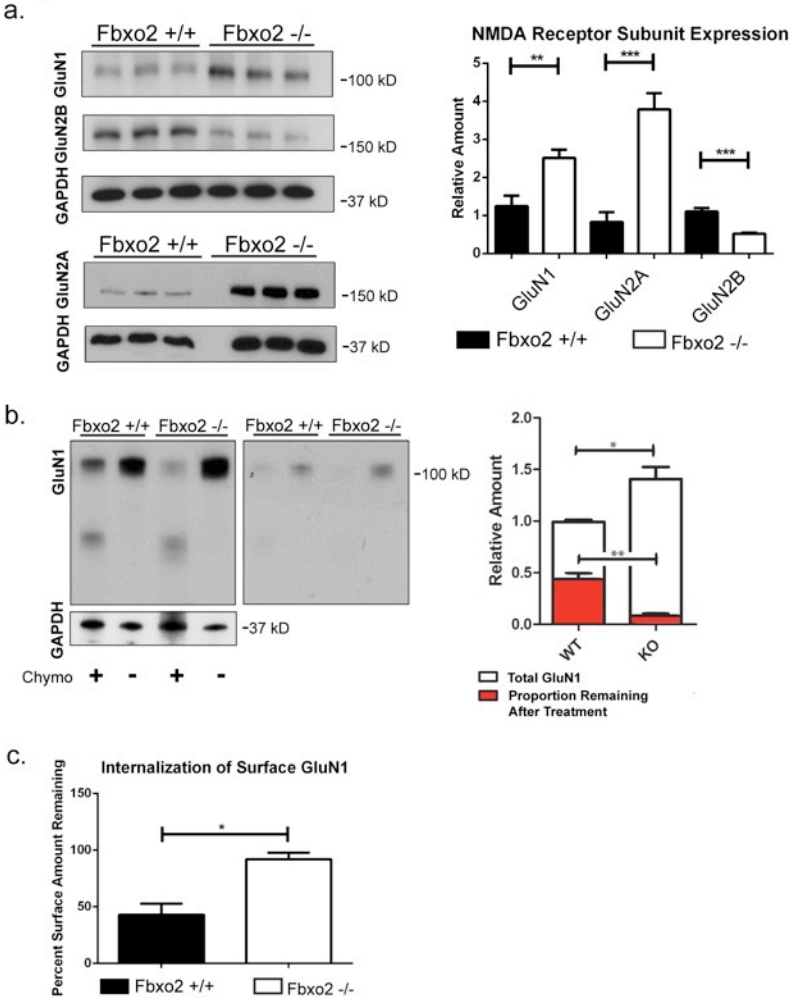

Figure 18. NMDA receptor levels and cell surface localization are increased in cultured *Fbxo2* -/- hippocampal neurons

Figure 19

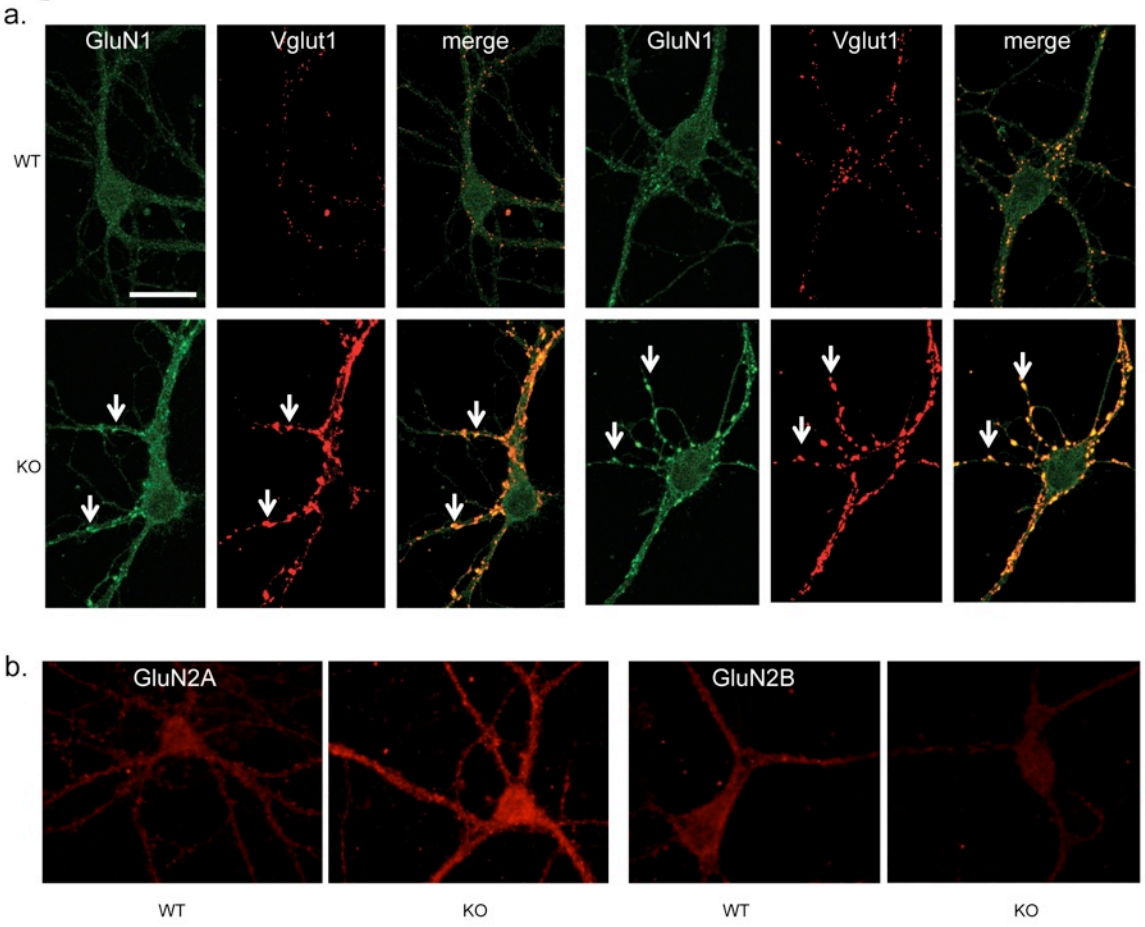

Figure 19. Greater GluN1 immunoreactivity colocalizes with the presynaptic marker VGlut1 in cultured hippocampal neurons

Figure 20

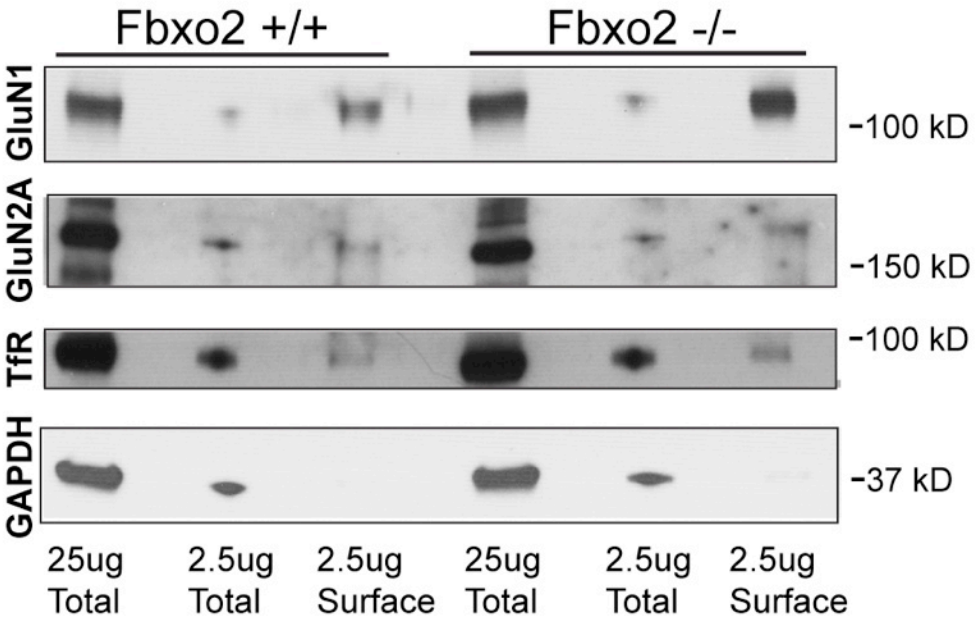

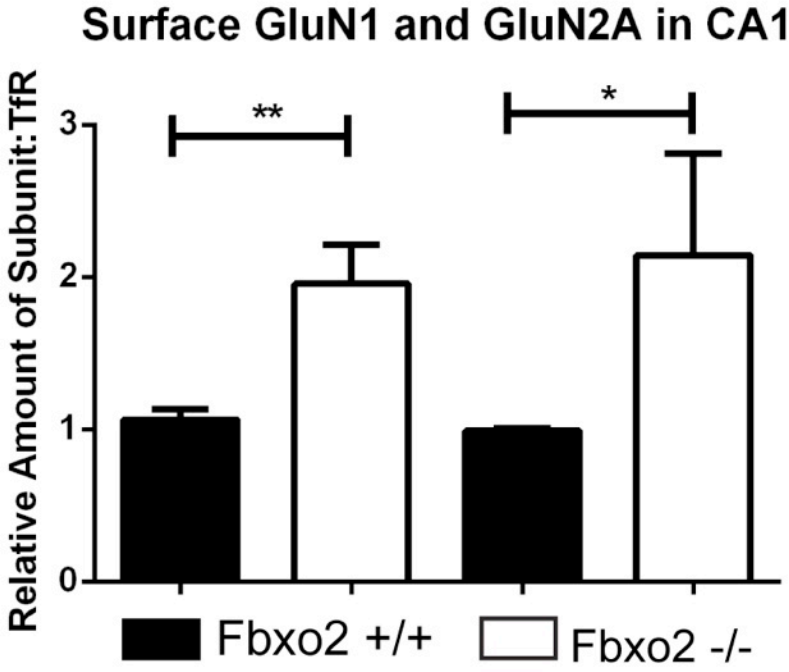

Figure 20. Enhanced Surface Localization of GluN1 and GluN2A in Hippocampi of Fbxo2 -/- mice

Figure 21

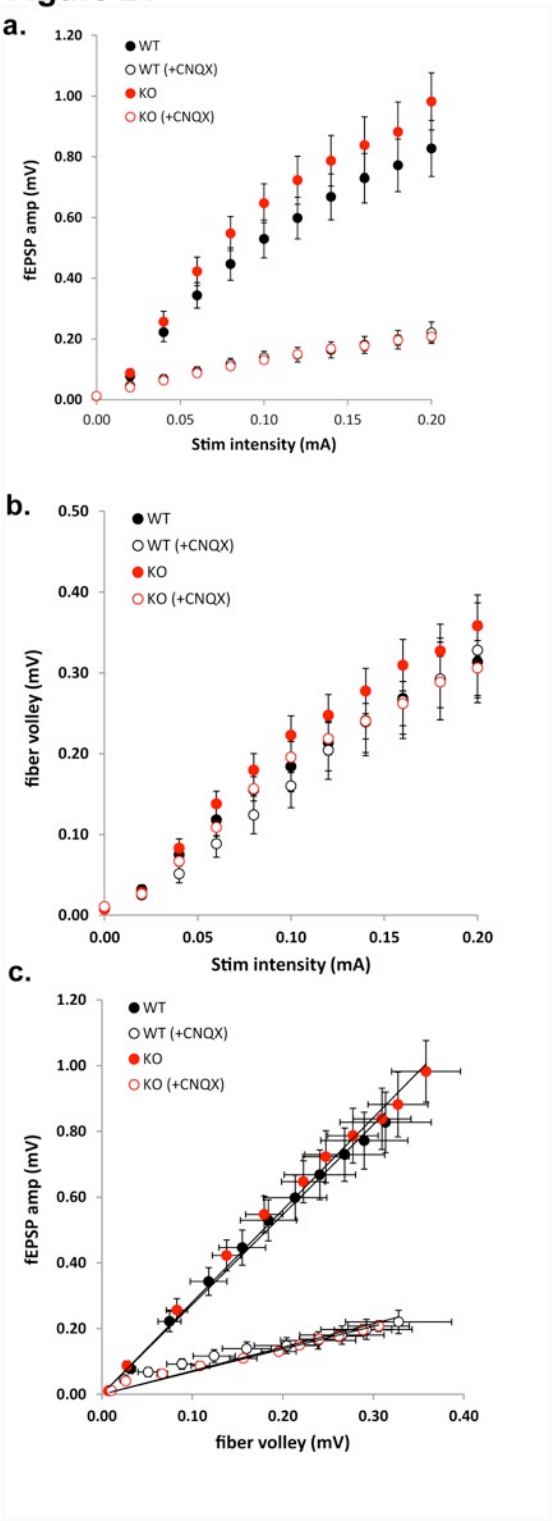

Figure 21. The loss of Fbxo2 does not alter hippocampal synaptic transmission

Figure 22

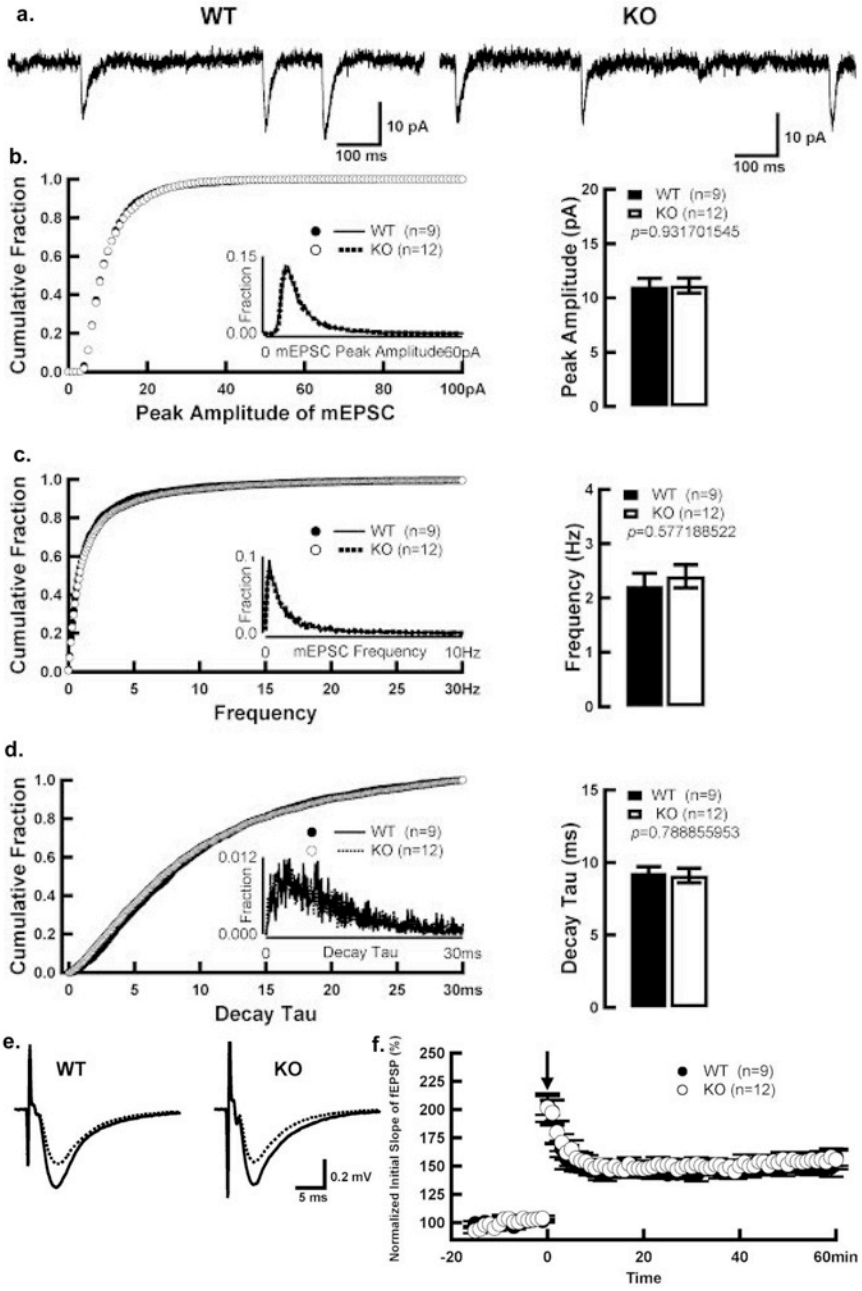

Figure 22. The loss of Fbxo2 does not alter hippocampal synaptic miniature synaptic currents or LTP induction

Figure 23

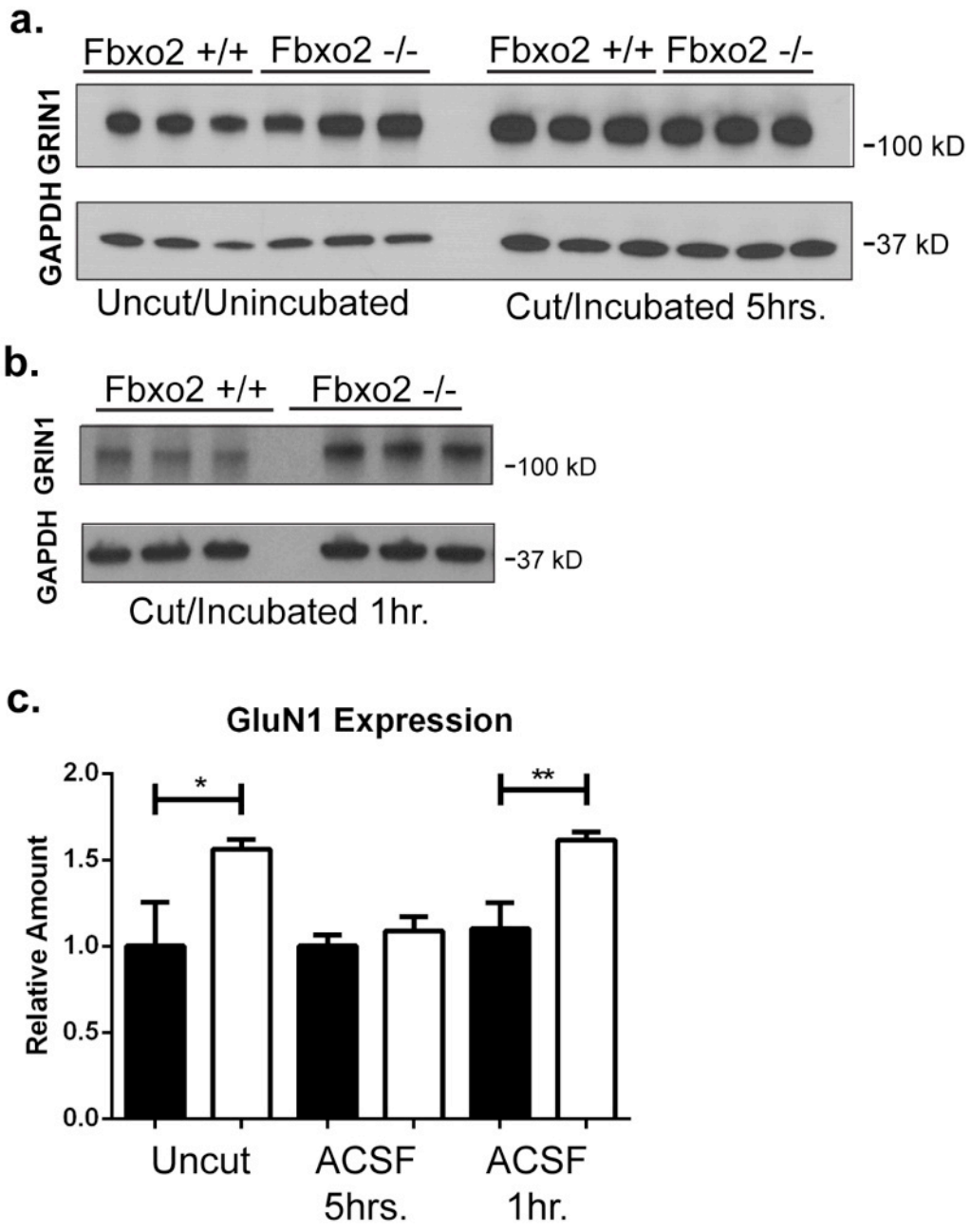

Figure 23. GluN1 levels are equilibrated following lengthy incubation in ACSF.

Figure 24

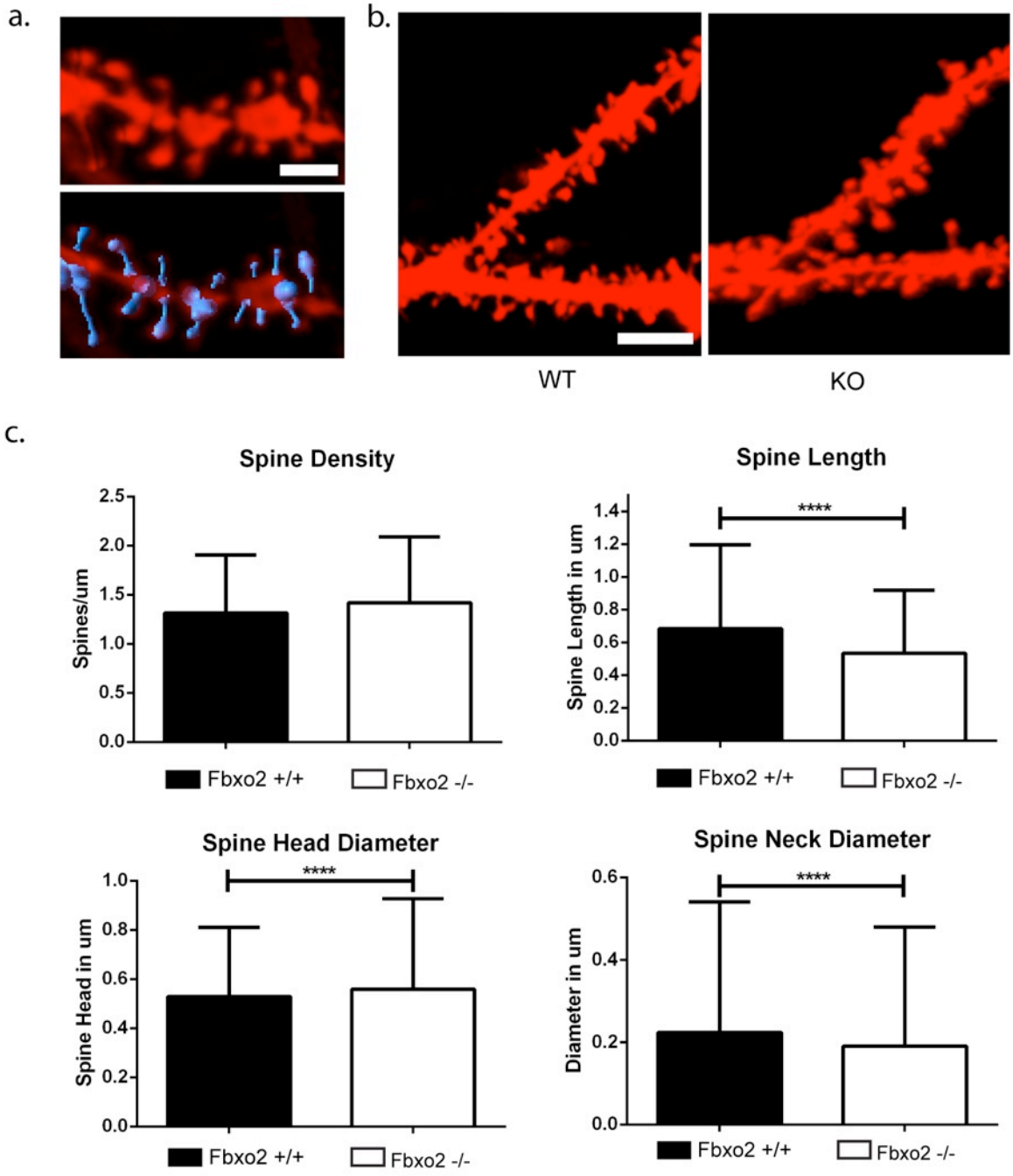

Figure 24. Dendritic Spine Density is not affected by the loss of Fbxo2

Figure 25

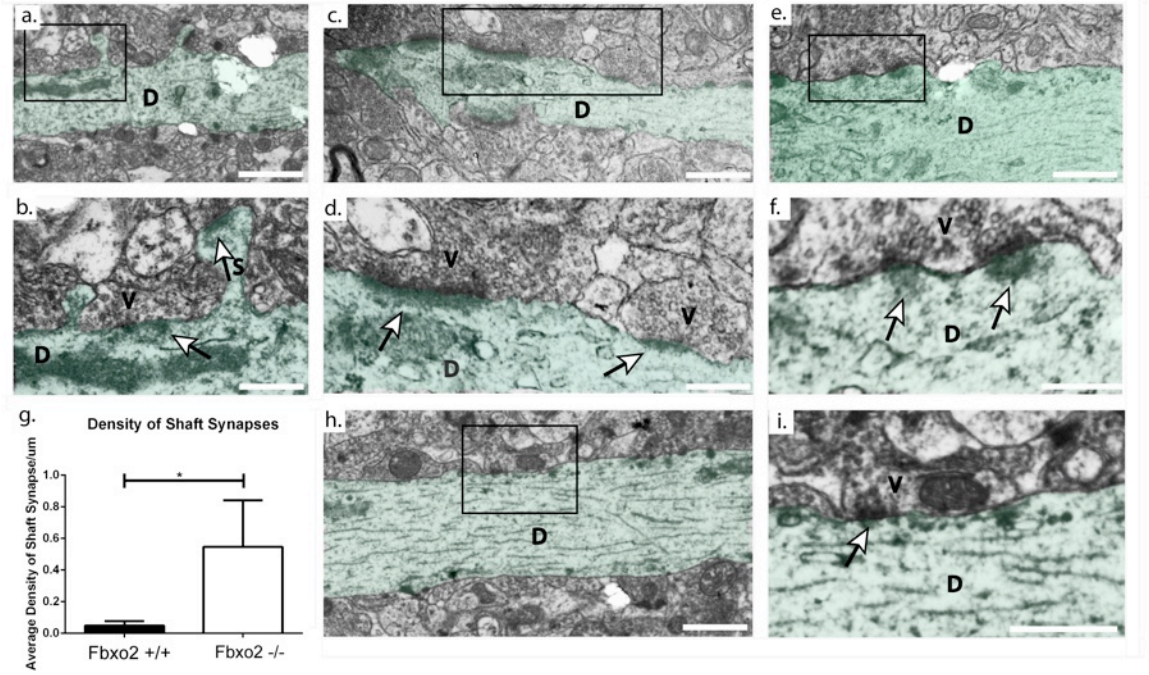

Figure 25. Increased density of axo-dendritic shaft synapses in CA1 of *Fbxo2* -/- mice

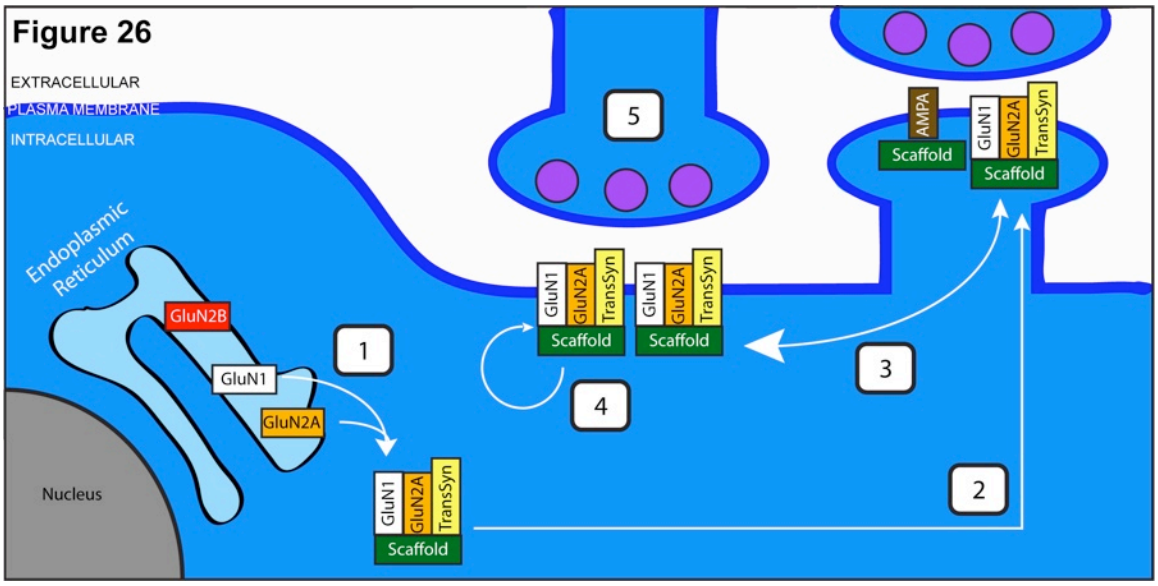

Figure 26. Proposed Model for the Altered Handling of NMDA receptors and Aberrant Formation of Axo-Dendritic Shaft Synapses in the Absence of Fbxo2

Bibliography

1. Hardingham, G. E. (2009) Coupling of the NMDA receptor to neuroprotective and neurodestructive events. *Biochem Soc Trans* **37**, 1147-1160
2. Morris, R. G., Anderson, E., Lynch, G. S., and Baudry, M. (1986) Selective impairment of learning and blockade of long-term potentiation by an N-methyl-D-aspartate receptor antagonist, AP5. *Nature* **319**, 774-776
3. Lee, J. L., Milton, A. L., and Everitt, B. J. (2006) Reconsolidation and extinction of conditioned fear: inhibition and potentiation. *J Neurosci* **26**, 10051-10056
4. Lai, T. W., Shyu, W. C., and Wang, Y. T. (2011) Stroke intervention pathways: NMDA receptors and beyond. *Trends Mol Med* **17**, 266-275
5. Gladding, C. M., Sepers, M. D., Xu, J., Zhang, L. Y., Milnerwood, A. J., Lombroso, P. J., and Raymond, L. A. (2012) Calpain and STriatal-Enriched protein tyrosine phosphatase (STEP) activation contribute to extrasynaptic NMDA receptor localization in a Huntington's disease mouse model. *Hum Mol Genet* **21**, 3739-3752
6. Li, S., Hong, S., Shepardson, N. E., Walsh, D. M., Shankar, G. M., and Selkoe, D. (2009) Soluble oligomers of amyloid Beta protein facilitate hippocampal long-term depression by disrupting neuronal glutamate uptake. *Neuron* **62**, 788-801
7. Snyder, E. M., Nong, Y., Almeida, C. G., Paul, S., Moran, T., Choi, E. Y., Nairn, A. C., Salter, M. W., Lombroso, P. J., Gouras, G. K., and Greengard, P. (2005) Regulation of NMDA receptor trafficking by amyloid-beta. *Nat Neurosci* **8**, 1051-1058
8. Parsons, C. G., Stoffler, A., and Danysz, W. (2007) Memantine: a NMDA receptor antagonist that improves memory by restoration of homeostasis in the glutamatergic system--too little activation is bad, too much is even worse. *Neuropharmacology* **53**, 699-723
9. Rowland, L. M., Astur, R. S., Jung, R. E., Bustillo, J. R., Lauriello, J., and Yeo, R. A. (2005) Selective cognitive impairments associated with NMDA receptor blockade in humans. *Neuropsychopharmacology* **30**, 633-639
10. Pollak, T. A., McCormack, R., Peakman, M., Nicholson, T. R., and David, A. S. (2013) Prevalence of anti-N-methyl-d-aspartate (NMDA) antibodies in patients with schizophrenia and related psychoses: a systematic review and meta-analysis. *Psychol Med*, 1-13
11. Monyer, H., Sprengel, R., Schoepfer, R., Herb, A., Higuchi, M., Lomeli, H., Burnashev, N., Sakmann, B., and Seeburg, P. H. (1992) Heteromeric NMDA receptors: molecular and functional distinction of subtypes. *Science* **256**, 1217-1221
12. Barria, A., and Malinow, R. (2002) Subunit-specific NMDA receptor trafficking to synapses. *Neuron* **35**, 345-353
13. Hardingham, G. E., and Bading, H. (2010) Synaptic versus extrasynaptic NMDA receptor signalling: implications for neurodegenerative disorders. *Nat Rev Neurosci* **11**, 682-696

14. Al-Hallaq, R. A., Conrads, T. P., Veenstra, T. D., and Wenthold, R. J. (2007) NMDA di-heteromeric receptor populations and associated proteins in rat hippocampus. *J Neurosci* **27**, 8334-8343
15. Lee, I., and Kesner, R. P. (2002) Differential contribution of NMDA receptors in hippocampal subregions to spatial working memory. *Nat Neurosci* **5**, 162-168
16. Horak, M., Chang, K., and Wenthold, R. J. (2008) Masking of the endoplasmic reticulum retention signals during assembly of the NMDA receptor. *J Neurosci* **28**, 3500-3509
17. Huh, K. H., and Wenthold, R. J. (1999) Turnover analysis of glutamate receptors identifies a rapidly degraded pool of the N-methyl-D-aspartate receptor subunit, NR1, in cultured cerebellar granule cells. *J Biol Chem* **274**, 151-157
18. Kato, A., Rouach, N., Nicoll, R. A., and Bredt, D. S. (2005) Activity-dependent NMDA receptor degradation mediated by retrotranslocation and ubiquitination. *Proc Natl Acad Sci U S A* **102**, 5600-5605
19. Yoshida, Y., Chiba, T., Tokunaga, F., Kawasaki, H., Iwai, K., Suzuki, T., Ito, Y., Matsuoka, K., Yoshida, M., Tanaka, K., and Tai, T. (2002) E3 ubiquitin ligase that recognizes sugar chains. *Nature* **418**, 438-442
20. Sans, N., Petralia, R. S., Wang, Y. X., Blahos, J., 2nd, Hell, J. W., and Wenthold, R. J. (2000) A developmental change in NMDA receptor-associated proteins at hippocampal synapses. *J Neurosci* **20**, 1260-1271
21. Jeyifous, O., Waites, C. L., Specht, C. G., Fujisawa, S., Schubert, M., Lin, E. I., Marshall, J., Aoki, C., de Silva, T., Montgomery, J. M., Garner, C. C., and Green, W. N. (2009) SAP97 and CASK mediate sorting of NMDA receptors through a previously unknown secretory pathway. *Nat Neurosci* **12**, 1011-1019
22. Hanus, C., and Schuman, E. M. (2013) Proteostasis in complex dendrites. *Nat Rev Neurosci* **14**, 638-648
23. Prybylowski, K., and Wenthold, R. J. (2004) N-Methyl-D-aspartate receptors: subunit assembly and trafficking to the synapse. *J Biol Chem* **279**, 9673-9676
24. Nelson, R. F., Glenn, K. A., Zhang, Y., Wen, H., Knutson, T., Gouvion, C. M., Robinson, B. K., Zhou, Z., Yang, B., Smith, R. J., and Paulson, H. L. (2007) Selective cochlear degeneration in mice lacking the F-box protein, Fbx2, a glycoprotein-specific ubiquitin ligase subunit. *J Neurosci* **27**, 5163-5171
25. Sutton, M. A., Wall, N. R., Aakalu, G. N., and Schuman, E. M. (2004) Regulation of dendritic protein synthesis by miniature synaptic events. *Science* **304**, 1979-1983
26. Atkin, G., Hunt, J., Minakawa, E., Sharkey, L., Tipper, N., Tennant, W., and Paulson, H. L. (2014) F-box only protein 2 (Fbxo2) Regulates Amyloid Precursor Levels and Processing. *J Biol Chem*
27. Hall, R. A., and Soderling, T. R. (1997) Quantitation of AMPA receptor surface expression in cultured hippocampal neurons. *Neuroscience* **78**, 361-371

28. Crump, F. T., Dillman, K. S., and Craig, A. M. (2001) cAMP-dependent protein kinase mediates activity-regulated synaptic targeting of NMDA receptors. *J Neurosci* **21**, 5079-5088
29. Parnas, D., and Linial, M. (1998) Highly sensitive ELISA-based assay for quantifying protein levels in neuronal cultures. *Brain Res Brain Res Protoc* **2**, 333-338
30. Thomas-Crusells, J., Vieira, A., Saarma, M., and Rivera, C. (2003) A novel method for monitoring surface membrane trafficking on hippocampal acute slice preparation. *J Neurosci Methods* **125**, 159-166
31. Kim, B. G., Dai, H. N., McAtee, M., Vicini, S., and Bregman, B. S. (2007) Labeling of dendritic spines with the carbocyanine dye DiI for confocal microscopic imaging in lightly fixed cortical slices. *J Neurosci Methods* **162**, 237-243
32. Swanger, S. A., Yao, X., Gross, C., and Bassell, G. J. (2011) Automated 4D analysis of dendritic spine morphology: applications to stimulus-induced spine remodeling and pharmacological rescue in a disease model. *Mol Brain* **4**, 38
33. Iliff, A. J., Renoux, A. J., Krans, A., Usdin, K., Sutton, M. A., and Todd, P. K. (2013) Impaired activity-dependent FMRP translation and enhanced mGluR-dependent LTD in Fragile X premutation mice. *Hum Mol Genet* **22**, 1180-1192
34. Nelson, R. F., Glenn, K. A., Miller, V. M., Wen, H., and Paulson, H. L. (2006) A novel route for F-box protein-mediated ubiquitination links CHIP to glycoprotein quality control. *J Biol Chem* **281**, 20242-20251
35. Helenius, A., and Aebi, M. (2004) Roles of N-linked glycans in the endoplasmic reticulum. *Annu Rev Biochem* **73**, 1019-1049
36. Jurd, R., Thornton, C., Wang, J., Luong, K., Phamluong, K., Kharazia, V., Gibb, S. L., and Ron, D. (2008) Mind bomb-2 is an E3 ligase that ubiquitinates the N-methyl-D-aspartate receptor NR2B subunit in a phosphorylation-dependent manner. *J Biol Chem* **283**, 301-310
37. Rinaldi, T., Kulangara, K., Antoniello, K., and Markram, H. (2007) Elevated NMDA receptor levels and enhanced postsynaptic long-term potentiation induced by prenatal exposure to valproic acid. *Proc Natl Acad Sci U S A* **104**, 13501-13506
38. Foster, K. A., McLaughlin, N., Edbauer, D., Phillips, M., Bolton, A., Constantine-Paton, M., and Sheng, M. (2010) Distinct roles of NR2A and NR2B cytoplasmic tails in long-term potentiation. *J Neurosci* **30**, 2676-2685
39. Tang, Y. P., Shimizu, E., Dube, G. R., Rampon, C., Kerchner, G. A., Zhuo, M., Liu, G., and Tsien, J. Z. (1999) Genetic enhancement of learning and memory in mice. *Nature* **401**, 63-69
40. Elias, G. M., Elias, L. A., Apostolides, P. F., Kriegstein, A. R., and Nicoll, R. A. (2008) Differential trafficking of AMPA and NMDA receptors by SAP102 and PSD-95 underlies synapse development. *Proc Natl Acad Sci U S A* **105**, 20953-20958

41. Tyan, S. H., Shih, A. Y., Walsh, J. J., Maruyama, H., Sarsoza, F., Ku, L., Eggert, S., Hof, P. R., Koo, E. H., and Dickstein, D. L. (2012) Amyloid precursor protein (APP) regulates synaptic structure and function. *Mol Cell Neurosci* **51**, 43-52
42. Kwon, H. B., and Sabatini, B. L. (2011) Glutamate induces de novo growth of functional spines in developing cortex. *Nature* **474**, 100-104
43. Skeberdis, V. A., Chevaleyre, V., Lau, C. G., Goldberg, J. H., Pettit, D. L., Suadicani, S. O., Lin, Y., Bennett, M. V., Yuste, R., Castillo, P. E., and Zukin, R. S. (2006) Protein kinase A regulates calcium permeability of NMDA receptors. *Nat Neurosci* **9**, 501-510
44. Gardoni, F., Bellone, C., Cattabeni, F., and Di Luca, M. (2001) Protein kinase C activation modulates alpha-calmodulin kinase II binding to NR2A subunit of N-methyl-D-aspartate receptor complex. *J Biol Chem* **276**, 7609-7613
45. Lin, Y., Jover-Mengual, T., Wong, J., Bennett, M. V., and Zukin, R. S. (2006) PSD-95 and PKC converge in regulating NMDA receptor trafficking and gating. *Proc Natl Acad Sci U S A* **103**, 19902-19907
46. Ali, D. W., and Salter, M. W. (2001) NMDA receptor regulation by Src kinase signalling in excitatory synaptic transmission and plasticity. *Curr Opin Neurobiol* **11**, 336-342
47. Bourne, J. N., and Harris, K. M. (2011) Coordination of size and number of excitatory and inhibitory synapses results in a balanced structural plasticity along mature hippocampal CA1 dendrites during LTP. *Hippocampus* **21**, 354-373
48. Megias, M., Emri, Z., Freund, T. F., and Gulyas, A. I. (2001) Total number and distribution of inhibitory and excitatory synapses on hippocampal CA1 pyramidal cells. *Neuroscience* **102**, 527-540
49. Ehlers, M. D. (2003) Activity level controls postsynaptic composition and signaling via the ubiquitin-proteasome system. *Nat Neurosci* **6**, 231-242
50. Dong, C., Upadhya, S. C., Ding, L., Smith, T. K., and Hegde, A. N. (2008) Proteasome inhibition enhances the induction and impairs the maintenance of late-phase long-term potentiation. *Learn Mem* **15**, 335-347
51. Huber, K. M., Kayser, M. S., and Bear, M. F. (2000) Role for rapid dendritic protein synthesis in hippocampal mGluR-dependent long-term depression. *Science* **288**, 1254-1257
52. Huang, Y. Y., and Kandel, E. R. (2007) 5-Hydroxytryptamine induces a protein kinase A/mitogen-activated protein kinase-mediated and macromolecular synthesis-dependent late phase of long-term potentiation in the amygdala. *J Neurosci* **27**, 3111-3119
53. Cui-Wang, T., Hanus, C., Cui, T., Helton, T., Bourne, J., Watson, D., Harris, K. M., and Ehlers, M. D. (2012) Local zones of endoplasmic reticulum complexity confine cargo in neuronal dendrites. *Cell* **148**, 309-321
54. Hanus, C., and Ehlers, M. D. (2008) Secretory outposts for the local processing of membrane cargo in neuronal dendrites. *Traffic* **9**, 1437-1445
55. Gong, B., Chen, F., Pan, Y., Arrieta-Cruz, I., Yoshida, Y., Haroutunian, V., and Pasinetti, G. M. (2010) SCFFbx2-E3-ligase-mediated degradation of

BACE1 attenuates Alzheimer's disease amyloidosis and improves synaptic function. *Aging Cell* **9**, 1018-1031
56. Huang, F., Zeng, X., Kim, W., Balasubramani, M., Fortian, A., Gygi, S. P., Yates, N. A., and Sorkin, A. (2013) Lysine 63-linked polyubiquitination is required for EGF receptor degradation. *Proc Natl Acad Sci U S A* **110**, 15722-15727
57. Fallon, L., Belanger, C. M., Corera, A. T., Kontogiannea, M., Regan-Klapisz, E., Moreau, F., Voortman, J., Haber, M., Rouleau, G., Thorarinsdottir, T., Brice, A., van Bergen En Henegouwen, P. M., and Fon, E. A. (2006) A regulated interaction with the UIM protein Eps15 implicates parkin in EGF receptor trafficking and PI(3)K-Akt signalling. *Nat Cell Biol* **8**, 834-842
58. Petralia, R. S., Al-Hallaq, R. A., and Wenthold, R. J. (2009) Trafficking and Targeting of NMDA Receptors.
59. Lussier, M. P., Nasu-Nishimura, Y., and Roche, K. W. (2011) Activity-dependent ubiquitination of the AMPA receptor subunit GluA2. *J Neurosci* **31**, 3077-3081
60. Houde, M., Bertholet, S., Gagnon, E., Brunet, S., Goyette, G., Laplante, A., Princiotta, M. F., Thibault, P., Sacks, D., and Desjardins, M. (2003) Phagosomes are competent organelles for antigen cross-presentation. *Nature* **425**, 402-406
61. Guermonprez, P., Saveanu, L., Kleijmeer, M., Davoust, J., Van Endert, P., and Amigorena, S. (2003) ER-phagosome fusion defines an MHC class I cross-presentation compartment in dendritic cells. *Nature* **425**, 397-402
62. Ultanir, S. K., Kim, J. E., Hall, B. J., Deerinck, T., Ellisman, M., and Ghosh, A. (2007) Regulation of spine morphology and spine density by NMDA receptor signaling in vivo. *Proc Natl Acad Sci U S A* **104**, 19553-19558
63. Nikonenko, I., Jourdain, P., Alberi, S., Toni, N., and Muller, D. (2002) Activity-induced changes of spine morphology. *Hippocampus* **12**, 585-591
64. Fortin, D. A., Davare, M. A., Srivastava, T., Brady, J. D., Nygaard, S., Derkach, V. A., and Soderling, T. R. (2010) Long-term potentiation-dependent spine enlargement requires synaptic Ca2+-permeable AMPA receptors recruited by CaM-kinase I. *J Neurosci* **30**, 11565-11575
65. Petrini, E. M., Lu, J., Cognet, L., Lounis, B., Ehlers, M. D., and Choquet, D. (2009) Endocytic trafficking and recycling maintain a pool of mobile surface AMPA receptors required for synaptic potentiation. *Neuron* **63**, 92-105
66. Meier, J., Vannier, C., Serge, A., Triller, A., and Choquet, D. (2001) Fast and reversible trapping of surface glycine receptors by gephyrin. *Nat Neurosci* **4**, 253-260
67. Newpher, T. M., and Ehlers, M. D. (2008) Glutamate receptor dynamics in dendritic microdomains. *Neuron* **58**, 472-497
68. Lai, H. C., and Jan, L. Y. (2006) The distribution and targeting of neuronal voltage-gated ion channels. *Nat Rev Neurosci* **7**, 548-562
69. Tovar, K. R., and Westbrook, G. L. (2002) Mobile NMDA receptors at hippocampal synapses. *Neuron* **34**, 255-264

70. Bassand, P., Bernard, A., Rafiki, A., Gayet, D., and Khrestchatisky, M. (1999) Differential interaction of the tSXV motifs of the NR1 and NR2A NMDA receptor subunits with PSD-95 and SAP97. *Eur J Neurosci* **11**, 2031-2043
71. Gardoni, F., Mauceri, D., Fiorentini, C., Bellone, C., Missale, C., Cattabeni, F., and Di Luca, M. (2003) CaMKII-dependent phosphorylation regulates SAP97/NR2A interaction. *J Biol Chem* **278**, 44745-44752
72. Chang, F. L., and Greenough, W. T. (1984) Transient and enduring morphological correlates of synaptic activity and efficacy change in the rat hippocampal slice. *Brain Res* **309**, 35-46
73. Nikolakopoulou, A. M., Davies, H. A., and Stewart, M. G. (2006) Passive avoidance training decreases synapse density in the hippocampus of the domestic chick. *Eur J Neurosci* **23**, 1054-1062
74. Jones, T. A., Klintsova, A. Y., Kilman, V. L., Sirevaag, A. M., and Greenough, W. T. (1997) Induction of multiple synapses by experience in the visual cortex of adult rats. *Neurobiol Learn Mem* **68**, 13-20
75. Helmeke, C., Ovtscharoff, W., Jr., Poeggel, G., and Braun, K. (2001) Juvenile emotional experience alters synaptic inputs on pyramidal neurons in the anterior cingulate cortex. *Cereb Cortex* **11**, 717-727
76. Ethell, I. M., and Pasquale, E. B. (2005) Molecular mechanisms of dendritic spine development and remodeling. *Prog Neurobiol* **75**, 161-205
77. Knott, G. W., Holtmaat, A., Wilbrecht, L., Welker, E., and Svoboda, K. (2006) Spine growth precedes synapse formation in the adult neocortex in vivo. *Nat Neurosci* **9**, 1117-1124
78. Aoto, J., Ting, P., Maghsoodi, B., Xu, N., Henkemeyer, M., and Chen, L. (2007) Postsynaptic ephrinB3 promotes shaft glutamatergic synapse formation. *J Neurosci* **27**, 7508-7519
79. Zha, X. M., Green, S. H., and Dailey, M. E. (2005) Regulation of hippocampal synapse remodeling by epileptiform activity. *Mol Cell Neurosci* **29**, 494-506
80. Kirov, S. A., Sorra, K. E., and Harris, K. M. (1999) Slices have more synapses than perfusion-fixed hippocampus from both young and mature rats. *J Neurosci* **19**, 2876-2886
81. Segev, I., and Rall, W. (1988) Computational study of an excitable dendritic spine. *J Neurophysiol* **60**, 499-523
82. Arellano, J. I., Benavides-Piccione, R., Defelipe, J., and Yuste, R. (2007) Ultrastructure of dendritic spines: correlation between synaptic and spine morphologies. *Front Neurosci* **1**, 131-143
83. Bloodgood, B. L., Giessel, A. J., and Sabatini, B. L. (2009) Biphasic synaptic Ca influx arising from compartmentalized electrical signals in dendritic spines. *PLoS Biol* **7**, e1000190

Chapter Four: Conclusions and Future Directions

In the preceding chapters I have explored the contributions of ubiquitin-mediated processes to neuronal health and function. In Chapter 1, I began by describing examples of the diverse, significant roles for ubiquitination in the most common neurodegenerative diseases. In Chapter 2, I explored the dysregulation of Amyoid Precursor Protein levels, localization, and processing following the loss of a single protein in the Ubiquitin Proteasome System, the brain-enriched E3 ligase substrate adaptor protein Fbxo2. In Chapter 3, I investigated the subunit-selective regulation of NMDA receptors by Fbxo2, and the complex homeoplastic regulation of these receptors and associated synaptic structures at the cell surface in the absence of Fbxo2. Here, I consider the broader implications of the work described in Chapters 2 and 3 on the need for further study of, and therapeutic intervention into, the problems associated with ubiquitination described in Chapter 1. I will focus my discussion on Alzheimer's Disease (AD) because of the links I have established in the preceding chapters to Fbxo2.

The question of potential clinical relevance underlies all of the work undertaken in our laboratory. Several factors influence the potential for translating our discoveries into meaningful insights into human disease and the design of potential therapies.

The first of these factors is the interchange between human disease and animal models. A great deal of what we believe about the protein-mediated

mechanism of human disease stems from studies of animal models which seldom faithfully recapitulate the features of human disease. These models often employ the expression of human or humanized proteins in non-human systems at levels which greatly exceed the physiologic levels of similar murine proteins. The expression of these proteins can be driven through extra-chromosomal means, and in doing so greatly change the landscape of gene transcription for the protein of interest. In the case of Fbxo2, our next logical step would be to ask whether the regulation of endogenous murine Amyloid Precursor Protein (APP) by Fbxo2 extends to mutant APP in AD mouse models. However, there is some question as to whether overexpressed, mutant APP is processed in the same way as endogenous APP (201). Alternative processing of mutant APP could occur in a manner that is independent of the expression of Fbxo2, and, given the massive over-expression of mutant APP in AD mouse models, actually mask smaller changes in the handling of endogenous APP. This could result in no detectable difference in amyloid levels between AD mice and AD mice lacking *Fbxo2* even if Fbxo2 does normally help regulate endogenous APP. Alternatively, Fbxo2 may facilitate the degradation of mutant and wild-type APP in vivo equally. The studies necessary to elucidate this point will require careful consideration of the appropriate AD mouse model, but could shed light on an important contribution to the processing of APP.

To address the need for model systems with greater fidelity to the biological problem, it would be of interest to suppress Fbxo2 expression in Induced Pluripotent Stem Cells (IPSCs) from AD patients and healthy adults of

various ages differentiated into neurons. While neurons in a dish will never recreate the complex connectivity of an intact brain, the study of wild-type and mutant human APP expressed in human cells at endogenous levels would allow us to determine whether what we observed here in mice also holds true in human neurons, and whether it extends to mutant APP as well.

In designing experiments with animal models, further consideration must also be given to the question of whether the reduction of Fbxo2 levels reported in AD patient tissue (90) occur early in disease or only as a late-stage phenomenon. While no mutations associated with *Fbxo2* have yet been reported for AD or any other neurodegenerative disease, the timing of any reduction in Fbxo2 levels could be critical in determining the impact such a change has. In the studies by Gong et al., transient changes to Fbxo2 levels resulted in an observed effect on BACE1 (90). In our studies, we were able to observe that same effect in a transient transfection model but not invivo, where the loss of Fbox2 was chronic. Similarly, the greatest difference in APP levels between wild-type and *Fbxo2* knockout mice occurred at 3 months of age, at the time point when Fbxo2 expression is highest in the wild-type brain. As the knockout animals aged, however, the observed increase in APP expression began to revert to levels matching those of wild-type mice, around 9 months of age. Intriguingly, the difference in GluN1 does not appear to normalize with aging, while the difference in GluN2A levels over time mirrors that of APP (Atkin, unpublished data). These findings suggest that additional, compensatory changes allow the brain to adapt to the loss of *Fbxo2* and normalize APP

handling. Thus, if the impact of *Fbxo2* knockout on the metabolism of APP and associated glycoproteins in the Amyloid Pathway is temporally restricted, the effect of reduced Fbxo2 levels on the pathogenic pathways of AD might well depend on when that decline in Fbxo2 first occurs. Access to patient brain tissue at several ages and degrees of disease severity would help greatly in clarifying this important point. Additionally, the creation of a conditional *Fbxo2* knockout mouse could reveal the significance of reduced Fbxo2 levels beginning at different ages and, when crossed with AD model mice, different stages of amyloid plaque deposition.

Another important consideration in assessing the potential clinical significance of Fbxo2 modulation pertains to the proliferation of synapses. The loss of synapses is observed in numerous neurodegenerative diseases and is considered the best morphological correlate for cognitive decline. This loss of synapses seems like an obvious problem in which modulating Fbxo2 activity could prove beneficial, as our studies reveal a significant increase in synapses in vitro and in vivo in the absence of Fbxo2. And yet our morphological examination of these structures suggests they are aberrantly localized, and our electrophysiological studies reveal that they do not participate in synaptic transmission or potentiation in a detectable manner. We must consider, then, that even if we were able to reduce Fbxo2 levels in a disease context and increase the numbers of synaptic connections, it might fail to benefit to cognitive function. Restoring synapse number without attention to the localization and composition of those additional synapses may not improve cognition. If the loss

of Fbxo2 increases the levels of one or more proteins necessary for the formation of synaptic connections, perhaps additional, combined interventions could redirect those additional synaptic building blocks to sites where neurons are optimally able to incorporate their function, such as spinous synapses. The precise mechanisms leading to the loss of synapses in disease states have yet to be understood, but perhaps this decline could be balanced out by the combined efforts of knocking down *Fbxo2* and increasing other mechanisms regulating synaptogenesis in order to achieve normal numbers of functional synapses and preserve cognitive functions.

Here, again, a conditional *Fbxo2* knockout mouse could prove useful to assess the potential for staving off age-related synaptic loss. The idea of creating an over-expression model of *Fbxo2* also raises fascinating scientific questions about the intersection of protein quality control and synaptic plasticity systems. In *Fbxo2* knockout mice, the overabundance of NMDA receptors (and likely other synapse-related proteins) does not compromise the regulation of dendritic spine number or architecture and synaptic transmission. The unchanged level of the AMPA receptor subunit GluR1 in knockout mice suggests a possible mechanism by which additional proteins may compensate for the effects of Fbxo2 loss. Such a mechanism could include the removal of AMPA receptors in an effort to sustain the Mg2+ block on NMDA receptors, or an increase in activity-dependent kinases whose modification of NMDA receptor subunits results in diminished NMDA receptor function, Protein Kinase C has been shown to do (1). What remains to be seen is whether the converse is true:

could decreasing NMDA receptors by over-expressing *Fbxo2* limit the formation of synapses if necessary minimum levels of substrate proteins aren't met? Or could other as yet unknown mechanisms compensate by inactivating Fbxo2 or limiting its access to high-mannose glycans on substrate proteins?

Finally, the potential unintended consequences of knocking down *Fbxo2* must be addressed when we consider the possibility of regulating Fbxo2 levels as a therapeutic intervention. Fbxo2 is merely one component of the UPS, and functions by complexing with other components to facilitate ubiquitination. Diverse combinations of UPS agents are able to form into a wide array of multi-subunit complexes that can allow for the recognition and handling of a large number of substrates (2). Fbxo2 has been shown to function with CHIP (3), but in our own unpublished work has also be found to interact with the RING-type E3 ligase Trim3 (Atkin, unpublished data). Trim3 is also involved in synaptic plasticity, facilitating the activity-dependent degradation of the post-synaptic scaffolding protein GKAP (4). Additional studies using mass spectroscopy of brain samples from wild-type and *Fbxo2* knockout mice revealed interaction between Fbxo2 and AP2A2, which is involved in the trafficking of surface proteins including synaptic receptors, and with the calcium-activated kinase CAMKII, an important regulator of long-term potentiation (Atkin, unpublished data). Fbxo2 was originally identified for its recognition of high-mannose glycans on potential substrates (5). Nearly half of all proteins are glycosylated as part of their synthesis and maturation (6). Thus, the list of proteins eligible for recognition and handling by Fbxo2 is potentially enormous. However, because our studies

revealed subunit-selective regulation of NMDA receptors in vivo by Fbxo2, the presence of high-mannose glycans may be necessary but not sufficient for substrate recognition. Taken together, these findings suggest that many proteins important for the health and function of neurons could be regulated by Fbxo2, but that further investigation will be needed to move possible substrates from the list of eligible candidates to proven substrates. These further investigations will also need to consider that Fbxo2 recognition of substrates may be restricted to specific activity-dependent states in neurons. Without a better understanding of the scope of proteins regulated by Fbxo2, altering its expression cannot be embraced as a potential therapy for Alzheimer's Disease or cognitive decline. Examining the large-scale proteomic changes following *Fbxo2* knockout in cultured neurons or brain is certainly feasible. And although such a study would not necessarily provide an exhaustive description of every protein whose level changes in the absence of Fbxo2, it would shed informative light on the broad scope of major changes. From there, a more refined strategy to target specific Fbxo2 substrates could be designed.

The etiology of Alzheimer's Disease appears extraordinarily complex. And while considerable time, effort, and money have been spent attempting to identify the individual events leading to disease, no effective treatments have resulted. The selective inhibition of secretase enzymes and the targeted elimination of Amyloid-Beta have not yet improved disease outcomes in human clinical trials. It may be that a less discriminate, less discrete intervention is called for. UPS agents like CHIP and Fbxo2 have the potential to influence a wide array of

substrate proteins and cellular processes. Modifying these agents might yield extensive, complex, and difficult to unravel proteomic changes, but the chance to improve neuronal health and cognitive function underscores that these are crucial areas of further investigation.

Bibliography

1. Perez, R. G., Squazzo, S. L., and Koo, E. H. (1996) Enhanced release of amyloid beta-protein from codon 670/671 "Swedish" mutant beta-amyloid precursor protein occurs in both secretory and endocytic pathways. *J Biol Chem* **271**, 9100-9107
2. Gong, B., Chen, F., Pan, Y., Arrieta-Cruz, I., Yoshida, Y., Haroutunian, V., and Pasinetti, G. M. (2010) SCFFbx2-E3-ligase-mediated degradation of BACE1 attenuates Alzheimer's disease amyloidosis and improves synaptic function. *Aging Cell* **9**, 1018-1031
3. Markram, H., and Segal, M. (1992) Activation of protein kinase C suppresses responses to NMDA in rat CA1 hippocampal neurones. *J Physiol* **457**, 491-501
4. Skaar, J. R., Pagan, J. K., and Pagano, M. (2009) SnapShot: F box proteins I. *Cell* **137**, 1160-1160 e1161
5. Nelson, R. F., Glenn, K. A., Miller, V. M., Wen, H., and Paulson, H. L. (2006) A novel route for F-box protein-mediated ubiquitination links CHIP to glycoprotein quality control. *J Biol Chem* **281**, 20242-20251
6. Hung, A. Y., Sung, C. C., Brito, I. L., and Sheng, M. (2010) Degradation of postsynaptic scaffold GKAP and regulation of dendritic spine morphology by the TRIM3 ubiquitin ligase in rat hippocampal neurons. *PLoS One* **5**, e9842
7. Yoshida, Y., Chiba, T., Tokunaga, F., Kawasaki, H., Iwai, K., Suzuki, T., Ito, Y., Matsuoka, K., Yoshida, M., Tanaka, K., and Tai, T. (2002) E3 ubiquitin ligase that recognizes sugar chains. *Nature* **418**, 438-442
8. Apweiler, R., Hermjakob, H., and Sharon, N. (1999) On the frequency of protein glycosylation, as deduced from analysis of the SWISS-PROT database. *Biochim Biophys Acta* **1473**, 4-8